France

Pyrenees-Orientales departement

Programme and funding

European Regional Development Fund

Execution of the study

Office National des Forêts

Restauration des Terrains en Montagne

Défense des Forêts contre l'Incendie

Final report

Erosion hazard assessment after a fire

October 2022

Commune of Cerbère

Experimental set-up:

Goals

Installation

Implementation

Results

Outlook

<u>Front page photograph</u>: view of the experimental erosion-measurement plot installed in the area burnt by the wildfire of 31 July 2021 in the CERBÈRE state forest (PYRÉNÉES-ORIENTALES)
Photo: ONF/RTM, 2 November 2021

EXECUTIVE SUMMARY

In the global context of climate change, periods of drought around the Mediterranean are becoming increasingly severe and long-lasting, and are significantly increasing the number of fires and the areas burnt. With increasingly dense built areas at the foot of the relief, the hydraulic risks induced after a fire are likely to be aggravated. This results in much more reactive catchment areas, leading to more frequent flooding and overflowing watercourses being triggered by less intense rainfall than before.

After a fire on a slope overlooking human structures, the sudden change in the landscape often causes psychological trauma in the population, which can lead to an exaggerated perception of the risks induced by rainfall episodes. This perception bias can lead to a desire to quickly implement solutions for restoring burnt soils that ultimately prove to be ineffective and costly.

The hydraulic processes induced after a fire, and in particular the increase in runoff and soil erosion, have been the subject of numerous studies and feedback throughout the world, with very varied estimates, most of which are difficult to apply in a Mediterranean context.

As part of the European MONTCLIMA project, a first in-depth analysis of the potential aggravation of the hydraulic risks induced by the fire of 2019 in the municipality of MONZE (AUDE, FRANCE) was carried out. Its aim was not to quantify the hydraulic processes precisely, but rather to describe the mechanisms involved. To complete this analysis, we proposed the implementation of an experimental "post-fire erosion hazard assessment" set-up intended to enrich scientific knowledge on these hydraulic processes induced in a Mediterranean context on burnt soils made up of weathered shale.

The principle of this experimental set-up consisted in installing measuring instruments on a slope recently impacted by a major wildfire in a pre-identified sector. The 51-hectare fire that occurred on 31 July 2021 on the international border ridge overlooking the town of CERBÈRE was an opportunity to set up three experimental plots of 100 m^2 each to measure hydrological and erosive processes. With the help of precise knowledge of the rainfall regime thanks to the installation of a rain gauge, the effects of the fire were quantified by comparing the volumes of runoff and sediment between two burnt plots and one vegetated control plot unaffected by the fire.

After one measurement season, from October 2021 to September 2022, and despite a general lack of rainfall in the study area, the experimental set-up yielded the following results:

- burnt soils reacted more quickly (from the beginning of the rainfall) and more readily (for lower rain intensities);
- burnt soils produced a hydrological response from a rainfall intensity of about 20 mm/h;
- unburned soils produced a hydrological response for rainfall intensities above 40 mm/h;
- runoff rates were up to six times higher on the burnt erosion plots than on the vegetated control plot;
- erosion rates were up to 14 times higher on the burnt erosion plots than on the vegetated control plot;
- runoff and erosion rates decreased with time and with the amount of vegetation cover on the ground;
- the natural dynamic process of vegetation recolonisation was strong, and after 10 months the vegetation on the ground reached a coverage rate of around 70% to 90%.

The results of this experiment should be treated with caution as they are based on measurements taken during a single hydrological season, in a context of rainfall deficit with few exceptional rainfall episodes.

By comparing these results with the literature, and taking into account the difference in scale between the MONTCLIMA project's experimental plots (100 m^2) and larger burnt catchments integrating hydro-sedimentary processes, we conclude that fires can as much as **double the runoff rate** compared to the pre-fire configuration.

As far as erosive processes are concerned, even if the results show a large sudden increase in the rate of erosion, with a ratio greater than 10, it is difficult to establish a trend on the basis of this experiment alone.

The changes in the hydro-sedimentary regime of the burnt watersheds are transitory: in the experimental set-up, the natural dynamics of vegetation recolonisation provided good ground cover after only 10 months. This dynamic depends on many factors, but an overview of the literature indicates that **3 to 5 years after the fire,** the hydrological and sedimentary processes **return to normal**.

Understanding this temporal evolution of the processes in the medium term requires the monitoring of the experimental system to continue beyond the end of the MONTCLIMA project. The RTM Department will carry out minimal monitoring during the 2022-2023 hydrological season, in association with a local university unit to capitalise and update this knowledge.

Thanks to the MONTCLIMA project, the results of the experiment were used by the RTM Department of the PYRÉNÉES-ORIENTALES in operational studies on the evaluation of the potential increase in hydraulic risks induced by the fires of OPOUL-PÉRILLOS and SALSES-LE-CHÂTEAU (28 June 2022) and of CAUDIÈS-DE-FENOUILLÈDES (15 August 2022).

In particular, it was possible to formalise, in **an objective and quantified manner**, **a protocol for intervention after a fire**, with **a suitable timeframe for the implementation of actions** to **mitigate the hydraulic risks involved**.

GLOSSARY

The following specific terms are used in this report:

- ***Experimental set-up***: set of three erosion plots, a rain gauge and digital cameras to confirm the presence of runoff and monitor vegetation recolonisation
- ***Rain gauge***: a device for continuous measurement of rainfall; a rain gauge consists of a stand and a cylindrical cover (sensor) installed on top of the stand
- ***Erosion plot***: a set-up comprising:
  - a plot of approximately 100 m^2 with borders;
  - a runoff collector/settler;
  - an approach channel with a flow measurement device (HS-Flume);
  - a digital camera to monitor the equipment.
- ***Borders***: whether rigid (wooden planks) or flexible (ballast bags), these are used to delimit a precise surface for the study of erosion
- ***Settler***: a tank that collects and measures the soil elements removed by the runoff (sand and gravel)
- ***Approach channel***: a straight channel located upstream of the HS-Flume to allow the running water to align with the general direction of flow and facilitate measurement
- ***HS-Flume***: the equipment used to measure flow (flow meter). This equipment has a very specific geometry and gives a simple relationship between the measured water level and the flow rate value
- ***Digital camera***: Observation device to monitor equipment and reduce the risk of vandalism

  ----

- ***Runoff coefficient***: ratio between the amount of water that runs off and the total amount of water that falls (rainfall). This ratio is always less than 1
- ***Splash effect***: the effect of raindrops impacting the soil and dislodging solid matter which is then carried away by gullying and contributes to soil erosion
- ***Hydrophobicity***: the tendency of a soil to become impermeable. In certain soil and vegetation configurations, fire can strongly modify the pedological characteristics of the soil and increase its hydrophobicity

  ----

- ***RTM***: *Restauration des Terrains en Montagne* (Restoration of Mountain Land) – a department of the National Forestry Office (ONF) specialising in natural risks (avalanche, landslides, flooding, overflowing watercourses)
- ***DFCI***: *Défense des Forêts Contre l'Incendie* – a department of the ONF specialising in the prevention of forest fires

LITERATURE REFERENCES

Badia, D., & Marti, C. (2000). Seeding and mulching treatments as conservation measures of two burnt soils in the central Ebro valley, NE Spain. Arid Soil Research and Rehabilitation, 14(3), 219-232.

Ballais, J. L., Bosc, M. C., & Sandoz, A. (1992). *La morphogenèse sur la montagne Sainte-Victoire après l'incendie : l'exemple du ruissellement* (1989-1992). *Méditerranée*, *75*(1), 43-52.

Ballais, J. L. (1993). *L'érosion consécutive à l'incendie d'août 1989 sur la montagne Sainte-Victoire : trois années d'observations* (1989-1992) (Erosion resulting from the fire of August 1989 on the Montagne Sainte-Victoire: three years of observations (1989-1992)). *Bulletin de l'Association de géographes français*, *70*(5), 423-437.

Bartet, J. H., & Combes, F. (1984). Remise en valeur d'un territoire incendié, communes de Saint-André-les-Alpes, Angles, Vergons (Alpes de Haute Provence). *Forêt Méditerranéenne*, *6*(1), 27-38.

Bautista, S., Bellot, J., & Vallejo, V. R. (1996). Mulching treatment for postfire soil conservation in a semiarid ecoset-up. *Arid Land Research and Management*, *10*(3), 235-242.

Bodí, M. B., Martin, D. A., Balfour, V. N., Santín, C., Doerr, S. H., Pereira, P., ... & Mataix-Solera, J. (2014). Wildland fire ash: production, composition and eco-hydro-geomorphic effects. Earth-Science Reviews, 130, 103-127.

Bonnet, V., & Tatoni, T. (2003). Analyse spatiale et fonctionnelle de la réponse de la végétation après incendie en basse Provence calcaire. *Forêt Méditerranéenne*, *24*(4), 385-402.

Booker, F. A., Dietrich, W. E., & Collins, L. M. (1993). Runoff and erosion after the Oakland firestorm. California Geology, 46(6), 159-173.

Cannon, S. H. (2001). Debris-flow generation from recently burned watersheds. Environmental & Engineering Geoscience, 7(4), 321-341.

Cerdà, A., & Doerr, S. H. (2005). Influence of vegetation recovery on soil hydrology and erodibility following fire: an 11-year investigation. International Journal of Wildland Fire, 14(4), 423-437.

Cerda, A. (2009). *Fire effects on soils and restoration strategies* (Vol. 5). CRC Press.

Combes, F. (1990). Après le feu... la boue. *Revue forestière française*, *42*(S), 303-306.

DeBano, L. F. (2000, March). Fire-induced water repellency: an erosional factor in wildland environments. In Proceedings of Conference Land Stewardship in the 21st century. The Contributions of Watershed Management (pp. 307-310). Tucson: Arizona.

Díaz-Fierros, F., Benito, E., & Soto, B. (1994). Action of forest fires on vegetation cover and soil erodibility. *Soil erosion and degradation as a consequence of forest fires. Geoforma Ediciones, Logroño*, 163-176.

Doerr, S. H., Shakesby, R. A., Blake, W. H., Chafer, C. J., Humphreys, G. S., & Wallbrink, P. J. (2006). Effects of differing wildfire severities on soil wettability and implications for hydrological response. Journal of Hydrology, 319(1-4), 295-311.

Hoefen, T. M., Kokaly, R. F., Martin, D. A., Rochester, C. J., Plumlee, G. S., Mendez, G., ... & Fisher, R. N. (2009). Sample collection of ash and burned soils from the October 2007 southern California Wildfires (No. 2009-1038). US Geological Survey.

Kribeche, H., Bautista, S., Gimeno, T., Blade, C., & Vallejo, V. R. (2013). Evaluating the effectiveness of post fire emergency rehabilitation treatments on soil degradation and erosion control in semi-arid Mediterranean areas of the Spanish South East. Arid Soil Research and Rehabilitation, 27(4), 361-376.

Lavabre, J., Torres, D. S., & Cernesson, F. (1993). Changes in the hydrological response of a small Mediterranean basin a year after a wildfire. Journal of Hydrology, 142(1-4), 273-299.

Lavabre, J., & Martin, C. (1997). Impact d'un incendie de forêt sur l'hydrologie et l'érosion hydrique d'un petit bassin versant. *Human Impact on Erosion and Sedimentation*, (245), 39.

Martin, C., Bernard-Allée, P., Béguin, E., Levant, M., & Quillard, J. (1993). *Conséquences de l'incendie de forêt de l'été 1990 sur l'érosion mécanique des sols dans le Massif des Maures* (Repercussions on physical soil erosion in the forests of the "Massif des Maures" following the fire of Summer 1990). *Bulletin de l'Association de géographes français*, *70*(5), 438-447.

Martin, C., Martin-Decome, A., & Allée, P. (2008). *Prédiction de l'érosion hydrique après incendie de forêt dans la partie occidentale du massif des Maures (Var, France). Etudes de géographie physique*, *35*, 51-64.

Martins, M. A., Machado, A. I., Serpa, D., Prats, S. A., Faria, S. R., Varela, M. E., ... & Keizer, J. J. (2013). Runoff and inter-rill erosion in a Maritime Pine and a Eucalypt plantation following wildfire and terracing in north-central Portugal. Journal of Hydrology and Hydromechanics, 61(4), 261.

Mataix-Solera, J., & Guerrero, C. (2007). *Efectos de los incendios forestales en las propiedades edáficas. Incendios forestales, suelos y erosión hídrica*, 5-40.

Moody, J. A., & Martin, D. A. (2009). Forest fire effects on geomorphic processes. In Fire effects on soils and restoration strategies (pp. 57-96). CRC Press.

Moody, J. A., Shakesby, R. A., Robichaud, P. R., Cannon, S. H., & Martin, D. A. (2013). Current research issues related to post-wildfire runoff and erosion processes. Earth-Science Reviews, 122, 10-37.

Moody, J. A., & Nyman, P. (2013). Variations in soil detachment rates after wildfire as a function of soil depth, flow properties and root properties. US Department of the Interior, US Geological Survey.

Moody, J. A., & Ebel, B. A. (2014). Infiltration and runoff generation processes in fire-affected soils. Hydrological Processes, 28(9), 3432-3453.

Neary, D. G., Ryan, K. C., & DeBano, L. F. (2005). Wildland fire in ecosystems: effects of fire on soils and water. *Gen. Tech. Rep. RMRS-GTR-42-vol. 4. Ogden, UT: US Department of Agriculture, Forest Service, Rocky Mountain Research Station. 250 p.*, *42*.

Pietraszek, J. H. (2006). Controls on Post-fire Erosion at the Hillslope Scale, Colorado, Front Range (Doctoral dissertation, Colorado State University).

Prats, S. A., Malvar, M. C., Vieira, D. C. S., MacDonald, L., & Keizer, J. J. (2016). Effectiveness of hydromulching to reduce runoff and erosion in a recently burnt pine plantation in central Portugal. Land degradation & development, 27(5), 1319-1333.

Rey, F., Ballais, J. L., Marre, A., & Rovéra, G. (2004). *Rôle de la végétation dans la protection contre l'érosion hydrique de surface. Comptes rendus géoscience*, *336*(11), 991-998.

Shakesby, R. A., & Doerr, S. H. (2006). Wildfire as a hydrological and geomorphological agent. Earth-Science Reviews, 74(3-4), 269-307.

Thomas, G., Rosalie, V., Olivier, C., & Antonio, L. P. (2021). Modelling forest fire and firebreak scenarios in a mediterranean mountainous catchment: Impacts on sediment loads. Journal of environmental management, 289, 112497.

Vallejo, R., Serrasolses, I., Alloza, J. A., Baeza, M. J., Bladé, C., Chirino, E., ... & Vilagrosa, A. (2009). Long-term restoration strategies and techniques. *Fire effects on soils and restoration strategies. Science Publishers Inc, Enfield*, 373-398.

Wohlgemuth, P. M., & Robichaud, P. R. (2007). The effects of selected postfire emergency rehabilitation techniques on small watershed sediment yields in southern California.

Woods, S. W., & Balfour, V. N. (2008). The effect of ash on runoff and erosion after a severe forest wildfire, Montana, USA. International Journal of Wildland Fire, 17(5), 535-548.

CONTENTS

1 THE GOALS OF THE PROJECT

1.1 THE EFFECT OF CLIMATE CHANGE ON THE INCREASE IN FIRES

In recent years, *"regional increases in temperature, aridity and drought have increased the frequency and intensity of fires"*, with a spatial spread that goes far beyond the regions that were frequently affected previously. Over the next few decades, *"At a global warming of 2°C with associated changes in precipitation, global land area burned by wildfire is projected to increase by 35% (medium confidence)." (Source: Intergovernmental Panel on Climate Change – Working Group II; contribution to the Sixth Assessment Report)*

By drying out vegetation, climate change increases the meteorological hazard[1] of forest fires and lengthens the fire season. Météo France[2] researchers have studied the evolution of this hazard over the past century and for the next few decades: it has been increasing since the 1960s and is expected to increase further during the 21st century. Especially in the Mediterranean basin, all climate models predict a drying out. This area is thus defined as a climate change hotspot in the latest IPCC report.

The evolution and modelling of the French Meteorological Fire Index (MFI) from 1958 to 2100 show a steady increase in the frequency of days with meteorological forest fire hazard and a lengthening of the fire season (starting earlier in spring and ending later in autumn). The regions exposed to this hazard are also expected to extend towards the north of France.

The mean value of the MFI increased by 18% between the periods [1961-1980] and [1989-2008]. By 2040, the mean MFI is expected to be 30% higher than for the period [1961-2000]. Some simulations show that this increase could reach up to 75% by 2060. By that time, a year like 2003 would become the norm for meteorological forest fire hazard.

MÉTÉO FRANCE researchers have cross-referenced this evolution of the meteorological fire hazard with the maps of vulnerability to forest fires of the main forest stands, drawn up by the National Forestry

[1] The **French Meteorological Fire Index (MFI)** expresses the meteorological hazard associated with forest fires.
This hazard is estimated by considering the probability of an outbreak of fire and its potential for spread. MÉTÉO FRANCE assesses the MFI daily throughout France. This index is calculated from simple meteorological data: temperature, air humidity, wind speed and precipitation. These data are fed into a numerical model that simulates the moisture conditions of the vegetation and the resulting **meteorological fire hazard**. Weather observations and forecasts are used to calculate a daily MFI. Climate projections allow us to study its evolution in the longer term.

[2] Extract from a MÉTÉO FRANCE publication: https://meteofrance.com/le-changement-climatique/observer-le-changement-climatique/changement-climatique-et-feux-de-forets

Office (ONF) and the National Forest Inventory (IFN). Potential sensitivity maps for summer forest fires in recent times [1989-2008] and the medium term [2031-2050] were drawn up.

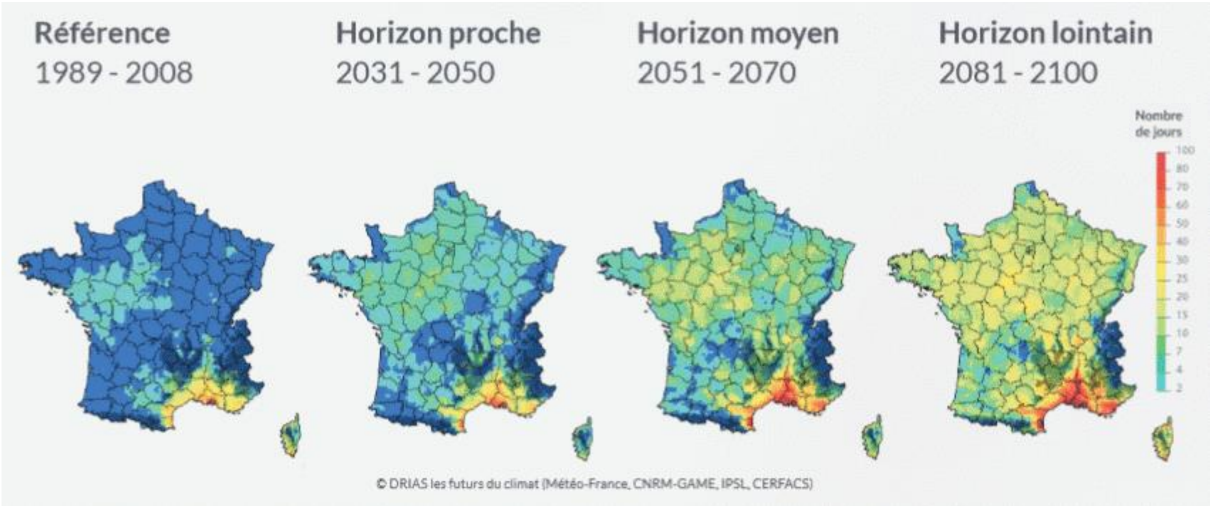

Figure 1: Number of days with meteorological fire index above 40 (high emissions scenario)

1.2 FIRES AGGRAVATE NATURAL RISKS

After a wildfire, in mountainous terrain, the potential aggravations concern the following risks *(Extract from the DGPR document, ONF 2021: Synthèse des études post-incendie de forêt et bilan des méthodologies*):

- **Risk of falling trees**

  Fire causes the death or weakening of trees, which greatly increases the risk of tree falls. This risk occurs when wooded areas are affected by a fire of moderate or high severity. In most cases, the trees fall months or possibly years after the fire has caused their death by heating the living parts (meristems), accentuated by degradation by various decomposers (entomofauna and fungi in particular). In the case of trees that are already partially dead or desiccated, tree fall can occur during or immediately after the fire.

  Falling trees can lead to the aggravation of other risks (erosion, rock falls, overflowing watercourses, avalanches).

- **Risk of falling rocks and stones**

  In the zones of origin, fire facilitates the movement of rocks through the combined effect of heat-induced soil destructuring and increased erosion due to the loss of vegetation cover.

  In rockfall propagation zones, the destruction or damage of the forest by fire can lead to a sudden loss of the protective screen function and therefore greatly increase the probability of danger to important elements.

  Protective structures can also be damaged, diminishing their effectiveness in reducing the probability of stones and rocks falling (active structures) or reaching other important elements (passive structures): wooden structures can be totally destroyed, dry stone walls destabilised, concrete or metal structures can be damaged by thermal effects, with the appearance of problems with anchoring and the resistance and durability of building materials.

- **Risk of gullying and erosion**

  During a fire, the heat destructures the surface soil and destroys the plant litter and the herbaceous layer, facilitating the genesis of erosion and gullying phenomena. Furthermore, the layer of ash deposited on the ground during the fire is highly mobile, and is easily washed away at the first rainfall. Erosion and gullying occur mainly in the first year after the fire and up to the third year. After this period, the most destructured fraction of the soil has already been washed away and the herbaceous and shrub layer is again present to protect the soil.

These post-fire phenomena can then have two types of consequences:

- natural risks: erosion and gullying lead to the bottoms of thalwegs becoming filled with gravel and scouring of the slopes, as well as on the tracks. Indirectly, erosion favours the movement of stones and rocks, which will actually fall later when watercourses overflow.
- the environment: soils are not only an important reservoir of biodiversity and carbon, but also a substrate for the development of the whole local biosphere. Although not very visible, the impact of fires on ecosystems can be very strong (directly through flames, then indirectly through erosion). This impact is all the more serious when fires are intense and/or frequent; in this case, the ecosystems are increasingly degraded (monospecific scrubland or maquis, grasslands, scree, deserts).

❖ **Risk of flooding and overflowing watercourses**

The destruction of the vegetation cover and the weakening of the soil by fire considerably aggravate the processes of runoff and gullying and therefore the risk of flooding and overflowing watercourses, including far downstream of the catchment areas affected by the fire. Post-fire damage usually occurs at already problematic locations (crossings, bridges, culverts, restricted stretches of watercourses, flooding areas, etc.).

An aggravating factor is the formation of logjams of burnt wood along the river system.

The transport of solids is most significant during the first rainfall episodes after the fire (departure of ash and the upper fraction of the soil disintegrated by the fire). It is therefore essential to assess this risk very quickly, before the autumn period of intense Mediterranean rainfall. This risk disappears as soon as a cover of at least 50% of the burnt surface is reconstituted, either artificially (mulching) or more often naturally (herbaceous plants, shoots or seedlings of shrub or tree species, etc.).

❖ **Avalanche risk**

In potential avalanche zones, the destruction of protective forest stands by fire can considerably increase the avalanche risk (more frequent avalanches with larger volumes). Fire can also damage and weaken avalanche defence structures of any material (metal, reinforced concrete, wood, stone).

1.3 THE STATE OF CURRENT KNOWLEDGE ON RUNOFF AND EROSION

For this case study, we were **only** interested in **the phenomena of runoff and soil erosion** after a fire.

1.3.1 CHANGES IN HYDROLOGICAL REGIME

1.3.1.1 DESCRIPTION OF THE PROCESSES

In a catchment area, there are several types of flows:

- ***"Slow" underground flows***, involving the infiltrated part of the rainwater slowly transiting through aquifers towards the outlets;
- ***"Rapid" surface flows***, which mainly concern surface runoff processes and subsurface runoff. Runoff is the fringe of water that flows more or less freely over the surface of the soil after rainfall. The amount of surface runoff depends on the intensity of rainfall and its capacity to rapidly saturate the first few centimetres of the soil, before infiltration and percolation, which are slower phenomena, become predominant.

Apart from any water intercepted by vegetation, the available rainfall at the soil surface is divided between water that infiltrates and contributes, through a slower flow through the soil layers, to groundwater recharge and base flow, and surface runoff when the intensity of the rainfall exceeds the infiltration capacity of the soil (which itself varies, among other things, according to soil moisture).

This surface runoff, where excess water flows down the slopes by gravity, forms the bulk of rapid flood flow. The steeper the slopes, the more surface runoff predominates compared to infiltration.

Flow when rainfall exceeds the infiltration capacity of the soil (known as Horton overland flow) is considered relevant for explaining the hydrological response of basins in semi-arid climates (as in the Mediterranean context) as well as during conditions of high rainfall intensity.

The percentage of vegetation interception varies with climate conditions and decreases as the intensity of rainfall increases. For a given rainfall, interception is better if it is light, fine rain rather than a downpour.

Foliage interception losses are highest for small rainfall events (<15 mm) and low-intensity rainfall (about 50% of rainfall). For heavy rainfall (>15 mm), interception losses decrease to 10-20% of rainfall.

Interception losses may be lower when foliage is shaken by strong winds. Thus, the amount of water flowing down the trunk and precipitation on the ground increases with rainfall intensity and wind speed; the storage capacity of the foliage is not constant.

The loss of vegetation after a fire has two consequences:

- the forest layer: the absence of forest cover leads to an increase in effective rainfall of around 10-20%.
- the vegetation layer at ground level: the role of the vegetation contributes to a slowing down of the hydrological dynamics. In the absence of ground vegetation, the hydrological response is much more rapid, and can be almost immediate in small catchments.

Figure 2: Distribution of the rainfall level during a constant-intensity shower (according to Réméniéras, 1976) – extract from Page 198 of *Hydrologie I – une science de la nature ; une gestion sociétale*, A. Musy, C. Higy, E. Reynard - Presses polytechniques et universitaires romandes)

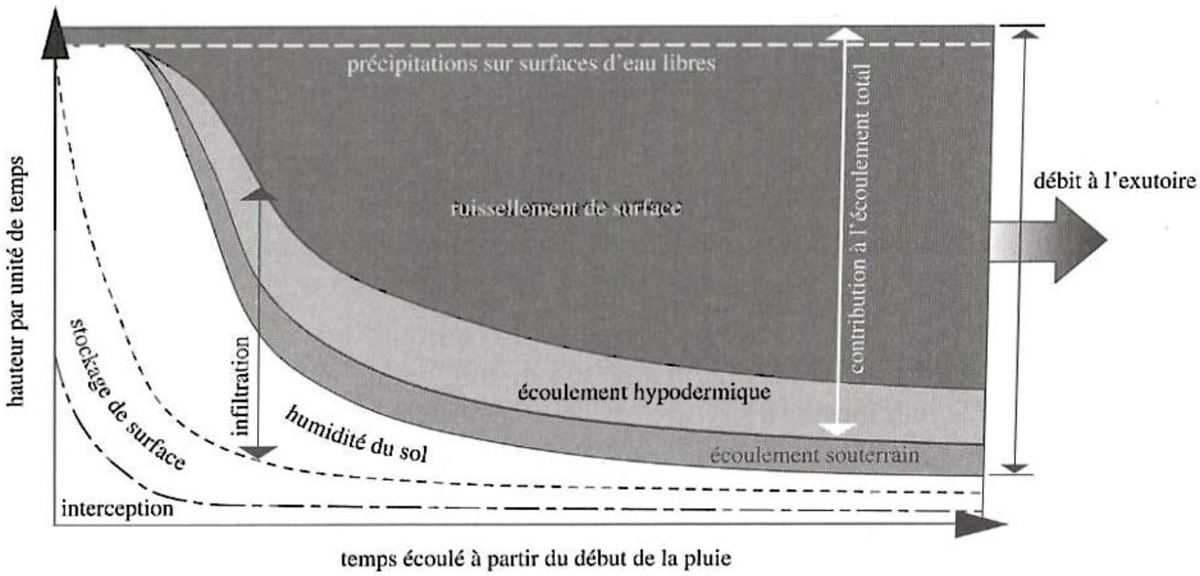

Figure 2 summarises the temporal contribution of the different types of flows that participate in the formation of a flow at the outlet of a natural catchment.

Interception (tree vegetation) and ***surface storage*** (micro-topography, ground vegetation) are important for low rainfall. For intense rainfall generating flooding episodes, they only play a secondary role. This role is even more marginal where vegetation has been lost by fire. The amount of water impacting the soil is then increased by up to 20% compared to a non-fire configuration.

The proportion of ***moisture in the soil*** increases the deeper the soil. In the Mediterranean region, shallow soils are very often found, where soil wetting reaches a saturation level quite quickly after the onset of rain.

In the Mediterranean context, the share of ***surface runoff*** predominates, especially for intense rainfall. Following a fire, this runoff is even greater and occurs more quickly after the start of the rain.

1.3.1.2 IMPACT OF A FIRE ON THE INCREASE IN FLOODING (FREQUENCY AND FLOW)

A wildfire very often changes the hydrological regime of a catchment area because it changes the input parameters:

- The strong decrease in the **interception** effect of crown cover due to its disappearance (and of vegetation more generally) generates greater **effective rainfall** than when vegetation is fully present;
- The **runoff coefficient** is increased because the land use is strongly modified: the disappearance of low vegetation no longer allows for the slowing of runoff, which preferentially runs down any slope rather than partially infiltrating the soil;
- Potential **hydrophobicity** of the soil[3] (a **crust of cinders** generated by the percolation of organic waxes from the burning of plants) which strongly reduces the infiltration capacity of the soil;
- The **"splash" effect** of raindrops that strongly impact the soil, aggravated by the lack of any interception. This "splash" effect contributes to the formation of a crust, which considerably reduces the infiltration potential of the soil: whereas in a non-porous and loose soil, infiltration is of the order of 30-60 mm/h, with a crust this infiltration is heavily reduced, with values as low as 2-6 mm/h, i.e. 10 times less;
- **The washing away of the humus layer** in the case of a litter fire, which reduces the retention capacity of rainfall, and thus aggravates runoff (*Combes, 1990*);
- Decreased runoff **concentration time** due to increased runoff velocities on bare soil.

The lessons learned from the experimental catchment areas of the *Rimbaud* (sub-catchment area of 1.46 km^2 of the *Réal Collobrier*, VAR *département*, LAVABRE *(1992, 1996, 1997))* allow for a better understanding of the evolution of runoff phenomena and their impact on the hydrological regime.

Thus, following a fire in August 1990, which led to the disappearance of almost 85% of the Mediterranean-type plant cover (scrub, cork forest, sweet chestnut trees, maritime pines on weathered gneiss soils, fine and sandy soils) of the small *Rimbaud* catchment area, which has been equipped with measuring instruments and observed by CEMAGREF since 1967, the following consequences were observed:

- **sediment entrainment**, although surface runoff only generated the beginnings of gullies a few mm to a few cm deep; no bank undermining was observed;
- **increased peak flows**: the 10-year return period flow (estimated before the fire) was exceeded three times in the post-fire **year**, with average rainfall values. Paradoxically, these flows were not associated with intense rainfall events. The monitoring of rainfall and hydrometry led to the conclusion that after a fire, a rainfall with a return period of one year is sufficient to generate a peak flow with a return period of 10 years (estimated before the fire).
- a **decrease in the time of concentration of flows**. After the fire, the hydrological response of the basin was extremely sudden. The runoff response of the basin was almost concurrent with rainfall. The recession was also much faster than before. However, within about 2 years of vegetation recovery after the fire, this effect had disappeared.

[3] The phenomenon of hydrophobicity is very often mentioned in English-language studies on large coniferous fires and on homogeneous soils with a significant silty fraction. In a Mediterranean context, on rather coarse and gravelly soils, this hydrophobicity phenomenon seems less prevalent. A DGPR 2022-2023 action sheet is being drafted to assess the relevance of taking this phenomenon into account.

- an **increase in runoff coefficients**. In a Mediterranean context (*Réal Collobrier, Lavabre 1992*), the annual runoff rate in areas affected by fire can be **25% to 30%** higher than the reference situation before the fire.

  The study by *Lavabre (1992, 1997)* – *Figure 3* – even shows that flows for 24-hour rainfall of less than 100 mm (typically a 10-year rainfall) can increase by a factor of up to 3 between the pre-fire and post-fire flow values. In contrast, for heavy rainfall, there is no marked impact on flows.

  These results may be subject to several interpretation biases:

  - for heavy rainfall (> 100 mm): there are very few data in the post-fire situation; ultimately, there are only two rainfall episodes with which to build a trend. Furthermore, a threshold effect of the hydrological response before fire is observed from a daily rainfall of 140 mm.
  - For moderate and low rainfall (< 100 mm): the comparison is made with daily rainfall. However, for this small catchment area (1.46 km^2), runoff is very much linked to the maximum intensity of rainfall. Indeed, 100 mm of rain falling in one day will cause much less runoff than 100 mm of rain falling in a few hours. As *Figure 3* does not make this distinction, the **factor of 3 should be taken as a maximum**, as it is not known whether comparable quantities are being considered.

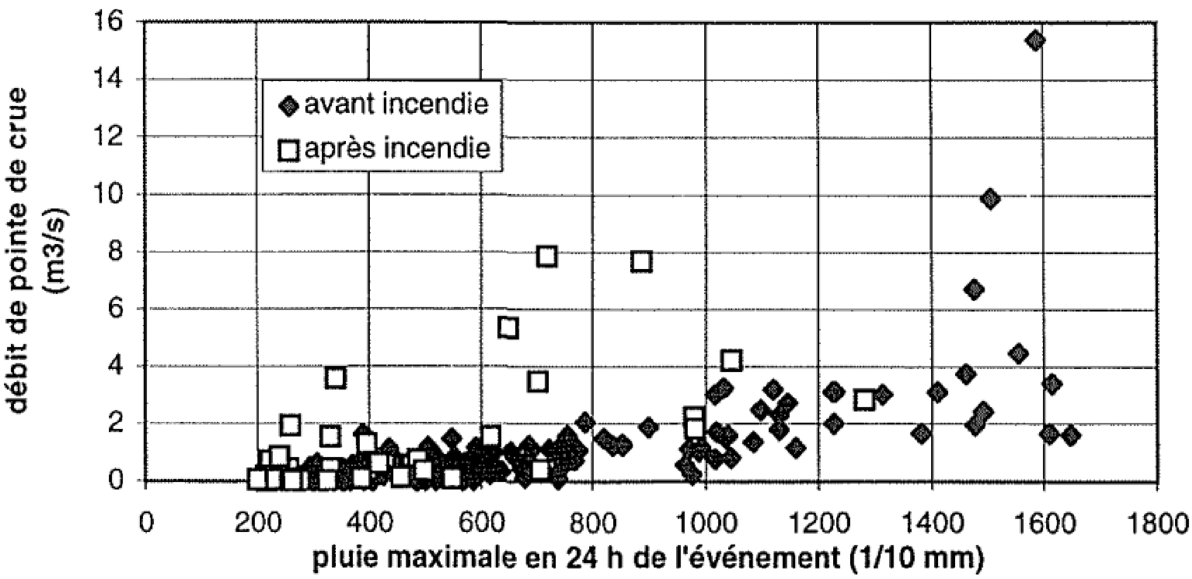

Figure 3: Relationship between peak flood flows and the 24-hour rainfall that caused the flood – from Lavabre, 1997

The more intense the rain, the greater the runoff: there will be more runoff following a short, violent storm than with long, not very intense rainfall (*Combes, 1990 "Après le feu...la boue"*).

Another study (*Shakesby; 2006*) moderates the increase in flows for heavy rainfall, estimating it at 30%. This is logically explained by the fact that for heavy rainfall, a high proportion of the precipitated water has already become runoff (this is the threshold effect observed in *Figure 3*).
Figure 4 compares runoff before and after a fire according to vegetation type. However, this graph does not provide information on the severity of the fire.

For example, for a stand of Ponderosa pine in Arizona (1), the infiltration capacity changes from 60 mm/h before fire to 35 mm/h after fire.
In holm oak stands in Spain, infiltration capacity remains almost constant. The impact of fire on increasing runoff is therefore not demonstrated in this case.
In conifer stands in Washington State, the impact of fire appears to be very strong on the modification of the infiltration capacity (by a factor of three):

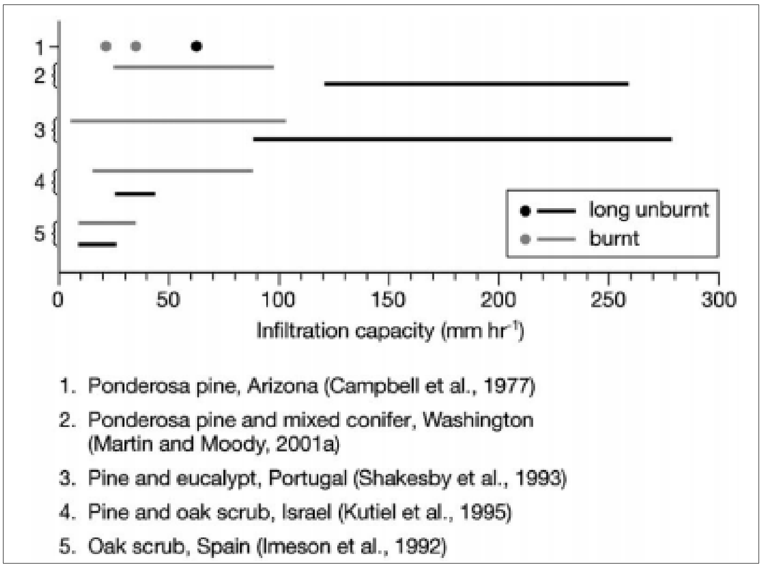

Figure 4: Infiltration capacities measured after a forest fire and on comparable unburned land, according to different authors. The lines represent ranges of values, and the dots represent individual values – from Shakesby, 2006

1.3.2 EROSION AND GULLYING

1.3.2.1 MECHANISMS OF SOIL DESTRUCTION

Fire, depending on its intensity, will change the properties of the soil in several ways:

1. **The formation of a carpet of ash on the ground**. Depending on the intensity of the fire, the ash produced can be either black to a thickness of often less than 1 cm (coals formed during a low-intensity fire) or grey-white to a thickness of up to 20 cm (fine, light ash from a high-intensity fire). Ash changes the porosity of the underlying soil in different ways: black, rather coarse ash remains porous and does not form a screen over the ground. In contrast, very fine grey ash clogs the soil interstices more quickly and effectively (*Woods, 2008*).

2. **Modification of the impermeability of the upper soil stratum** (generally to a depth of less than 6 cm) through the formation of a hydrophobic layer (MACDONALD, 2009). The hydrophobic nature of the soil caused by fire is often the main cause of increased runoff. Fire temperature is a critical factor in increasing the hydrophobic nature of post-fire soil (*DOERR, 2006*). In the case of deep, coarse-textured soil covered by scrub[4] and/or coniferous vegetation, the impact of the fire (for a duration of between 5 and 20 minutes) is as follows:

[4] The 2006 DOERR study focuses on "chapparal" soils, which are a type of scrub and bushland found in California, northwestern Mexico and the Mediterranean. This ecosystem belongs to the category of Mediterranean forests, woodlands and scrubland.

- If the soil temperature remains below 175°C, the fire does not change the composition of the soil much and it does not become more hydrophobic than before;
- If the soil temperature reaches values between 175°C and 200°C, the organic matter turns into wax, which clogs up the interstices of the soil, considerably increasing its hydrophobic nature. The rate of runoff then increases sharply;
- If the temperature reaches 280°C - 300°C or more, the top layer of soil disintegrates and the hydrophobic layer is formed underneath.

3. **Alteration of the surface soil structure**. In comparison, fire acts 10 to 100 times more intensely than frost in the long term to fracture rocks (*SHAKESBY, 2006*). Burnt soils become friable and much less cohesive, which generates a large quantity of fine materials (*COMBES, 1990*) that can be washed away by moderate and heavy rainfall. The most intense fires can destroy at least 80% of the surface layer and litter (MACDONALD, 2009).

Figure 5 summarises these mechanisms of soil degradation following a fire.

- In case (A), of a soil with a fairly impermeable tendency (strongly hydrophobic) that has not been burned over, the forest litter favours water retention, as do the cracks and preferential pathways created by the root systems. With the rainwater being retained in this way, the surface elements are not so strongly washed away;
- After a low to moderate intensity fire (B), the litter is consumed, releasing organic waxes that clog the preferential pathways of cracks and root systems. The soil becomes even more hydrophobic. There is no longer any surface litter to buffer the impact of raindrops and the risk of fine particles being carried away becomes significant.
- The passage of a high-intensity fire will cause the same damage as a moderate-intensity fire, and will also "bake" the surface layer of the soil. As long as the rainfall intensity remains moderate (C), the baked soil, which has become wettable, will buffer the runoff and limit the removal of material. On the other hand, as soon as the runoff becomes too high (D), the wettable soil is washed away, eroding large volumes of fine elements.
  The literature does not give an order of magnitude of the rainfall necessary to move from situation (C) to situation (D).

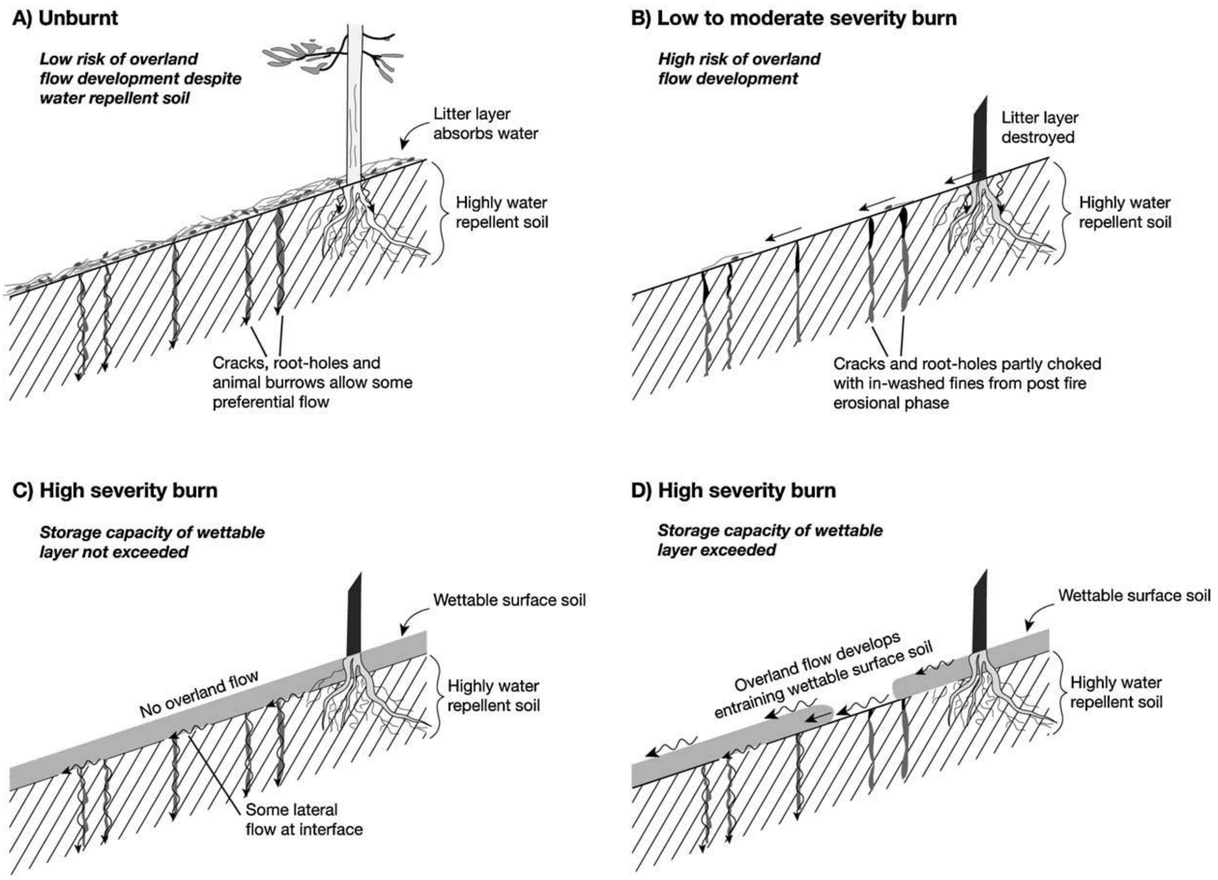

Figure 5: Structural and hydrological changes of the soil after a fire; (A) reference state without fire; (B) soil behaviour after a low to moderate intensity fire; (C and D) severe fire conditions

1.3.2.2 CONSEQUENCES FOR EROSION AND GULLYING

The degree of soil erosion depends on many factors, including:

- The **level of soil destructuring** induced by the heat of the fire (this destructuring being itself strongly linked to the geology, the vegetation cover, the relief, the previous hydric conditions, etc.);
- The **aggressiveness of the rains:** "splash effect", cumulative rainfall and hourly intensities.

Following a fire, the absence of crown cover considerably reduces the interception of rain by trees. The direct impact of raindrops on the soil contributes to a significant splash effect on the soil, which is all the greater when the rain comes from a thunderstorm (*Pietraszek, 2006*) because the drops have a larger diameter (summer thunderstorms, Mediterranean-type rain).

Raindrops falling on the ground produce a "splash effect" that can loosen soil material.

To give an order of magnitude of the aggressiveness of the splash effect, a rainfall equivalent to a 1 mm of water falling at a distance of 10 cm from the ground can loosen up to 10 grams of material per m^2 of soil, i.e. about 100 kilograms of soil per hectare. The splash effect is one of the main processes of hydraulic soil erosion. Even in the absence of runoff, it is likely to cause the creep of sedimentary particles. The larger the raindrop size, the stronger the splash effect: it is most evident during summer thunderstorms.

Given the many factors that control the degree of soil erosion, it is very difficult to estimate sediment production immediately after a fire. Some publications report erosion values:

- *Ballais, 1992*: Sainte-Victoire mountain (PACA Region)
  The bedrock is mainly limestone and the soils are composed of clays and marls. Measuring soil erosion from instruments (grade nails) installed immediately after the August 1989 fire, 650 times more water erosion was observed on burnt soils than on unburnt plots. The time required for morphodynamic stabilisation is experimentally evaluated at 1 year, considering the rather low rainfall. In the case of normal or excess rainfall, the study indicates, on the basis of bibliographic references, that equilibrium would rather be reached about 4 and 5 years after the fire.

- *Martin, 1993*: Massif des Maures – *Réal Collobrier* catchment area
  The bedrock is essentially made up of crystalline rocks (gneiss, micaschist, phyllades). There were already instruments installed on this catchment area (Cemagref hydrological study), which makes it the site with the richest rainfall record in the literature. The erosion study carried out after the fire of August 1990 concerned the quantitative monitoring of the sediment fill of the DFCI's reservoirs and the study of dedicated erosion plots.
  The specific degradation rate was more than 1500 t/km^2 over one year (1990-1991 season). In subsequent years, this rate decreased sharply.
  The fire caused a dramatic increase in soil erosion:
    - fine load: the before/after ratio was in the order of 1:100 to 1:5000.
    - coarse load: the before/after ratio was in the range of 1:600 to 1:3500.

  Soil losses on the small burnt catchments were higher than those observed on the burnt erosion plot. On the latter (area of 75 m^2 sloping at 11°) the measured soil loss was 883 t/km^2 on stony soil (gneiss and micaschist) during the first year after the fire. In comparison, on unburned woodland, there was hardly any soil loss.
  This publication gives erosion values following fires in different contexts:
    - an example in Arizona from 1959 (scrub type vegetation), the specific degradation rate is increased by a ratio of 1:400 (production of 19.5 t/km^2/year before fire versus 8400 t/km^2/year after fire). In some areas, the specific degradation rate even reached values of 25,000 t/km^2/year;
    - an example in the Australian Alps, the rate of specific degradation increased by a ratio of 1:100.

- *Lavabre, 1997*: Massif des Maures – *Réal Collobrier* catchment area
  This publication complements the previously mentioned study (*Martin, 1993*) with a longer analysis period to assess the effect of vegetation recovery on erosion reduction. This publication also specifies the specific degradation rates by year:
    - 1 year after the fire (1990): 569 t/km^2/year;
    - 2 years after the fire (1991): 66 t/km^2/year;
    - 3 years after the fire (1992): 76 t/km^2/year.

- *Shakesby, 1996*: Northern Portugal, pine and eucalyptus forest
  Soil losses for rather wet conditions (above normal rainfall) after a fire were:

	Number of years after the fire		
Type of forest	**1 year**	**2 years**	**3 years**
pine	6.73 t/ha	9.47 t/ha	-
eucalyptus	-	14.37 t/ha	2.88 t/ha

The literature indicates that alluvial production immediately after a fire can be increased on average by a range of ratios between 1:100 and 1:400.

This excessive sediment production occurs immediately after the fire. The soils, after the surface part has been washed away by the rains, return to their original sedimentary "equilibrium" 5 years after the fire (*BALLAIS, 1992*). This equilibrium is recovered all the more quickly because short vegetation quickly colonises the burnt soil. Sediment production can be divided by 8 after 3 years (*LAVABRE, 1997*).

Figure 6 summarises the temporality of the processes involved in the modification of sediment production after a wildfire, and then illustrates the mechanisms for returning to the pre-fire equilibrium.

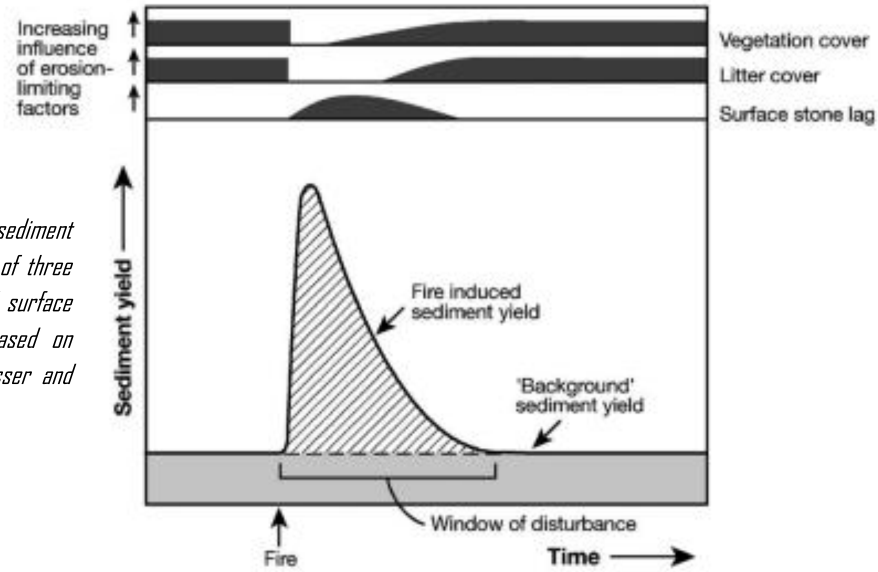

Figure 6: The hypothetical decline in sediment production after a forest fire and the role of three factors (vegetation cover, litter cover and surface stone lag) in reducing erosion rates (based on Swanson, 1981; Shakesby et al., 1994; Prosser and Williams, 1998).

2 METHODOLOGY USED

2.1 THE OBJECTIVES

Many publications deal with **changes in the hydrological regime after a fire**. Several configurations (soil type, slopes, vegetation) were analysed, and it was found that in the majority of cases post-flood flows are significantly increased. This increase is in a wide range between +30% and +800% (*Lavabre 1992, 1996, 1997; Shakesby 2006*). This range is based on a compilation of post-fire analyses from different countries (USA, AUSTRALIA, SPAIN, PORTUGAL, FRANCE) and a multitude of configurations. It does not specifically consider the impact of fires in the Mediterranean context.

In parallel, several publications (*Ballais, 1992; Martin, 1993; Lavabre, 1997; Shakesby, 1996*) have analysed **sediment production after a fire**. The values vary greatly depending on the configuration of the sites (geology, type of vegetation, rainfall context). Some publications mention an increase in water erosion by a ratio of 1 to 650 between the pre-fire and post-fire situation, with a return to normal after between 1 year (low rainfall) and 5 years (high rainfall). Other publications, in different contexts, suggest an increase in water erosion by a ratio of 1 to 6000, with sediment production rates highest in the year following the fire and decreasing up to 3 to 5 years after the fire.

The objective of this study was to use measurements to quantify very precisely the impact of a fire on the modifications of the hydro-sedimentary regime, in a configuration frequently encountered in the PYRÉNÉES-ORIENTALES *département*: wooded scrubland on predominantly shale.

2.2 THE EXPERIMENTAL APPROACH

Feedback and the literature on the change in hydrology after a fire indicate that runoff is systematically increased immediately after the fire. But the runoff multiplier coefficient in relation to a reference situation fluctuates greatly according to the sources, and is sometimes not well suited to the context of Mediterranean forests.

The most appropriate scientific reference concerns experiments carried out as part of a study on a catchment area burnt in 1990 (*Réal Collobrier catchment, Lavabre, publications from the 1990s*).

Locally, in the PYRÉNÉES-ORIENTALES *département*, there has never been an attempt to quantify erosion after a fire. The MONTCLIMA project, which can provide precise measurements of these phenomena, makes it possible to acquire detailed and local knowledge on this problem of soil erosion. This knowledge is possible thanks to hydro-sedimentary monitoring on erosion plots installed for this project.

2.2.1 SELECTED PRINCIPLE OF MEASURING INSTRUMENTATION

Determining the variables to be measured is an **essential prerequisite for the proper construction of the experimental set-up**, in terms of both the sizing of the equipment (collector volumes, channel shapes, organisation of the various measurement and "demonstrative" erosion representation modules) and the choice of the measurement range of the various sensors and their level of accuracy.

In the specific case of the CERBÈRE erosion plots, the variables to be measured are:

- the **rainfall** at short time-steps (amount and intensity of the rain);
- the **runoff rate** at short time-steps (flow rate and volume of liquid flows);
- the **quantity of eroded material** (mass of sand and gravel).

In order to have a precise knowledge of the liquid (hydrology) and solid (water erosion) flows, according to the type of land (burnt, not burnt), the instruments were designed to measure two categories of values, as illustrated in Figure 7:

- ❖ **principle of continuous (flow) measurement**:
  - o short time-step rainfall
  - o runoff rates
- ❖ **principle of overall (accumulated) measurement**:
  - o mass of eroded sediment

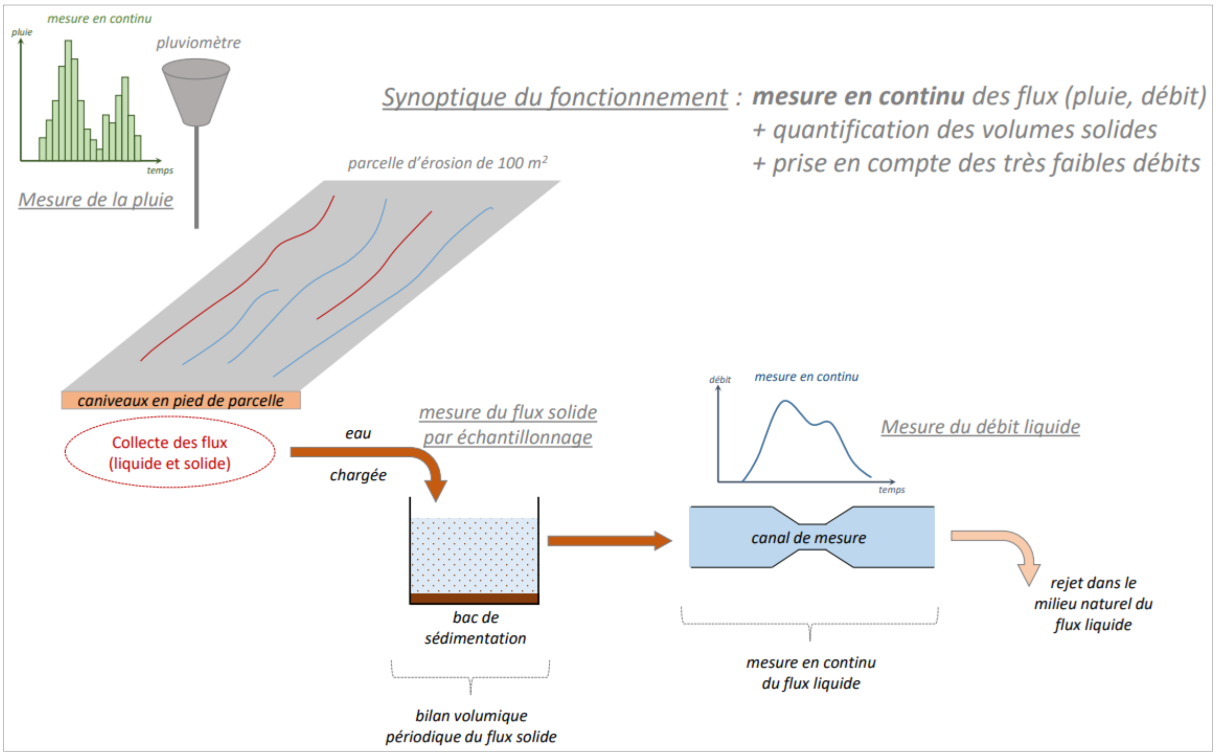

Figure 7: Schematic diagram of the operation of an experimental erosion plot

To easily demonstrate the impact of a fire on the increase in runoff and erosion, three experimental plots were established in order to be able to compare the different measurement results:

- ❖ 1 plot of shrubby scrubland that had been burnt over (**FIRE PLOT 1**);
- ❖ 1 plot of dense shrubby scrubland that had been burnt over (**FIRE PLOT 2**);
- ❖ 1 plot of dense shrubby scrubland, not burnt (**CONTROL PLOT**).

2.2.2 SITE SELECTION

The effects of fire on hydro-sedimentary soil changes can be assessed in two different ways:

- **possibility 1**: **ARTIFICIAL FIRE**
  An unburned site is selected and then one or more prescribed burns are carried out to "simulate" a wildfire. This makes it possible to choose the site in advance with several advantages: ease of access, land ownership issues, choice of slopes, choice of geology, choice of rainfall context, sufficient time to order the equipment, etc.).
  The set-up is then ready to be deployed as soon as the artificial fire passes, so that the variables can be measured immediately after the fire.
  However, an intentional fire is considered **a low-severity fire** and does not have the same effects on soil as an actual wildfire. With a lower temperature, it does not impact the soil and vegetation as much as a real fire would.

- **possibility 2**: **REAL WILDFIRE**
  A real wildfire is often of moderate to high severity and has a significant impact on the soil. It represents reality. The difficulty in instrumenting plots for this type of fire is that the set-up must be adapted rapidly to suit the location of the fire and that it is often not possible to install equipment immediately after the fire: difficulties linked to land ownership, access, implementation, etc.
  It may take 1-2 months after the fire to become operational. This timeframe is highly dependent on the location of the site and the land ownership.

For this project, in order to assess the reality of the phenomena as accurately as possible, we chose to **instrument plots after a real fire**.

In order to be able to respond as quickly as possible, all the equipment was designed and sized during the summer/autumn of 2021, **in anticipation** of a fire that might occur.

This **"opportunistic" strategy** required the pre-identification of interesting sites to be equipped with measuring instruments.

The pre-identified sites, according to their geological, rainfall and relief characteristics and their susceptibility to fire were, in order of priority (Figure 8): Côte Vermeille / Albères / Fenouillèdes / Bas Vallespir / Aspres / L'Aude – Corbières Alaric.

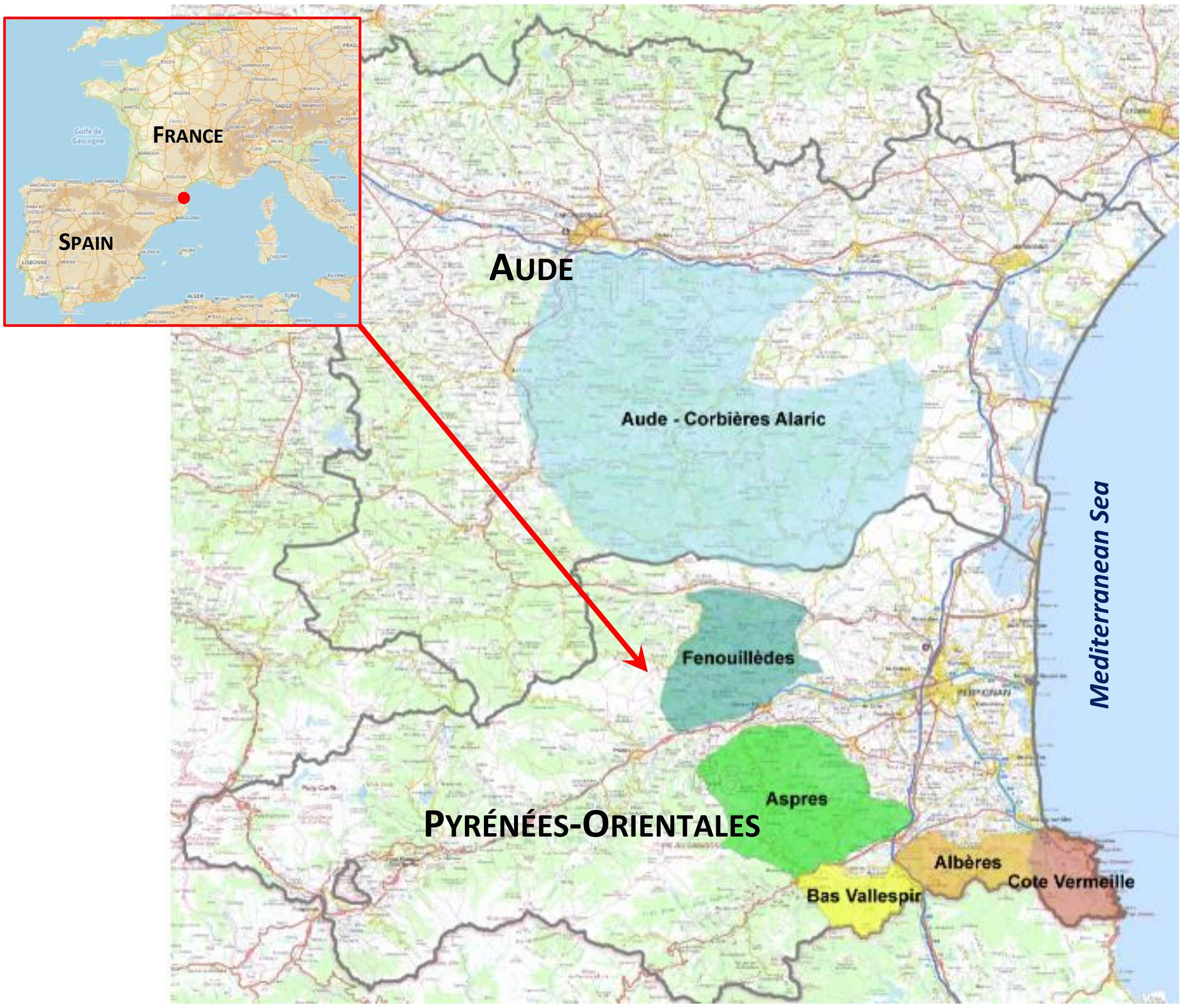

Figure 8: Location of possible sites to be equipped with measuring instruments in the event of a fire

The Côte Vermeille is a suitable experimental site because of the high likelihood of hydraulic risks induced by wildfires, to which the area is particularly vulnerable (Mediterranean vegetation, human activities, wind regime, significant slopes, schistose soils), as well as containing densely built areas and features.

In the summer of 2021, two fires occurred on the Côte Vermeille:

- the **fire of 16 June 2021 in the commune of PORT-VENDRES** below Fort Béar. This fire affected about 33 ha of scrubland on former agricultural terraces. Access is by footpath only and the land is mainly private;
- the **fire of 31 July 2021 in the commune of CERBÈRE** in the state forest (51 ha). The land is totally State-owned and access is very easy (well served by forest tracks).

The selection of a company to install the instruments was carried out on the basis of the PORT-VENDRES fire, with a site visit taking place on 31 August 2021. However, for ease of access and control of the land, we decided to instrument the burnt land in the commune of CERBÈRE.

On 31 July 2021, in the middle of the afternoon, a fire broke out in the southern part of the commune of CERBÈRE *(Figure 9)*. Driven by a strong tramontana wind, the fire which started along the RD914 road covered 51 ha as far as PORTBOU (10 ha burnt on the French side and 41 ha on the Spanish side).

Figure 9: Timeline of the fire, and resources deployed

(a): Start of the fire on 31/07/2021 at about 5 p.m. from the upper embankment of the RD914 road – horizontal view from the heights of CERBÈRE, Chemin des Vignes;

(b): Development of the fire under strong tramontana where it crossed the French-Spanish border;

(c): Final traces of the burnt areas straddling the French-Spanish border;

(d): Emergency response – an Air Tractor spraying retardant during the spread of the fire;

(e): Emergency response – extinguishing the fire with a water-bombing helicopter;

(f): Emergency response – tactical fire along the embankment of Chemin des Cachalots to slow the progress of the main fire.

The burnt vegetation was mainly composed of heath and scrub (50 ha) and marginally of fairly dense coniferous forest (1 ha). On the French side, all the burnt vegetation was in the managed CERBÈRE state forest. The overall fire severity index was High *(Figure 10)*. During the search for sites to locate the erosion plots, we selected a High severity index *(Figure 11)*.

Figure 10: Cerberus Fire Severity Index defined on the basis of the burning rate of plants

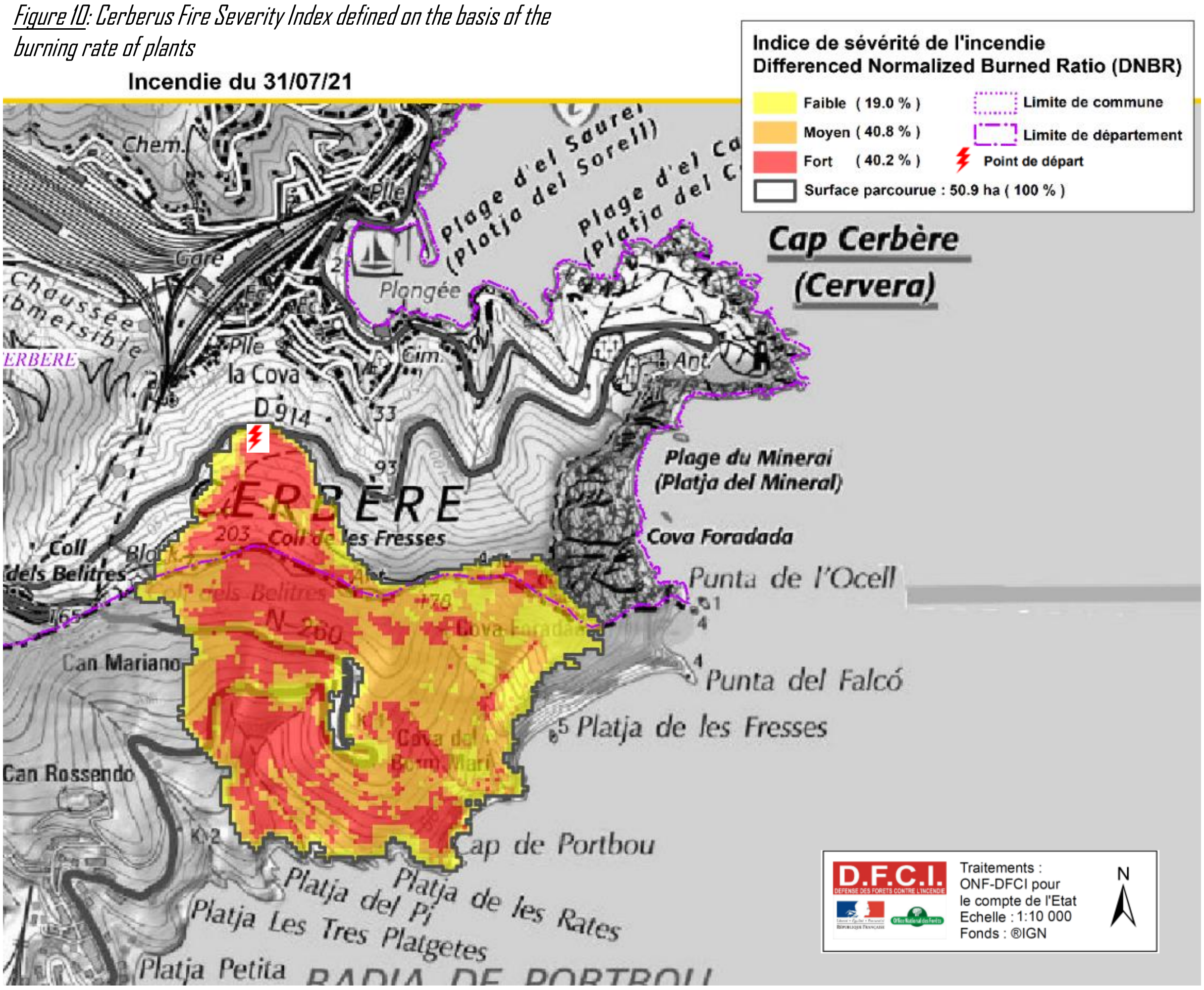

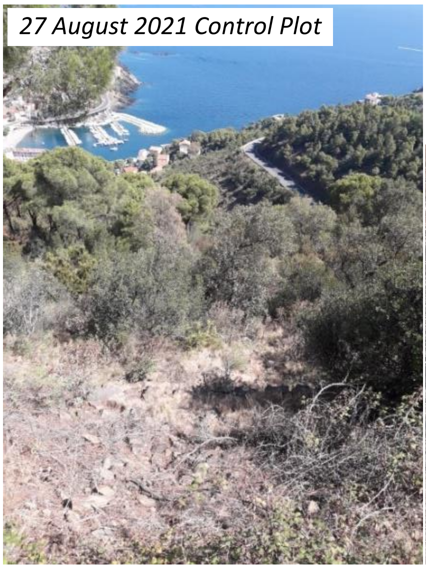

Figure 11: Soil condition before the establishment of the erosion test plots – Fire Plots 1 and 2 were selected for their High severity index

A Digital Terrain Model (DTM) was produced in October 2022 from a LIDAR[5] survey by drone. This DTM provided a detailed description of the topography of the burnt slope and the characteristics of the experimental plots. The shading on this DTM (Figure 12) shows the micro-relief and watersheds. Figure 13 shows the slope values of the hillside.

Figure 12: DTM obtained by LiDAR in October 2022. The acquisition area of this LiDAR survey is marked in red. Outside this perimeter, the DTM represented is that of the RGEAlti (2021 – 1 m steps).

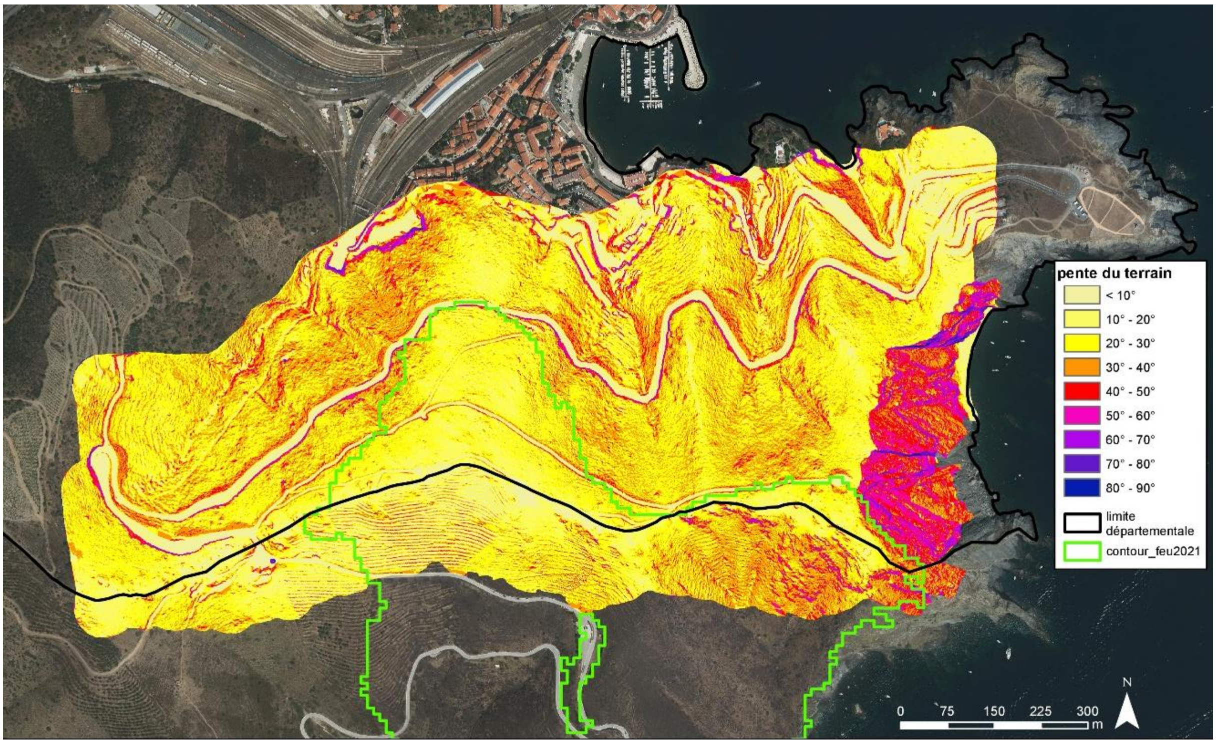

Figure 13: Slope map based on the LiDAR survey (October 2022) – the outline of the 31/07/2021 wildfire is shown in green

[5] LIDAR: Light Detection And Ranging. A remote measurement technique that allows for large-scale topographic surveys (point cloud) with the ability to describe the relief under vegetation.

2.2.3 SIZING OF THE SET-UP

2.2.3.1 QUANTIFICATION OF RAINFALL EVENTS

The quality of erosion measurements over small areas depends heavily on the ability of the set-up to accurately measure rainfall at short time steps, especially so as to be able to properly describe short and intense rainfall events.

Rainfall on the ground can be measured with several instrument technologies:

- Double-chambered bucket rain gauges, which describe the rainfall pattern perfectly, but have great difficulty in describing precipitation totals in the event of hail and snow;
- Weighing rain gauges, which give the water equivalent of all precipitation: liquid and solid. These instruments are suitable for use in remote mountain locations.
- Impact rain gauges, which "count" the number of impacts of drops per second on a rigid surface to deduce an equivalent water depth. The accuracy of this device is sometimes questionable, as the measurement can deviate by up to 20% from the actual rainfall. This system measures solid precipitation (hail and snow) very poorly.

Taking into account the location of the measurement site, and the need to have a good accuracy of measurement of short rains, we opted for a PrécisMéca rain gauge with a mechanical double-chambered bucket, with an opening of 400 cm^2 and an accuracy of 0.2 mm.

For simplicity and cost reasons, as the set-up needed to be visited periodically (at least once every 2 months), we chose not to transmit the data electronically. The records are then downloaded manually at each maintenance visit.

In an ideal configuration, this type of rain gauge should have been set up at each erosion plot. For reasons of economy and consistency of investment, as well as ease of maintenance and proximity of the plots to each other, we installed only one rain gauge, at the centre of the set-up.

Figure 14 illustrates the rainfall patterns that occur at the pre-identified sites. The PrécisMéca PLV400 rain gauge is suitable for measuring these rainfalls, which can be very heavy (> 100 mm/h).

Figure 14: Climatological data and rainfall characteristics from the Aurelhy and Shypre procedures at the different sites considered: Aspres (Caixas), Côte Vermeille (Cap Béar), Fenouillèdes (Força Réal), Albères (Perthus), Conflent (Rodès).

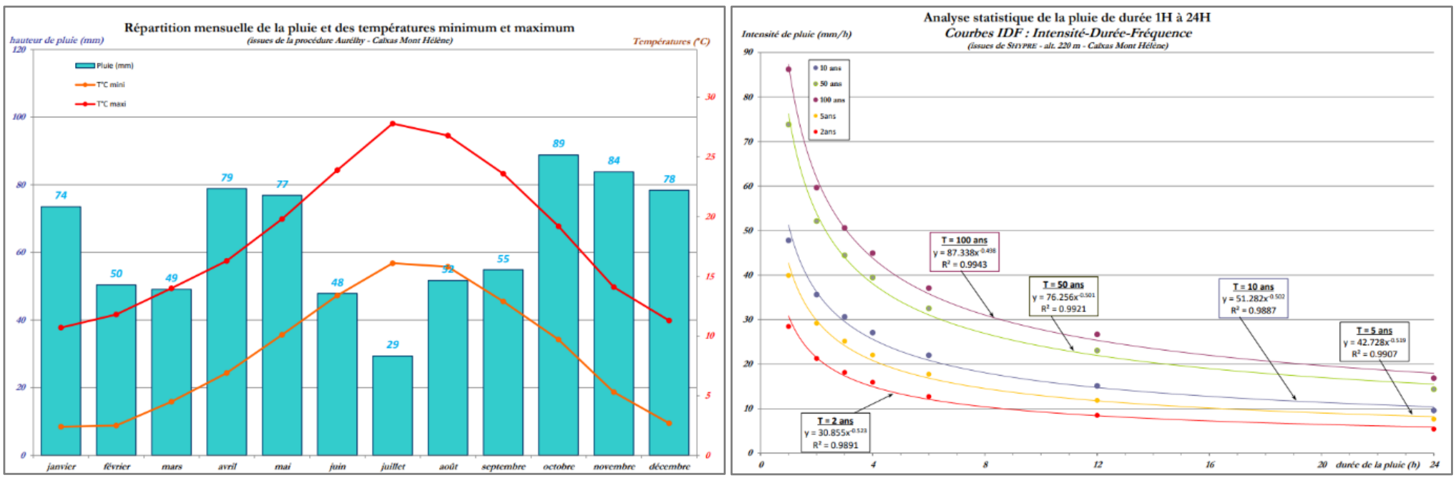

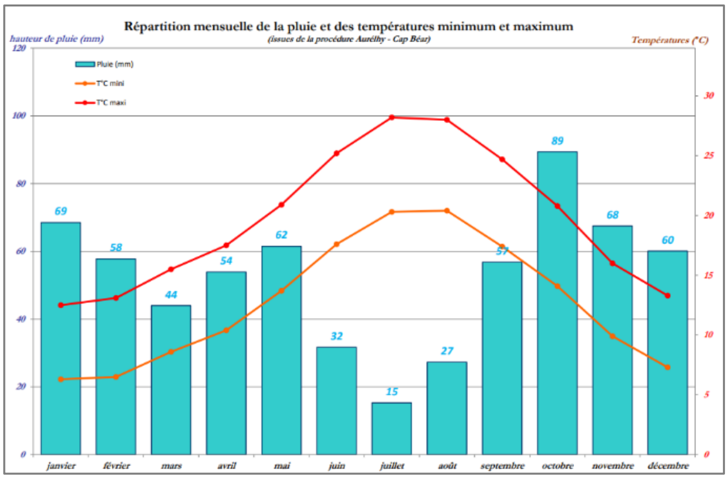
Répartition mensuelle de la pluie et des températures minimum et maximum
(issues de la procédure Aurélhy - Cap Béar)
hauteur de pluie (mm)
Températures (°C)
Pluie (mm)
T°C mini
T°C maxi
69
58
44
54
62
32
15
27
57
89
68
60
janvier
février
mars
avril
mai
juin
juillet
août
septembre
octobre
novembre
décembre

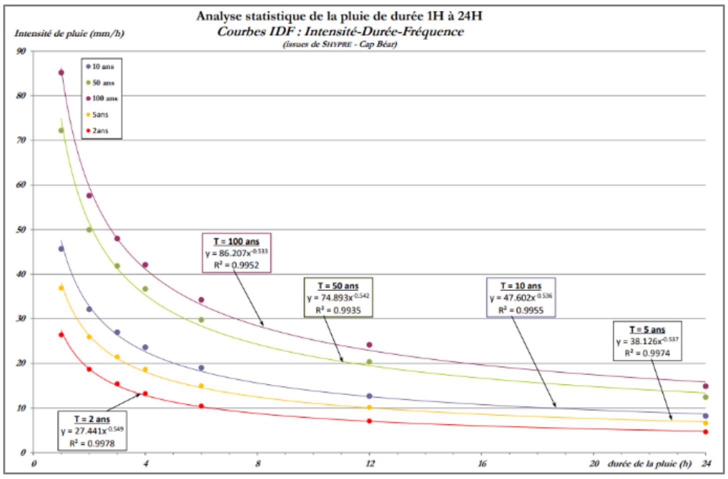
Analyse statistique de la pluie de durée 1H à 24H
Courbes IDF : Intensité-Durée-Fréquence
(issues de SHYPRE - Cap Béar)
Intensité de pluie (mm/h)
10 ans
50 ans
100 ans
5ans
2ans
T = 100 ans
y = 86.207x$^{-0.533}$
R² = 0.9952
T = 50 ans
y = 74.893x$^{-0.542}$
R² = 0.9935
T = 10 ans
y = 47.602x$^{-0.536}$
R² = 0.9955
T = 5 ans
y = 38.126x$^{-0.537}$
R² = 0.9974
T = 2 ans
y = 27.441x$^{-0.549}$
R² = 0.9978
durée de la pluie (h)

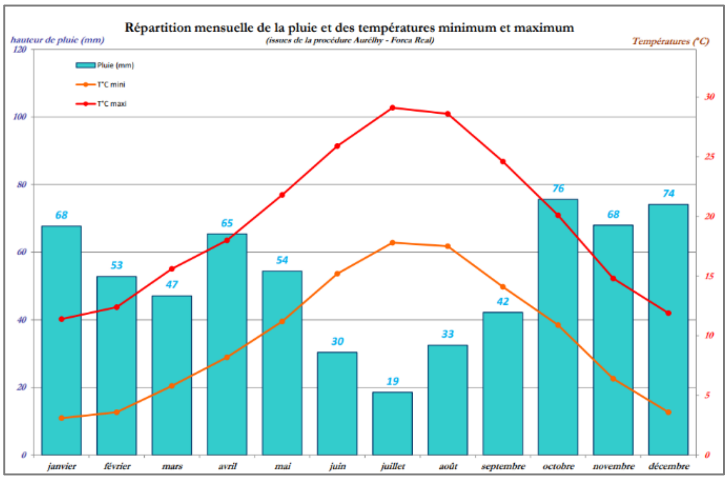
Répartition mensuelle de la pluie et des températures minimum et maximum
(issues de la procédure Aurélhy - Forca Real)
hauteur de pluie (mm)
Températures (°C)
Pluie (mm)
T°C mini
T°C maxi
68
53
47
65
54
30
19
33
42
76
68
74
janvier
février
mars
avril
mai
juin
juillet
août
septembre
octobre
novembre
décembre

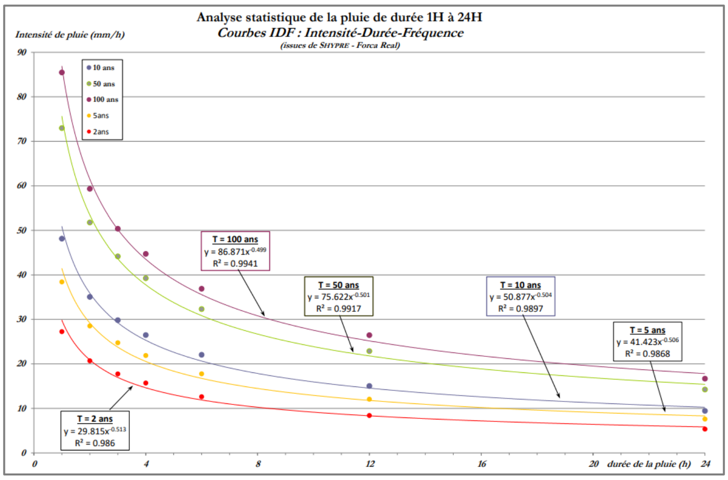
Analyse statistique de la pluie de durée 1H à 24H
Courbes IDF : Intensité-Durée-Fréquence
(issues de SHYPRE - Forca Real)
Intensité de pluie (mm/h)
10 ans
50 ans
100 ans
5ans
2ans
T = 100 ans
y = 86.871x$^{-0.499}$
R² = 0.9941
T = 50 ans
y = 75.622x$^{-0.501}$
R² = 0.9917
T = 10 ans
y = 50.877x$^{-0.504}$
R² = 0.9897
T = 5 ans
y = 41.423x$^{-0.506}$
R² = 0.9868
T = 2 ans
y = 29.815x$^{-0.513}$
R² = 0.986
durée de la pluie (h)

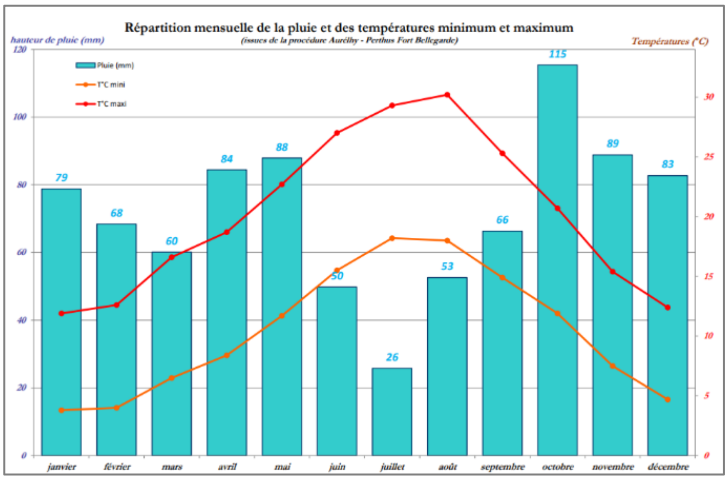
Répartition mensuelle de la pluie et des températures minimum et maximum
(issues de la procédure Aurélhy - Perthus Fort Bellegarde)
hauteur de pluie (mm)
Températures (°C)
Pluie (mm)
T°C mini
T°C maxi
79
68
60
84
88
50
26
53
66
115
89
83
janvier
février
mars
avril
mai
juin
juillet
août
septembre
octobre
novembre
décembre

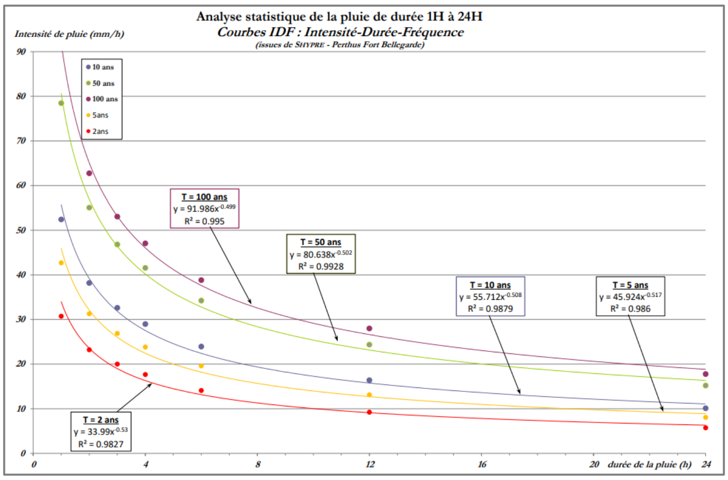
Analyse statistique de la pluie de durée 1H à 24H
Courbes IDF : Intensité-Durée-Fréquence
(issues de SHYPRE - Perthus Fort Bellegarde)
Intensité de pluie (mm/h)
10 ans
50 ans
100 ans
5ans
2ans
T = 100 ans
y = 91.986x$^{-0.499}$
R² = 0.995
T = 50 ans
y = 80.638x$^{-0.502}$
R² = 0.9928
T = 10 ans
y = 55.712x$^{-0.508}$
R² = 0.9879
T = 5 ans
y = 45.924x$^{-0.517}$
R² = 0.986
T = 2 ans
y = 33.99x$^{-0.53}$
R² = 0.9827
durée de la pluie (h)

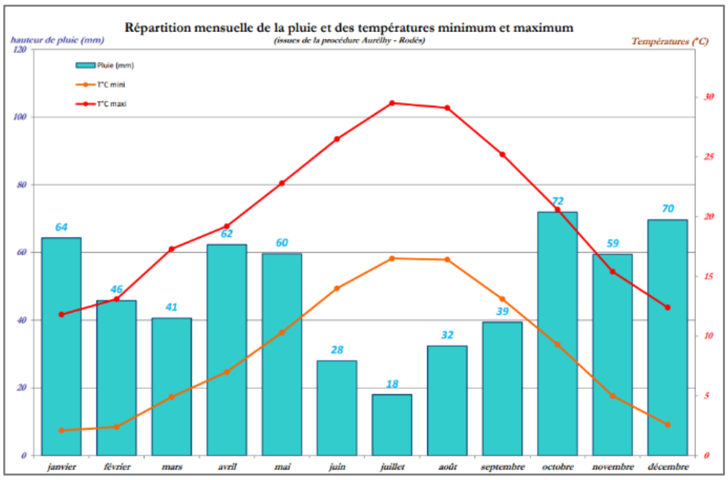
Répartition mensuelle de la pluie et des températures minimum et maximum
(issues de la procédure Aurélhy - Rodès)
hauteur de pluie (mm)
Températures (°C)
Pluie (mm)
T°C mini
T°C maxi
64
46
41
62
60
28
18
32
39
72
59
70
janvier
février
mars
avril
mai
juin
juillet
août
septembre
octobre
novembre
décembre

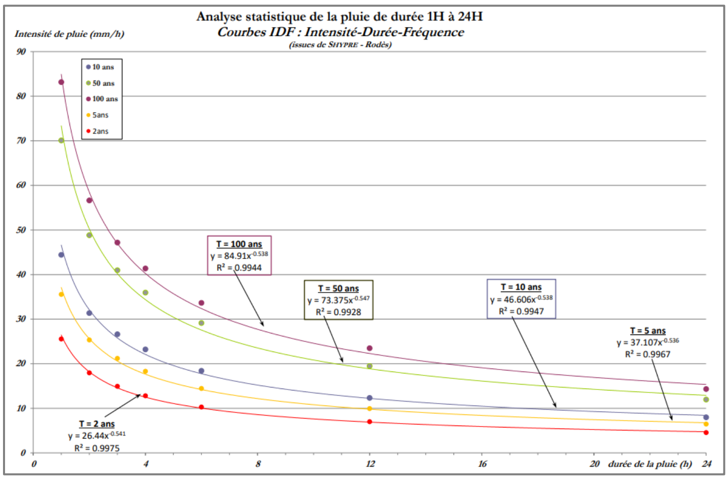
Analyse statistique de la pluie de durée 1H à 24H
Courbes IDF : Intensité-Durée-Fréquence
(issues de SHYPRE - Rodès)
Intensité de pluie (mm/h)
10 ans
50 ans
100 ans
5ans
2ans
T = 100 ans
y = 84.91x$^{-0.538}$
R² = 0.9944
T = 50 ans
y = 73.375x$^{-0.547}$
R² = 0.9928
T = 10 ans
y = 46.606x$^{-0.538}$
R² = 0.9947
T = 5 ans
y = 37.107x$^{-0.536}$
R² = 0.9967
T = 2 ans
y = 26.44x$^{-0.541}$
R² = 0.9975
durée de la pluie (h)

2.2.3.2 QUANTIFICATION OF RUNOFF OF THE PRECIPITATED WATER

For each rainfall event, the quantification of the liquid volume produced by the erosion plot from direct surface gullying is essential data; it indicates the volumes of water involved and ultimately provides an understanding of the capacity of the soils to favour or not favour water flow, as well as the concentration of the materials removed.

These quantifications are based on the integration method, since it was planned to set up erosion plots of approximately 100 m^2 in area. In concrete terms, this means measuring a liquid flow rate. In hydraulics, there are many methods of measuring flow. In this case, the most appropriate way is to measure with a calibrated channel.

This channel can either be assembled directly on site or pre-assembled at the factory. In the first case, the rating curve (water level/flow rate ratio) that needs to be determined depends very strongly on the correct construction of the structure. Measurement campaigns are then necessary for a period of one to several hydrological seasons.

In the second case, the factory pre-calibrated templates allow immediate quantification after implementation on site.

In order to save time for the measurement campaign, **we recommend the solution of a <u>factory pre-calibrated channel gauge</u>**.

In this case, several geometries are possible. They depend on:

- the maximum flow rate that needs to be measured;
- low flows representative of common rain showers;
- the accuracy of the measurements;
- the consideration of the risk of obstruction by floating objects;
- the consideration of any deposits (sand and gravel) that may form;
- ease of installation and maintenance;
- the cost of purchase, installation, commissioning and maintenance.

The most common structures that can meet these requirements include:

- The H-Flume-type channel[6] with its HS-Flume variant;
- The Kafaghi-Venturi-type measuring flume;
- The Parshall-type measuring flume.

Figure 15 provides a comparative overview of the main flow meters that can be used for this study. We should also mention some other less common measuring flumes, such as CUTTHROAT, LEOPOLD-LAGCO, etc., but they do not generally provide accurate measurements of small flows and have therefore been excluded from the comparative analysis of technical options.

[6] *The term H comes from the fact that this geometry corresponds to the eighth design of the flume (H being the eighth letter of the alphabet). This design combines the sensitivity of a thin-walled weir with the self-cleaning properties of a flume.*

	H-Flume	Parshall	Khafagi-Venturi	Palmer BOWLUS	Fluid Tipper
ILLUSTRATIONS					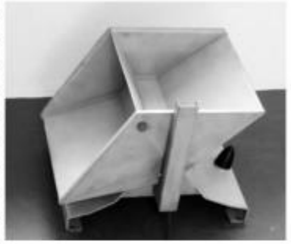
SCHEMAS	Il existe trois types « flume » : 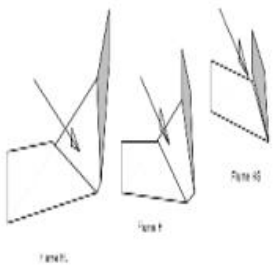 le H-Flume le HL-Flume pour les forts débits le HS-Flume pour les faibles débits Grâce à des géométries différentes, ils couvrent plusieurs gammes de débits.	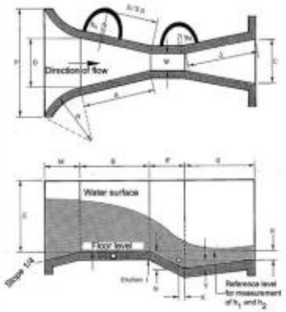 Le canal Parshall fonctionne sur le principe d'un rétrécissement (effet Venturi) combiné à une « marche » en fond. Comme tous les canaux, il permet aux écoulements de passer par le régime critique (de fluvial à torrentiel).	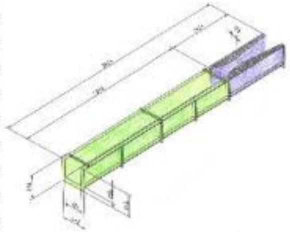 Le canal Khafagi-Venturi possède un fond plat et les écoulements subissent un rétrécissement (effet Venturi pour un passage en régime critique).	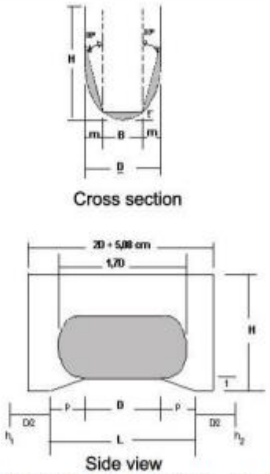 Fonctionnement également sur le principe du régime critique.	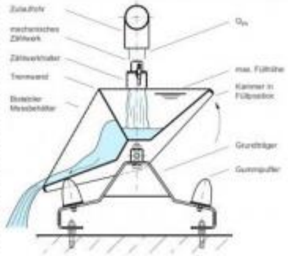 La mesure est basée sur le principe des volumes élémentaires, à l'image du fonctionnement des pluviomètres à augets.
AMPLITUDE DE MESURE DE DEBITS POSSIBLES (SELON MODELE)	• Hs-122 mm : 0,0046 l/s à 2,41 l/s • Hs-152 mm : 0,0056 l/s à 3,96 l/s • Hs-183 mm : 0,0066 l/s à 6,513 l/s • Hs-244 mm : 0,0086 à 13,31 l/s • Hs-305 mm : 0,0105 l/s à 23,22 l/s	• col de 25 mm : 0,13 l/s à 4,38 l/s • col de 51 mm : 0,4 l/s à 8,75 l/s • col de 76 mm : 0,82 l/s à 52,56 l/s	• QV302 : 0,5 l/s à 6,93 l/s • QV303 : de 0,5 l/s à 29 l/s	• diamètre 102 mm : 0,2 l/s à 2,2 l/s • diamètre 152 mm : 0,98 l/s à 8,9 l/s • diamètre 203 mm : 2,1 l/s à 18,96 l/s	• modèle 2 L → jusqu'à 0,25 l/s • modèle 5 L → jusqu'à 0,63 l/s • modèle 10 L → jusqu'à 1,3 l/s • modèle 16 L → jusqu'à 2 l/s • modèle 25 L → jusqu'à 3,1 l/s • modèle 40 L → jusqu'à 5 l/s
Canal d'amenée – caractéristiques	Longueur d'au moins 5 fois la hauteur d'eau maximum. Pente du canal d'amenée < 1 %	Longueur d'au moins 20 fois la dimension du canal d'arrivée d'eau Pente du canal d'amenée < 1 %	Longueur d'au moins 10 fois la hauteur d'eau maximum. Pente du canal d'amenée < 0,2 %	Longueur d'au moins 25 fois la dimension de la conduite d'amenée Pente du canal d'amenée < 2 %	Aucun, principe de la chute
Mage d'erreur renseignée	Le Flume de type Hs permet de mesurer les plus petits débits avec une étendue assez intéressante vers les débits les plus forts et une faible marge d'erreur.	± 3 % à condition d'un strict respect des dimensions de construction et d'installation	± 1 % sur la gamme de débit comprise entre 5 et 100 % du maximum	± 3 % A condition d'un strict respect des dimensions de construction et d'installation	Non précisé par le fabricant
Facilité de construction sur place à partir de plans	Difficulté = moyenne	Difficulté = forte (nombreux plans à assembler)	Difficulté = forte (courbure à respecter)	Difficulté = Forte	Inenvisageable
Prix (hors frais de port et douane)	3 000 $ pour un canal et le capteur de mesure de hauteur d'eau (y compris la batterie et le data logger) Aux USA	Environ 2000 € en europe	Environ 1 000 € en europe	inconnu	entre 1 600 € et 2 300 € H.T. selon modèle

*Figure 15: Possible equipment for measuring small flows – characteristics of each **flowmeter**, its advantages and limitations of use*

2.2.3.3 ESTIMATION OF RUNOFF ON A 100 M² PLOT

In order to choose the most suitable type of flowmeter for the measurement site, it is necessary to accurately determine the characteristic flow rates that can be produced by each plot.

Given the small size of the plots under consideration, it is entirely appropriate to use the **rational method** using the MONTANA coefficients for the study area.

$$\boxed{Q_T = \frac{C_R \cdot i(t_c,T) \cdot S}{3{,}6}}$$

where: Q_T = peak flow of return period T (m³/s)

C_R = runoff coefficient of the basin, function of T

$i_{mm/h}(t_c,T)$ = intensity of rainfall with duration t_c and return period T (mm/h)

S = catchment area (km²)

t_c = time of concentration[7] of the basin (h)

The Montana coefficients related to the rainfall context of the study area[8] are linked by the relationships:

$$\boxed{P_{mm}(t_c,T) = a_T \cdot t_c^{1-b}} \quad \text{and} \quad \boxed{i_{mm/h}(t_c,T) = a_T \cdot t_c^{-b}}$$

where: $P_{mm}(t_c,T)$ = amount of rainfall with duration t_c and return period T (mm)

a_T and b: Montana coefficients of the return period T representative of the rainfall regime at small time steps on the selected site.

As explained in §2.2.2. "Site Selection", we sized the set-up before having made the final choice of the site to be equipped. For this purpose, we carried out sizing on the different sites considered *(Figure 8)*. The Montana coefficients used are shown compiled in *Table I*.

		Caractérisation de la pluie de projet - coefficients de Montana					
		a_{2ans}	a_{5ans}	a_{10ans}	a_{50ans}	a_{100ans}	b
Sites potentiels	Caixas Mont Hélène	30.8	42.7	51.3	76.3	87.3	0.51
	Cap Béar	27.4	38.1	47.6	74.9	86.2	0.54
	ForcaRéal	29.8	41.4	50.8	75.6	86.9	0.50
	Perthus	34.0	45.9	55.7	80.6	92.0	0.51
	Rodès	26.4	37.1	46.6	73.4	84.9	0.54

Table I: Montana coefficients of the rainfall regime at the different sites considered

[7] *The time it takes for the drop of water that falls at the most remote point of the basin to reach the watershed outlet, following the longest hydraulic path.*
[8] *The selected rainfall value is a function of the basin's time of concentration, t_c.*

➤ DETERMINATION OF THE TIME OF CONCENTRATION t_c

With a plot area of approximately 100 m^2 (rectangular plot, 20 m down the slope and 5 m wide), the longest hydraulic path travelled by the runoff will be around 20 metres. This distance corresponds to a very short time of concentration, well below what is usually observed in catchment areas and which can be determined using several different hydrological methods of determining the time of concentration can be used. In the case of such small plots, these methods are outside their respective scope. Indeed, very few formulas have been constructed from very short concentration times. For example, the KIRPICH Formula, which is known to accurately estimate the times of concentration of very small catchments, was determined from a sample of basins ranging from 0.4 ha to 43 ha in size.

For comparison, the erosion plots to be studied have an area of about 0.01 ha, which is 40 times smaller than the smallest sample definition of the KIRPICH Formula.

The only applicable method, which generally gives very satisfactory results, is the so-called "speed method". This is a physically based formula detailed in the book Hydrology (*Musy and Higy, 2004*).

The time of concentration $\mathbf{t_c = t_h + t_r + t_e}$ is the sum of the following three terms:

- **wetting time t_h** → *time needed to saturate the soil before runoff occurs*
- **runoff time on an inclined plane t_r** → *travel time in diffuse flow*
- **flow time t_e** → *travel time in concentrated flow*

The main objective of the erosion plots is to measure **the ablation of the soil surface layer** under the effect of rainfall forcing and according to a defined state of degradation (burnt or not).

The processes related to gullying and concentrated flow do not reflect the ablation variable we wish to quantify. It is therefore important to avoid the occurrence of these phenomena in order not to distort the measurement. The small size of the plots will make it possible to avoid this. Therefore, the flow time t_e is arbitrarily assumed to be zero.

The wetting time is usually between 5 and 10 minutes. This wetting time can be considerably reduced in the following cases:

- rain on very dry ground will be difficult to absorb in the first few moments (as when a trickle of water runs easily at first off a very dry sponge). In the case of a very small area, runoff can travel a significant distance before the land becomes susceptible to infiltration;
- rain on soil that is already saturated with water. In this case, the wetting time is very short before the precipitated water starts to run off.

The **wetting time** is usually between **1 and 5 minutes**.

As far as runoff time is concerned, this corresponds to:

- a flow on an inclined plane with **unconcentrated flows**. In the present case, it is assumed that this type of flow occurs in the first 10 metres. As shown in Figure 16, the corresponding time would be in the order of 1.2 minutes, which corresponds to an average runoff velocity of about 15 cm/s;
- a flow on an inclined plane with **flows beginning to concentrate**. This phenomenon of flow concentration needs to be quantified, as it is largely responsible for materials being swept into the river system. In the present case, taking into account the slope of the land and the

type of soil, an average speed of around 1.5 m/s is assumed. This time corresponds to the 10-metre distance of flow near the bottom. It is very short, of the order of a few seconds (10 s).

The direct **runoff time** on the plot would therefore be in the region of **1 minute**.

Figure 16: Calculation of runoff time according to the physical-based method taken from MUSY and HIGY, 2004.

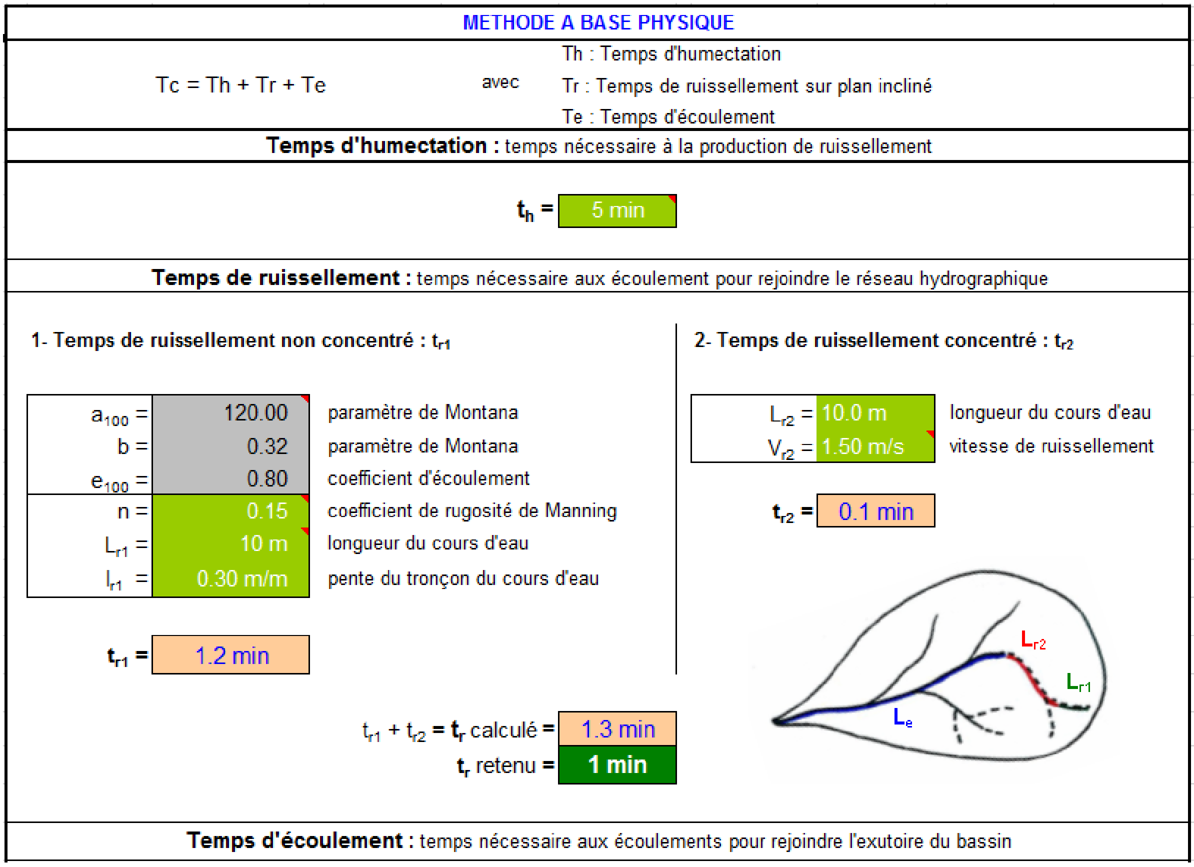

To summarise, the **concentration time** of a 100 m^2 erosion plot, depending on the initial soil moisture conditions, would be between **2 minutes** and **6 minutes**.

- *CHARACTERISTIC FLOW RATES*

Before choosing the instrumentation to be installed (flowmeter geometry and sensor performance), it is essential to specify the range of values expected for runoff from the erosion plot.

The flows to be measured will be generated by both common and exceptional rainfall events. In order to offer the widest possible measurement range, we used **100-year rainfall** as the **sizing** value for the flowmeter geometry.

Meteorological rain gauges rarely provide rainfall characteristics for a time step of less than 6 minutes. In the present case, despite the fact that the time of concentration is much shorter than the minimum time step for the determination of the Montana coefficients, we assume that the latter **are still applicable** for calculating the **order of magnitude** of the rainfall intensity.

Table 2 summarises the rainfall intensities that can be observed for small time steps (< 6 minutes) at the different pre-identified sites, and for several different return periods.

While for the 2-year return period, an average hourly intensity of around 100 mm/h is obtained, for the 100-year return period, a value close to 300 mm/h is obtained.

Table 2: Reference rainfall intensities at pre-identified sites

		Intensité de la pluie de projet				
	intensité pluie (mm/h)	**2ans**	**5ans**	**10ans**	**50ans**	**100ans**
Sites potentiels	Caixas Mont Hélène	100	138	166	247	282
	Cap Béar	95	132	165	260	299
	ForcaRéal	94	131	161	239	275
	Perthus	110	149	180	261	298
	Rodès	92	129	162	255	294

These rainfall intensities result in flows ranging from 0.51 l/s to 6.64 l/s on a drained plot of 100 m^2 *(Table 3)*.

Table 3: Range of runoff rates for pre-identified sites

		Calcul du débit projet selon la méthode rationnelle				
	Débit max (l/s)	**2ans**	**5ans**	**10ans**	**50ans**	**100ans**
	Coef. ruissellement	*0.2*	*0.3*	*0.5*	*0.6*	*0.8*
Sites potentiels	Caixas Mont Hélène	0.55	1.15	2.31	4.12	6.28
	Cap Béar	0.53	1.10	2.29	4.33	6.64
	ForcaRéal	0.52	1.09	2.23	3.98	6.11
	Perthus	0.61	1.24	2.50	4.35	6.62
	Rodès	0.51	1.07	2.24	4.24	6.54
	moyenne	*0.54*	*1.13*	*2.32*	*4.20*	*6.44*
	mini	*0.51*	*1.07*	*2.23*	*3.98*	*6.11*
	maxi	*0.61*	*1.24*	*2.50*	*4.35*	*6.64*

When implementing the set-up, the boundaries of the erosion plots must be adapted to the terrain (micro-relief, trees, rocks, etc.) and some plots may be slightly larger than 100 m^2. The expected flows could then be greater than those previously determined. In all cases, the flows will be below the value of 10 l/s.

The flow rate value of 10 l/s was chosen for sizing the **maximum** measurement **capacity** of the flow meter.

In order to measure all runoff values, it is essential to be able to quantify the very low flows generated by common rainfall events.

Ideally, the measurement range to be considered would be **[0 l/s - 10 l/s]**. However, the measuring instruments (flow meters and sensors) have threshold values that do not allow the measurement of flows close to zero.

Now that the project measurement range has been defined, and considering the different types of flowmeters that can be used *(Figure 15)*, comparing the project measurement range and the measurement ranges offered by the different possibilities of equipment enables the most suitable equipment to be chosen *(Figure 17)*.

Figure 17: Measuring ranges of the different flowmeters in comparison with the desired measuring range [0 – 10 l/s]

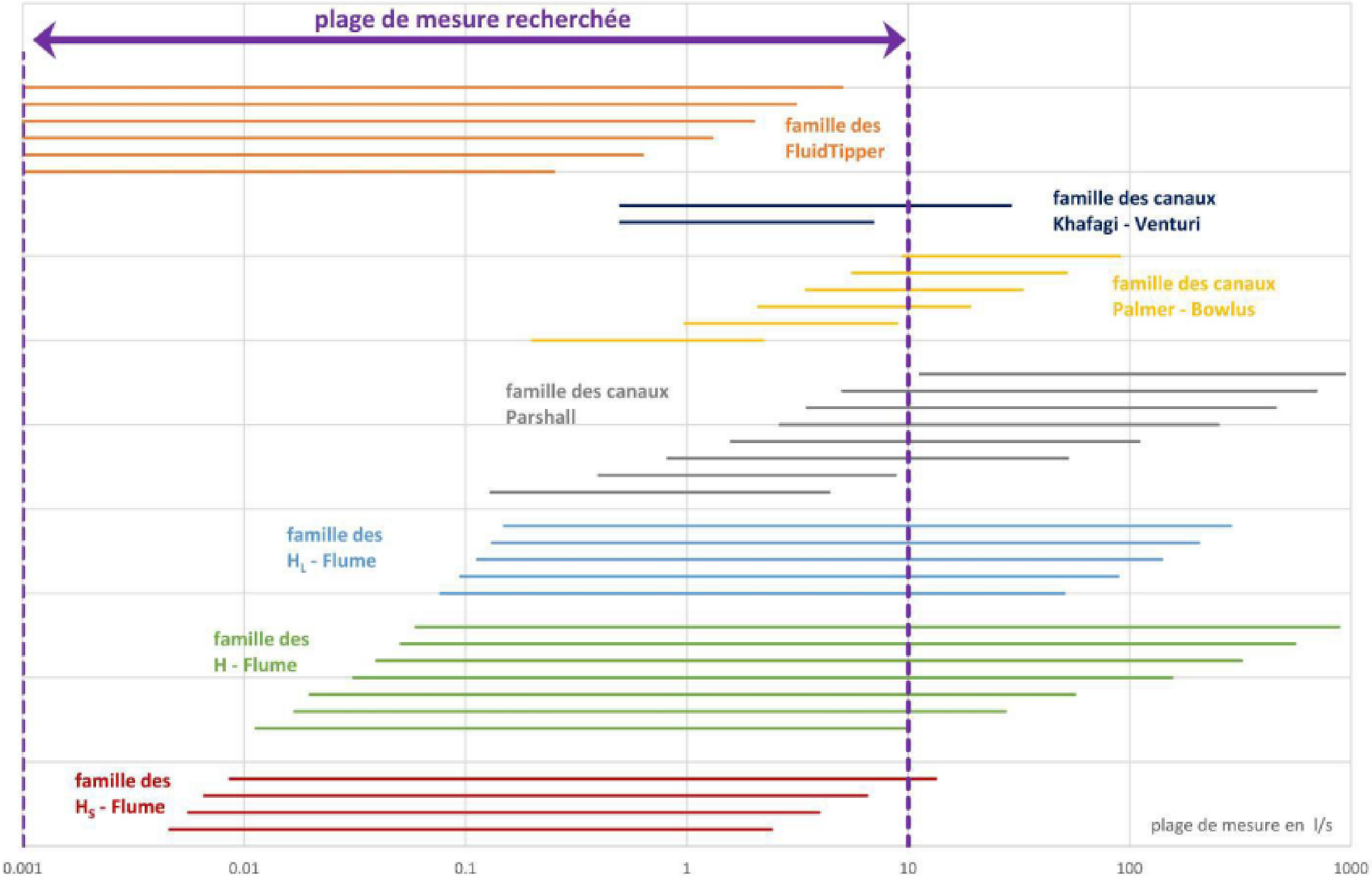

It can be seen that FluidTipper-type equipment (volume measurement using the double-chambered bucket principle) allows very low flow rates to be measured. However, they do not measure flows above 5 l/s, which does not meet our needs.

The HS Flume-type equipment covers the project measurement range to a large extent, except for very low flows (< 0.01 l/s). This type of flowmeter offers the **best measurement compromise**.

In view of the respective measuring ranges of each of the devices shown in the graph above in comparison with the desired range of [0 - 10 l/s], it appears that the 244 mm (0.8-foot) HS Flume model is the most suitable.

Indeed, at 13.31 l/s, the maximum measurement value of this model will ensure that exceptional rainfall is well taken into account. But what is most interesting is the ability of the device to measure very low flows (from 0.0086 l/s[9]).

In order to measure these low flows, the water level probes will need to be very accurate and placed below the level of the sill plate of the HS Flume, ideally in a stilling well.

[9] *To imagine this low flow-rate value, it is equivalent to taking almost 2 minutes to empty a 1 litre bottle.*

2.2.4 CHOICE OF EQUIPMENT AND INSTRUMENTS

The technical choices and specifications of the equipment and instruments are presented below.

2.2.4.1 PLOT BOUNDARIES

➢ *PRINCIPLE*

In order to be able to make accurate hydro-sedimentary measurements, it is essential to know the exact surface area receiving the rainfall. The area defined when constructing the plot must be constant throughout the life of the set-up.

Boundaries are set by laying borders. Usually the borders are sunk into the ground, and it is sometimes necessary to use a mechanical tool to make a thin, clean trench to insert the metal or wooden border plates.

During the installation of the borders, an important precaution must be observed: the installation work must not mobilise sediments, otherwise the erosion measurements would be considerably distorted by the impact of the work itself.

In the case of the CERBÈRE site, the soil is composed of highly weathered shale, with a significant proportion of stones. It is not possible to cut borders without releasing a large volume of material. To avoid this, we chose not to sink the borders, but rather to lay them down and compact them in such a way as to fit the unevenness of the ground.

Figure 18: Boundary lines of the Control Plot – 17/11/2021

➢ *CHOICE OF EQUIPMENT*

In order to fit the shape of the ground, we installed sand-filled, UV-resistant sleeves made from synthetic material *(Figure 18)*. These items were originally used as ballast bags for agricultural tarpaulins.

They are fixed together and held firmly down by steel reinforcing bars (rebars) driven into the ground.

2.2.4.2 RAIN MEASUREMENT

➢ PRINCIPLES FOR MEASUREMENT

The rainfall context of CERBÈRE often involves episodes of heavy rain (> 100 mm/h). The rain gauge in the set-up should allow for accurate measurement of these intense events. The site is also heavily impacted by stormy winds which the instrument will have to withstand.

Less intense events (< 100 mm/h) should also be accurately measured.

➢ CHOICE OF RAIN MEASURING EQUIPMENT

The following material was selected *(Figure 19)*:

- Brand: PARATRONIC
- Type: automatic with a double-chambered bucket
- Model: PLV400; aperture 400 cm^2; 0.2 mm/pulse; without heating
- Stand-alone power supply (battery)
- Data acquisition: 3-channel recorder without remote transmission
- Installed on a builder's prop, guyed with 3 mm diameter cable
- Measurement time-step chosen: 6 min, in line with that usually used by MÉTÉO FRANCE rain gauges
- Acquisition memory capacity for 6 min time step: 67 days

Figure 19: PLV400 rain gauge installed at the CERBÈRE experimental site, photo taken on 30 March 2022

Right::View without cover

2.2.4.3 MEASUREMENT OF RUNOFF

➢ *PRINCIPLES FOR MEASUREMENT*

A flow rate is by definition the ratio of a volume of water per unit of time. This quantity cannot be measured directly. To carry out the measurement, we use a flowmeter, i.e. a gauge with a well-defined geometry that allows us to establish an **unambiguous relationship between the flow rate and the water level** (rating curve). The measurement of the water level alone is therefore sufficient to determine the corresponding flow.

➢ *CHOICE OF FLOW METER (OR MEASURING FLUME OR GAUGE CHANNEL)*

In order to make custom-built flowmeters operational and specific to the topography of a site, it is essential to establish the rating curve. This requires a calibration campaign which can be long (several hydrological seasons), difficult (access and time issues) and onerous (need for personnel to be on site during flood events).

To overcome these constraints, we decided to use **a pre-calibrated HS-Flume gauge**.

HS-Flumes have the following advantages:

- Pre-calibrated at the factory for immediate use, provided that the installation instructions (horizontality, alignment with flows, etc.) are followed;
- No measurement drift as long as the geometry remains unchanged;
- Fairly easy and quick installation;
- Limitation of sediment deposition up to a certain value. The flat bottom makes cleaning easier;
- Modular, with low impact for the environment as it requires little earthwork.

The disadvantages of this type of flume gauge are as follows:

- The specific shape does not allow the installation of a protruding water-level measurement probe, as this would alter the pre-established rating curve; in this case, it is preferable to use a non-intrusive measurement by ultrasound or radar (which uses more power);
- When using a pressure probe (intrusive measurement in the flow), it is necessary to create a measurement well at a specific point in the convergent flow so that the probe does not alter the geometry of the installation;
- It is necessary to add an approach channel to carry the flows in order to obtain a water surface that is little disturbed and easily measurable;
- Horizontality of the equipment must be guaranteed to ensure the correct application of the rating curve.

The HS-Flume model chosen is the "small" version (hence the name HS, "s" for small) with a characteristic size of 0.8 foot (24.38 cm). *Figure 20* gives the geometrical characteristics of this measurement flume.

Figure 20: Standardised dimensions of the 0.8-foot HS-Flume and its approach channel

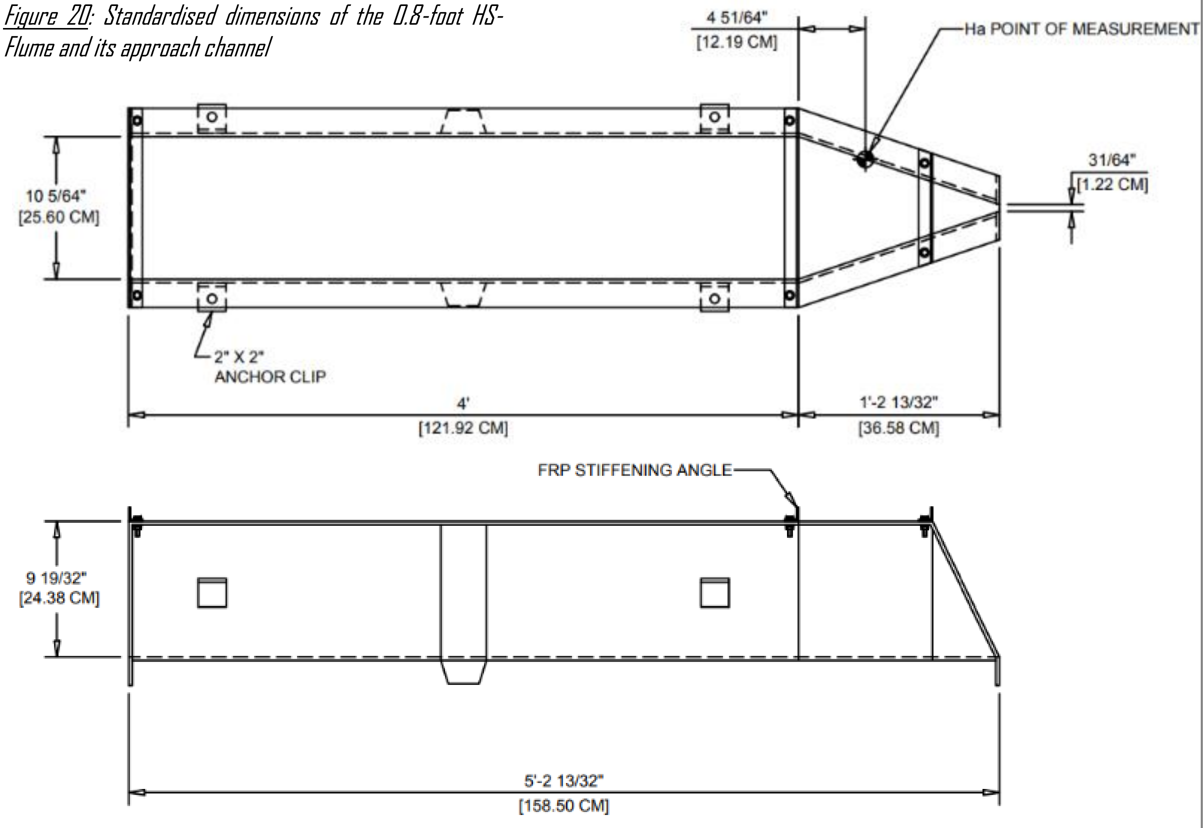

The geometry of the channel is quite simple as it is composed of an assembly of flat walls. It is quite simple to construct from the diagrams in *Figure 20* and *Figure 21*.

Nevertheless, in order to remain faithful to the factory pre-calibrated calibration curve, rigorous attention must be paid to respecting dimensions and angles.

As part of the MONTCLIMA project, the search for H-Flume-type hydrometric equipment led us to a single supplier[10].

However, taking into account the delivery times, the price and difficulties internal to the ONF for importing equipment from the UNITED STATES, we decided to manufacture this flowmeter ourselves *(Figure 22)*.

In order to simplify the construction, we chose 15 mm thick marine plywood as the material.

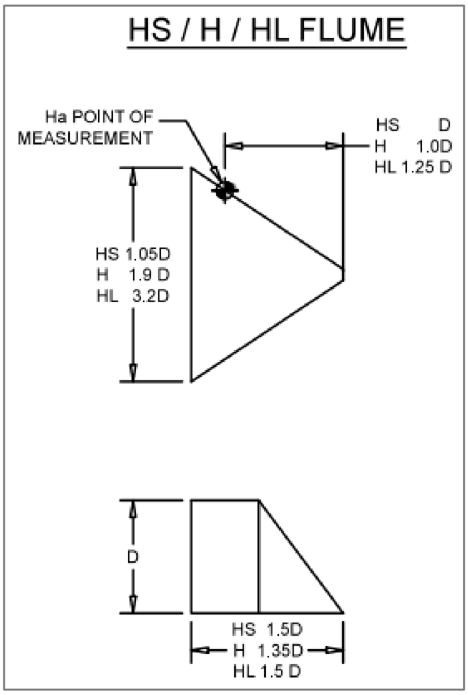

Figure 21: Details of the geometrical characteristics of the convergent and the water-level measurement point to respect the rating curve

[10] https://www.openchannelflow.com

The 0.8-foot HS-Flume has the following specifications:

- Minimum water level for measurement = 0.61 cm
- Maximum water level for measurement = 24.08 cm
- Minimum measurable flow rate = 0.0085 l/s
- Maximum measurable flow rate = 12.94 l/s

For comparison, the 0.6-foot HS-Flume, which is the model just below, has the following characteristics:

- Minimum water level for measurement = 0.61 cm
- Maximum water level for measurement = 17.98 cm
- Minimum measurable flow rate = 0.0065 l/s
- Maximum measurable flow rate = 6.259 l/s

It can be seen that the 0.6-foot HS-Flume does not cover the entire measurement range ([0 – 10 l/s]).

The 0.8-foot HS-Flume is therefore the most suitable gauge for the CERBÈRE erosion plot instrumentation project.

The rating curve for the 0.8-foot HS-Flume is given in *Figure 23*.

Figure 22: HS-Flume and its approach channel were manufactured in-house; the use of plywood reduces costs and facilitates construction.

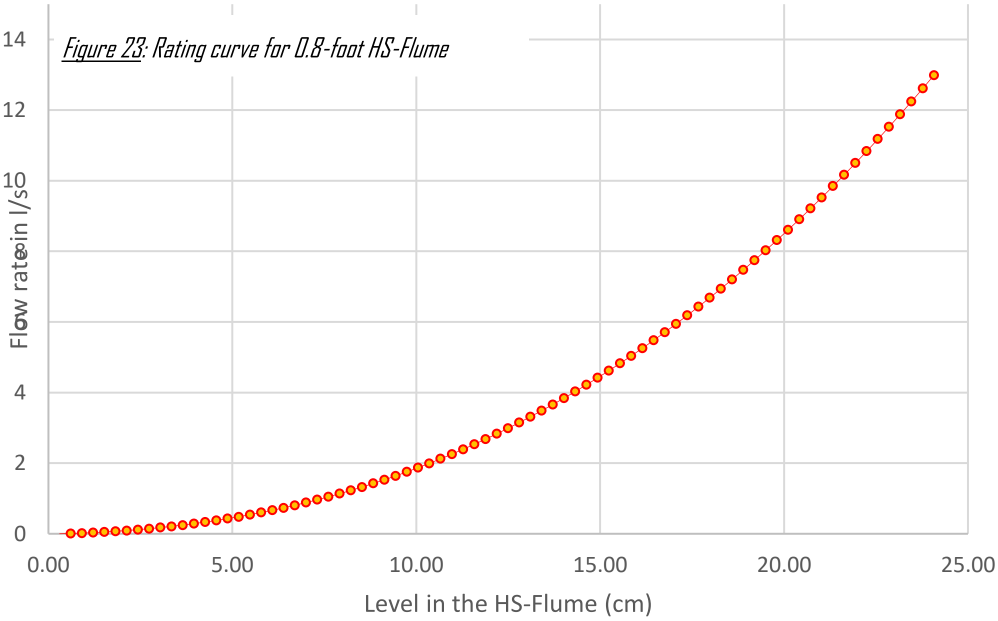

Figure 23: Rating curve for 0.8-foot HS-Flume

➢ CHOICE OF WATER-LEVEL MEASURING EQUIPMENT

The water level in the gauging flume can be measured either manually or automatically.

Given the very short response time of the erosion plots (between 2 min and 6 min), it is essential to carry out automatic measurement at small time steps.

As this is purely a research project, there is no need for real-time data. For this reason, we chose not to transmit sensor data remotely, which simplifies installation (no SIM card costs, no need to install a stand-alone power supply, less risk of vandalism).

There are several types of technology available for automatic measurement: piezometric measurement, non-intrusive ultrasonic measurement, non-intrusive radar measurement. The latter two technologies require the addition of a stand-alone power supply.

In order to simplify the instrumentation as much as possible, with a view to reducing costs and ensuring the robustness of the equipment, we decided to install a water-level measurement probe (piezometric measurement).

The water-level measuring instrument should offer the best trade-off between the following objectives:

- have a measuring range at least equal to the maximum amplitude to be measured (from 0 to about 30 cm);
- permit precise measurement (in the order of mm);
- have a very low drift over time (deviation from calibration);
- have a high degree of autonomy in terms of power and logging memory (several months);
- be sufficiently robust for installation in a natural environment (resistant to high temperatures, rapidly sweeping fire, strong winds);
- be discreet, to reduce the risk of vandalism;
- be as inexpensive as possible, and readily available when replacements are needed;
- not be very sensitive to silting;
- have a simple software solution for setting up and for downloading data.

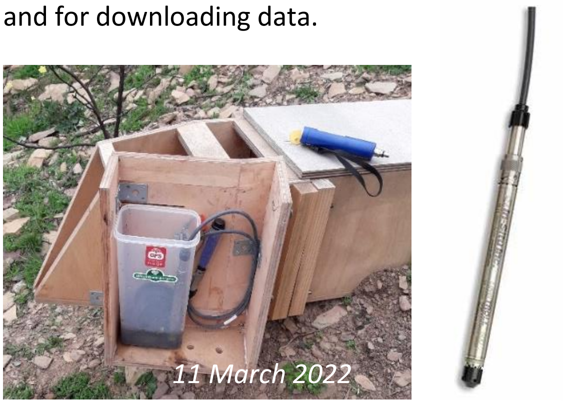

Figure 24: Level TROLL 500 probe with external measurement well

The measurement probe chosen was the Level TROLL 500 from InSitu *(Figure 24)*. This probe is the size of a large pen, 1.83 cm in diameter and 21.6 cm long.

The body is made of titanium and the measuring cell of ceramic. It is powered by a 3.6 V lithium internal battery.

The battery life is approximately 10 years in normal use. The internal memory allows the acquisition of 120,000 recordings. With measurement set at every 5 minutes, the memory can store information for over 200 days.

The VuSitu smartphone interface allows easy parameterisation of and downloading from the probes. The small diameter of the probe allows it to be easily and discreetly inserted into an external measurement well.

The selected model allows measurement over the range 0-3.5 m. The probe is ventilated, which means that the hydrostatic pressure is automatically corrected by the atmospheric pressure. The stated accuracy of the probe is +/- 1.75 mm which is perfectly satisfactory for the quantities to be measured. In order to overcome the disadvantages linked to the presence of the probe in the channel (disturbance of the flows in a calibrated gauge), the sensor should be installed in a dedicated measurement well.

Since the HS-Flume gauge has a well-defined geometry, the measurement of the water level must not be disturbed by the presence of the probe in the gauging channel. This requires the probe to be installed in an external measurement well.

This well has several advantages. It not only guarantees the rating curve that links the water level and the associated flow rate, but also smooths out the fluctuations of the water surface and therefore averages the measurement.

Figure 25 shows the installation of the hydrostatic pressure sensor (probe) in the flume's measurement well. In order to measure low flows (and therefore low water levels), the measuring probe should be positioned below the channel bottom. This configuration makes it prone to silting, but given the regular maintenance of the set-up, silting has little impact on the quality of water-level measurements.

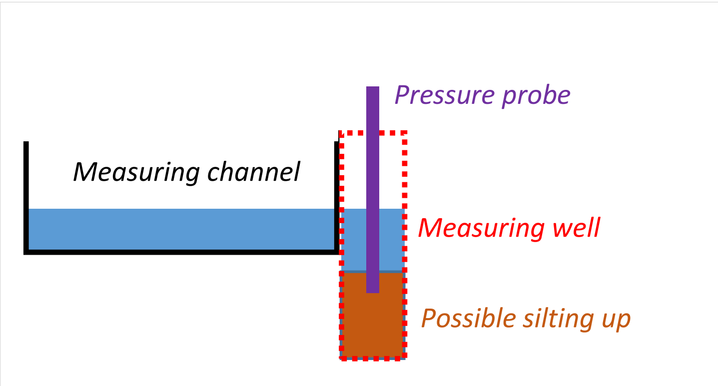

Figure 25: Installation diagram of the probe in its measurement well

2.2.4.4 MEASUREMENT OF SEDIMENT LOAD

➢ *PRINCIPLES FOR MEASUREMENT*

The sediment load from the erosion plots will be of three types:

- Suspended solids (SSs), of which there will be a significant volume that can only be quantified through turbidity measurement of flows (or by sampling and then analysing the concentration of samples);
- The load of heavy sediment, which will appear as silting of the bottom of the device;
- Uncontrollable deposits that are swept into the collector at the foot of the plot (pine needles, twigs, lumps of earth, stones).

As part of the project, given the intermittent nature of the flows and the technical difficulties of accurately measuring SSs, we chose to measure only the coarse sediments (sand and pebbles).

Thus, even if we do not measure the entire volume of eroded sediment, we can compare the same variable (coarse load) in relative terms between the control plot and the burnt plots.

➢ *CHOICE OF MEASURING EQUIPMENT*

In order to collect the coarse load, we placed a settling tank immediately below the plot's collector installation *(Figure 26)*. This 80 cm cubic tank allows the solid fraction to settle before the flows join the approach channel and then the HS-Flume for liquid flow measurement.

The bottom sediment load will not be quantified on a continuous basis, but rather during maintenance visits which often occur after significant rainfall events. Sediment can deposit in the settling tank, but also further down in the approach channel, as shown in *Figure 26*.

Deposits are collected periodically during maintenance visits using a brush and shovel. They are then dried naturally and any vegetation is removed. These deposits are then weighed with a precision balance to determine their mass.

Initially, in the design of the sediment tank, it was envisaged that baffles and filter screens would be installed to encourage the deposition of such matter.

In practice, it was found that these devices were not necessary and the bin was left "empty" to facilitate cleaning operations.

Figure 26: View of the settling tank and approach channel, with the HS-Flume in the background. In the foreground you can see the borders of the plot and the mat that forms the transition between the natural ground and the measuring device.

2.2.4.5 PROCESS OBSERVATION AND SUPERVISION

➢ *PRINCIPLES FOR MEASUREMENT*

The visual observation of these erosion plots has several goals:

- To **observe** the flow meter in operation and **confirm** the accuracy of the information from the water-level sensors;
- To monitor the **natural dynamics of vegetation recolonisation**, which is a marker of the extent of erosion;
- To carry out these observations on each of the erosion plots;
- To enable **supervision of equipment** and deter vandalism.

- <u>CHOICE OF OBSERVATION EQUIPMENT</u>

Given the frequency of maintenance visits (at least 8 times a year), and in order to limit operating costs (three SIM cards at around €30/month each), we did not consider remote transmission of images.

Observations are made using Digital Cameras (DCs) of the camera trap type. The 30-minute time lapse mode, combined with motion triggers, allows for very regular monitoring of equipment operation.

The hardware used is the BOLYGUARD SG 2060X. It can be set to produce images of different quality (low/medium/high). This DC can take pictures at night, thanks to an infrared flash.

On the burnt plots, the DCs were installed on builder's props. On the control plot, the DC was installed on a tree. *Figure 27* shows a typical layout for a DC and the quality of the images in day and night conditions.

Figure 27: Digital camera (DC) for the observation of the equipment in an erosion plot.

(a): Installation of the DC at a height of about 2.2 m on a stand in front of the plot.

(b): Close-up of the DC used

(c): Daytime image of Fire Plot I produced by the DC. In this picture, we can see a flow in the HS-Flume.

(d): Night-time image of Fire Plot I produced by the DC

2.2.5 SETTING UP THE MEASURING INSTRUMENTS

The equipment was installed during September and October 2021. The set-up became operational **on 21 October 2021**, less than 3 months after the fire (31 July 2021).

During these 3 months, there was no significant rainfall event that could begin to wash away the soil. At the time of implementing the set-up, the condition of the burnt soils can be considered to be identical to the day after the fire, except for the significant wind erosion in the sector, which transported very fine elements (soot) as well as the pine needles that began to cover and protect the soil.

Figure 28 presents the set-up schematically, which is composed of:

- **Three** erosion measurement **plots** with measuring equipment and probes
    - One burnt plot → **Fire Plot 1**
    - One burnt plot (steeper and with more vegetation) → **Fire Plot 2**
    - One plot unaffected by fire → **Control Plot**
- **One automatic rain gauge** located in the centre of the three erosion plots;
- **Three digital cameras**, each observing one plot.

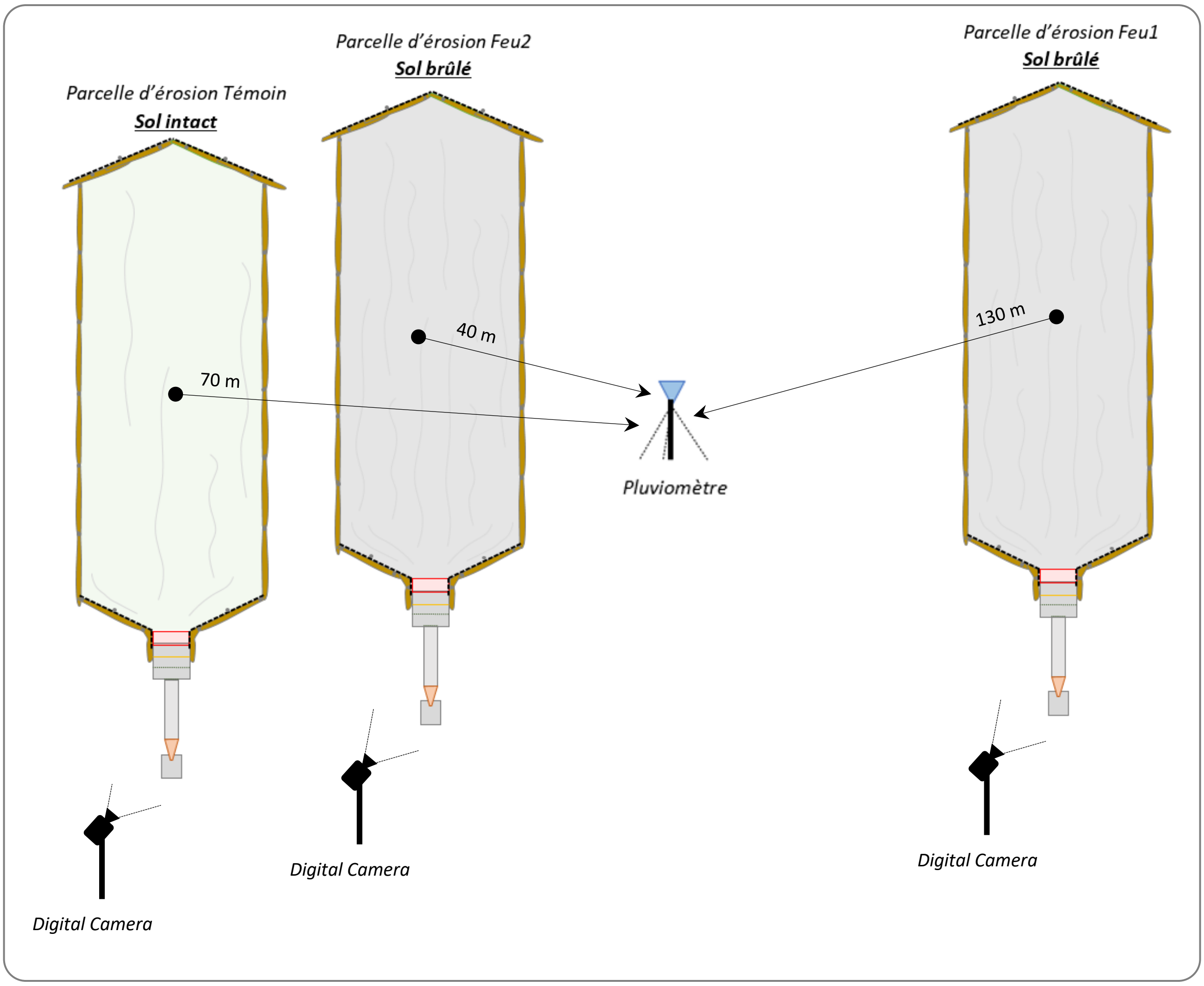

Figure 28: Overview of the set-up (principle and equipment) and distance between the erosion plots and the rain gauge

Figure 29 shows the whole set-up. The characteristics of the plots were as follows:

	Area	Longitudinal slope	Distance to rain gauge	Type of vegetation
Fire Plot 1	115 m^2	44%	130 m	Shrubby scrub
Fire Plot 2	107 m^2	53%	40 m	Dense shrubby scrub
Control Plot	114 m^2	56%	70 m	Dense shrubby scrub

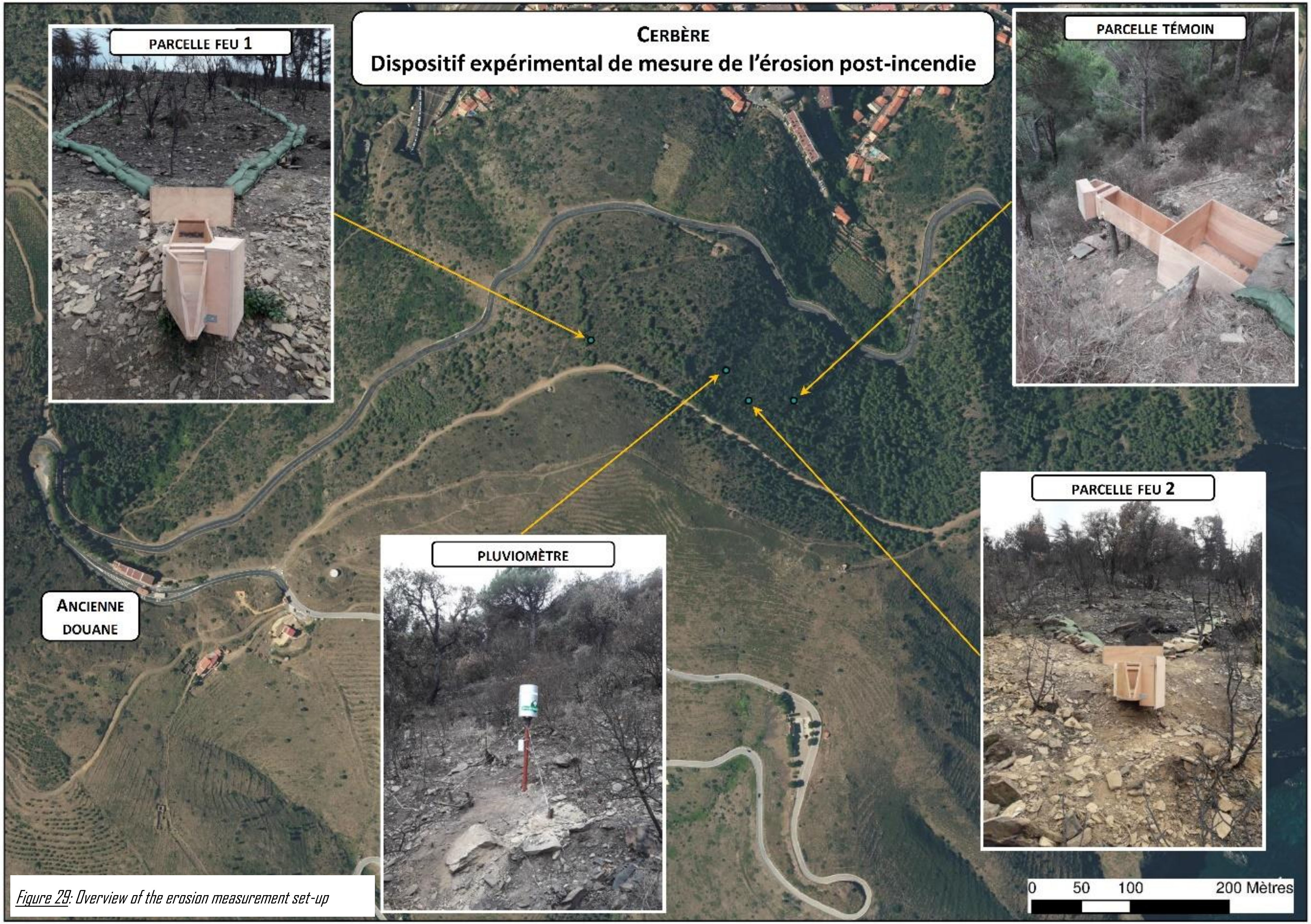

Figure 29: Overview of the erosion measurement set-up

The erosion plots were located on the upper part of the northern slope of the international border ridge. This slope overlooks the RD914 (departmental road) and the houses of CERBÈRE *(Figure 30)*.

Figure 30: Isometric view of the burnt and instrumented slope of the CERBÈRE state forest: the red line shows the outline of the fire of 31 July 2021; the erosion plots are shown in yellow. Image: HD LiDAR (Geopole, October 2022) overlaid on IGN RGEAlti 2021.

For ease of implementation, and above all to guarantee regular maintenance, these plots were set up along the edge of the forest track *(Figure 31)*, but were not disturbed by runoff from the track. Contrary to what is shown (analysis of Sentinel satellite images at 10 m spatial resolution), the Control Plot is entirely in the unburnt zone.

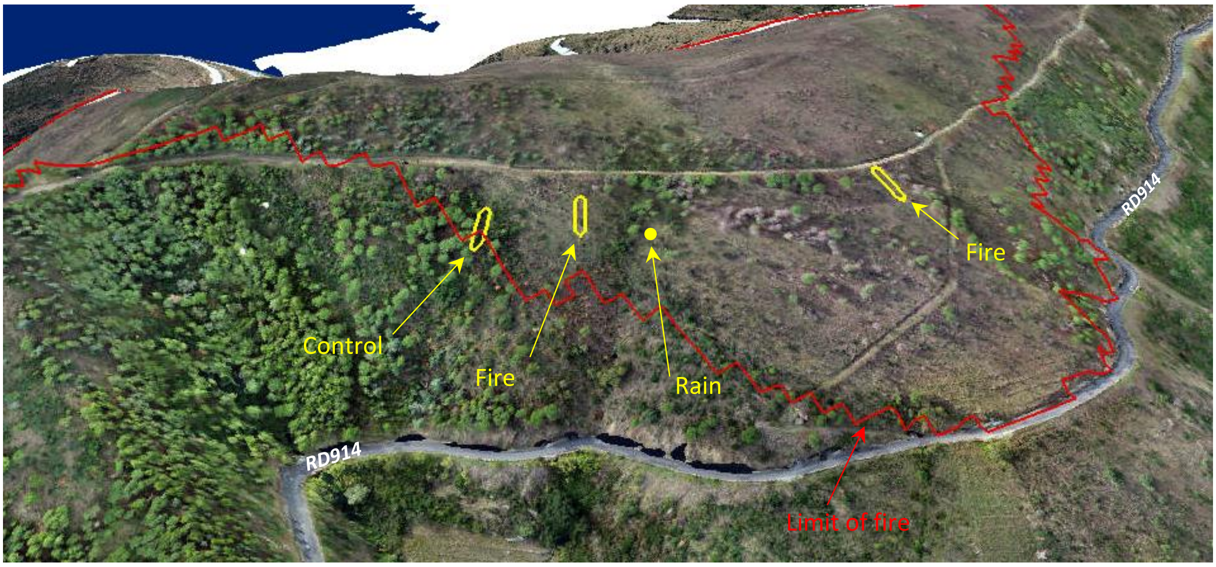

Figure 31: Precise location of equipment in the burnt area (Fire Plot 1, Fire Plot 2, rain gauge) and in the unburnt vegetation (Control Plot) - image: orthophotograph taken in October 2022 during the realisation of the Digital Terrain Model by LiDAR. The fire boundary is based on Sentinel satellite images (European Copernicus programme) with a resolution of 10 m. Contrary to appearances, the Control Plot is located at the edge of the fire, and entirely in the unburnt zone.

The three erosion plots were identical, and consisted of *(Figure 32)*:

- a **plot** with an area of approximately 100 m^2 delimited by **boundary markers** laid and packed into the natural ground (this choice of marker was necessary because the ground is very stony and thin boundary slabs cannot easily be sunk into it). The boundary markers at the bottom of the plot converged to channel the water to the measuring device;
- a wooden **sedimentation tank** 80 cm long to receive the runoff. Coarse material (sand and stones) and plant debris settle in this tank;
- a 1.2 m long **approach channel** to channel the flows;
- a 0.8 foot **HS-Flumes-type flowmeter** with an external measuring well. The measuring well is fitted with a **water-level logger** (Level TROLL 500 from INSITU). The specific shape of the flow meter gives the flow rate based on the measured water level;
- an **automatic camera** (time lapse and motion detection) to record the flows as they leave the flow meter.

On the terminal part of the plot, at the interface between the natural ground and the equipment, the boundary markers converge from a width of 5 metres to approximately 80 cm. This convergent system directs liquid and solid flows to the measuring equipment.

This interface is often a source of sediment contamination due to the construction work; the transition from a rough to a smooth surface locally favours gullying and the formation of furrows which distort the quantities to be measured. To solve this problem, a mat was laid on the ground to create a gradual transition of roughness and limit the gullying phenomenon before the settling tank *(Figure 33* and *Figure 34)*.

Once the flows have been concentrated by the converging boundaries, they pass into the settling (or sedimentation) tank. The settling tank allows the solid elements (sand and gravel) to sink to the bottom. In the design phase, it was planned to install grids to retain floats so that they would not interfere with the flow measurement. In the end, the first weeks of operation showed that these grids were not essential due to the low proportion of floaters occurring. The advantage of not having a grid is that it simplifies maintenance.

Beyond the settling tank is the approach channel, whose function is to channel the water efficiently so that the flow can be measured correctly.

The approach channel and the HS-Flume are installed almost horizontally, with a longitudinal slope not exceeding 1%. **Both of these elements were installed with great care**. Their foundations were consolidated so that they would not sink over time. An arrangement of stones and sandbags was used to set them at the right height. At the foot of the HS-Flume, stones were placed in order to return the flows to the natural environment without causing gullying that could destabilise the HS-Flume.

Figure 32: Illustration of the equipment making up an erosion plot

Figure 33: Schematic overhead view of the terminal part with the measuring equipment

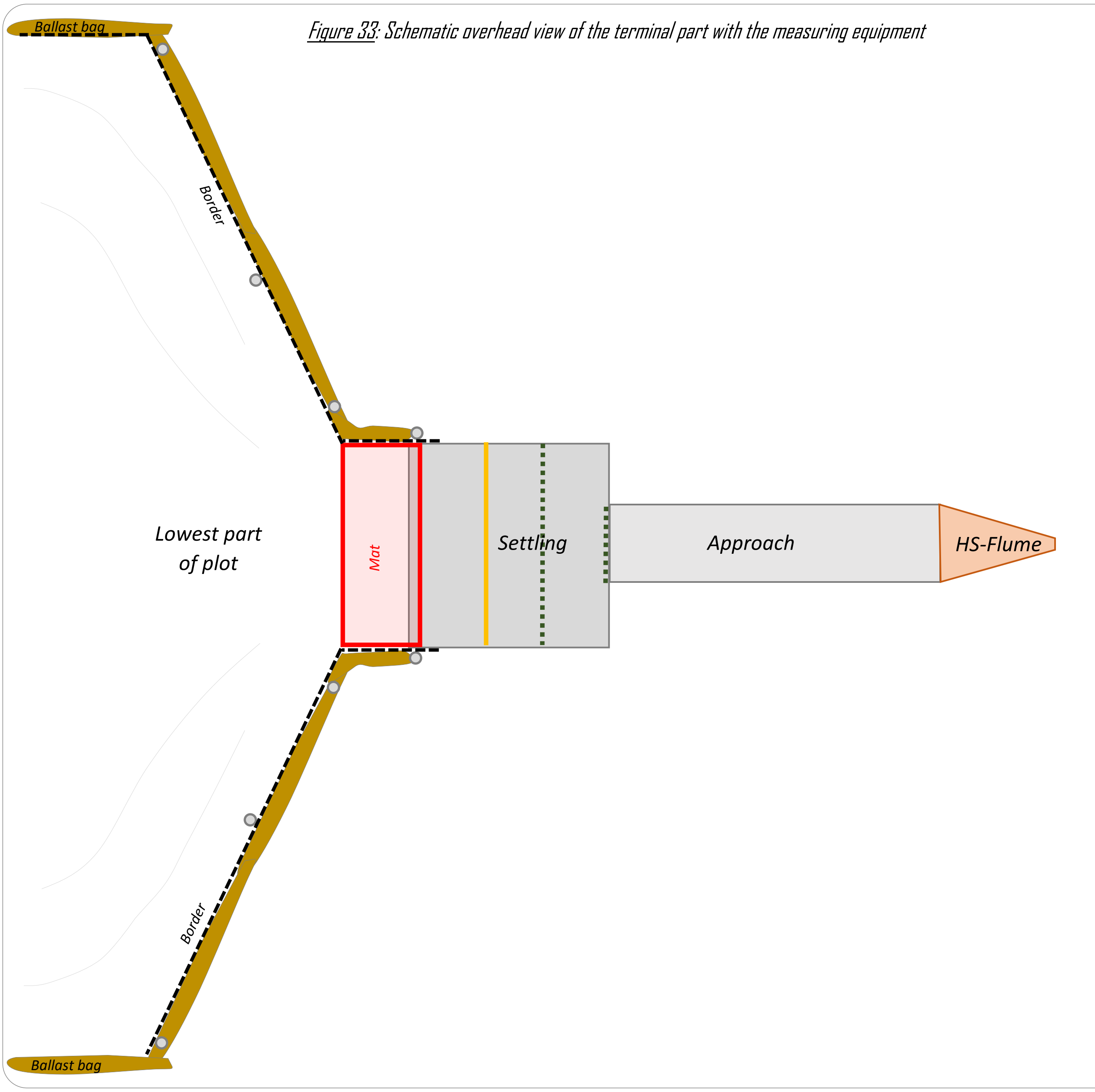

Figure 34: Schematic cross-section of the terminal part with the measuring equipment

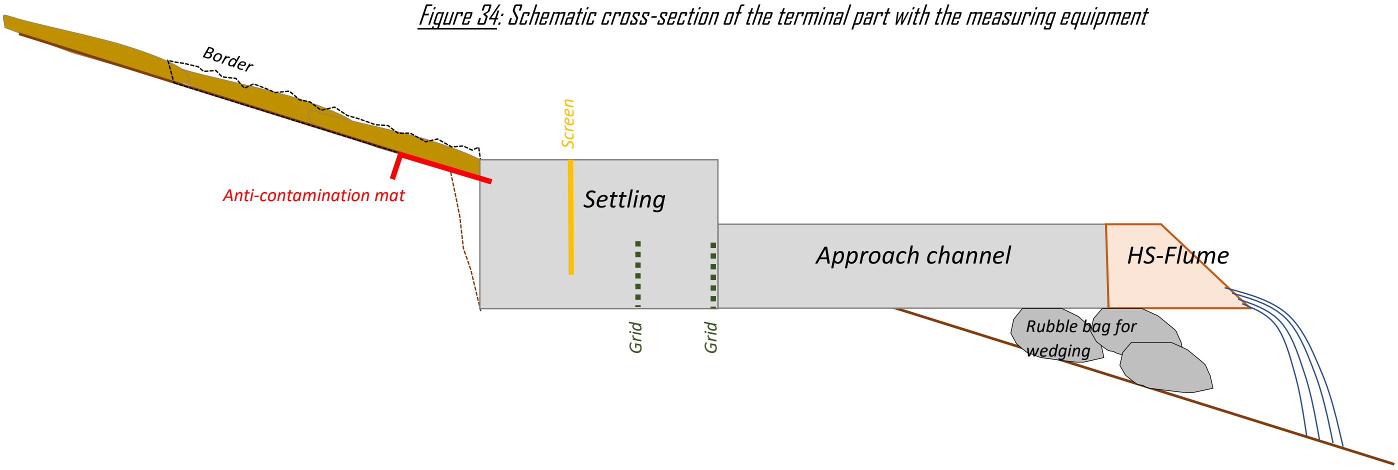

For this project, the ONF took charge of purchasing all the materials (instruments, materials for building the equipment, hardware, etc.), as well as the construction of the marine plywood caissons (settling tank, approach channel, HS-Flume).

A local company, CUTILLAS, carried out the work over 4 days, with a total of 18 man-days for the installation of the three plots and the installation of the rain gauge support *(Figure 35)*.

Thanks to the proximity of the track, a plot of land can be completed in almost a single day: delineation of the boundaries, laying of the border, earthworks to install the caissons, installation of the settling tank and the approach channel, and levelling the equipment.

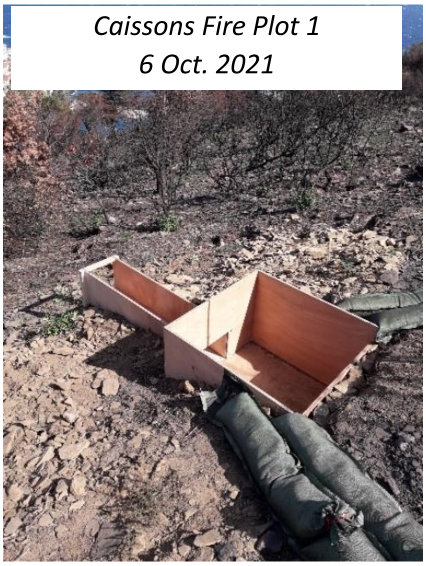

Figure 35: Installation of the equipment in October 2021 by CUTILLAS, with, from left to right and from top to bottom:

- *Marking out Fire Plot 1 before installation of the borders;*
- *Transporting the borders, pre-filled in the workshop;*
- *Earthworks and levelling of the caissons on Fire Plot 1;*
- *Earthworks for the equipment on the Control Plot;*
- *Installation of the caissons in the Control Plot. Due to the slope and the presence of a rocky slab, they are installed on stakes cut from Black Locust (or False Acacia, a common local species).*

To facilitate assembly and reduce the risk of breakage, the set-up was designed with individual components. The settling tank, approach channel and HS-Flume were then bolted together.

On the fourth day, the HS-Flumes were installed on the approach channels, and the borders were reinforced with ties and rebars driven into the ground. The guyed support for the rain gauge was also installed.

Figure 36: Rain gauge installed on 21 Oct. 2021

The external HS-Flume wells, as well as the containers and water-level probes, were installed on 21 October 2021 *(Figure 37)*.

We installed the more fragile rain gauge on its stand ourselves, on 21 October 2021 *(Figure 36)*, and then calibrated it. We also installed the brackets for the DCs ourselves during a maintenance visit to the set-up much later, on around 20 May 2022, due to a long delivery time from the supplier *(Figure 38)*.

Figure 37: External well and measuring probe

Figure 38: Digital cameras installed facing each of the plots. On Fire Plots 1 and 2, guyed supports were necessary. On the Control Plot, it was possible to use a pine tree right in front of the plot as a support.

2.2.6 IMPLEMENTATION AND MAINTENANCE

Despite great attention to the quality of the equipment and instruments, as well as their implementation, the **quality of the data produced** by the instruments is highly dependent on the initial calibration and, **above all, regular maintenance of the set-up**.

2.2.6.1 INITIAL CALIBRATION

The first thing to do is to check the solidity of the support and the tension of the guy wires, as well as the horizontality of the circular opening for receiving the rain.

The PLV400 double-chambered bucket rain gauge was already calibrated at the factory. When installing the instrument in the set-up, it was necessary to check the free mechanical movement of the buckets, as well as the cleanness of the openings *(Figure 39)*. The rain gauge is connected to a stand-alone data logger. This should be set to Universal Time (UTC), which is more convenient for handling clock changes between summer and winter time. The time step is 6 minutes and the unit of measurement is the millimetre. As a reminder, each tipping of the buckets is equivalent to 0.2 mm of rainfall.

Figure 39: Close-up of the rain gauge mechanism

The water-level sensors in the HS-Flume are located in their respective external wells *(Figure 40)*. The principle of the well is to preserve the geometry of the HS-Flume (the probe does not interfere with flows, and therefore does not alter the rating curve). This well is connected to the HS-Flume via a hole cut in the wall. In addition, the ceramic diaphragm that measures the pressure, and therefore the hydrostatic head, is located almost 2 centimetres from the end of the probe. In order to obtain a measurement as soon as the first flows occur, the external well is installed below the level of the sill plate of the HS-Flume.

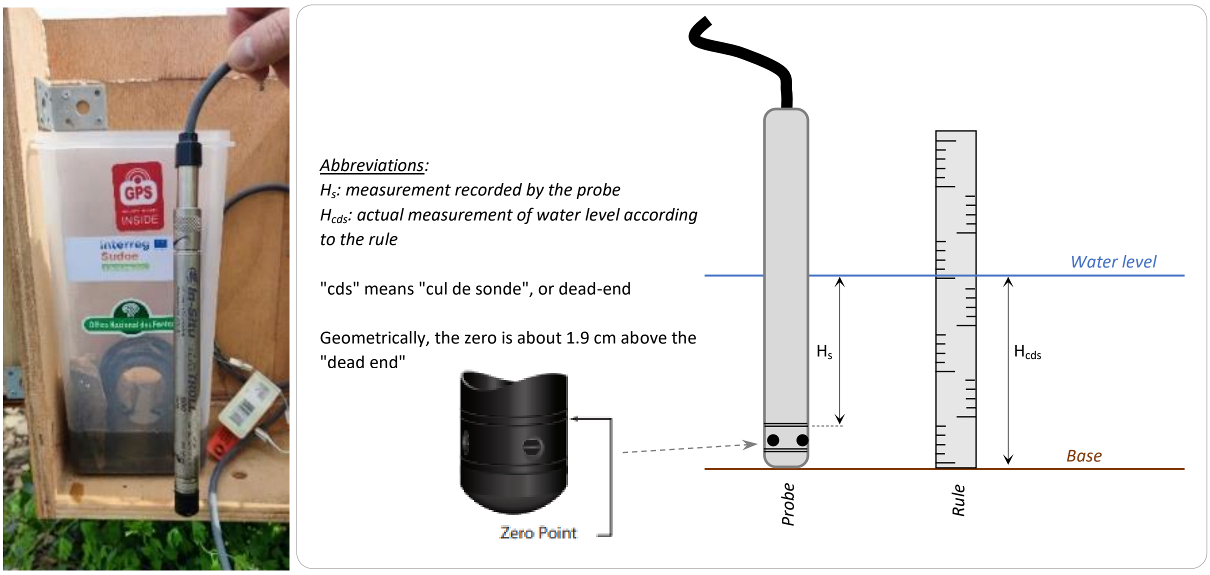

Figure 40: Installation of a water-level probe in its external well. The actual water level in the HS-Flume is different from that recorded by the automatic probe. The difference is determined at each maintenance visit.

Figure 40 illustrates the position of the external well in relation to the HS-Flume: while the water level is flush with the base of the HS-Flume, the probe is immersed in about 5 cm of still water. In this way, the start of runoff is measured correctly by the probe and the measured values are averaged (no outliers due to disturbance).

Figure 40 also shows the comparative quantities to be taken into account to obtain the true water level in the HS-Flume usable for calculating the runoff.

During each maintenance visit, and for each plot, the probe is removed from its well for cleaning of the ceramic membrane. When the probe is reinstalled in its measurement well, a comparison is made between the H_s and H_{cds} variables in order to verify that there is no drift of the probe (change over time in the difference between these two quantities).

For the digital cameras, an initial calibration was necessary to choose the shooting frame as well as the quality and frequency of the images, in order to find the best compromise in terms of power management and storage capacity on the memory cards.

2.2.6.2 MAINTENANCE

The maintenance of an experimental erosion measurement set-up is essential to ensure the quality of the instrument data. The intrusive measurement of sediment-laden flows poses a potentially high risk of partial or total clogging of the hydrostatic pressure probe orifices. Regular cleaning of these probes, as well as checking that they are working properly, is imperative.

Moreover, when designing the set-up, the frequency of maintenance was anticipated in the choice of instruments: data downloading must be regular. As an example, the choice of a 6-minute acquisition time step for the rain gauge means that data must be downloaded every 67 days at the most. After this period, the old data are overwritten.

Finally, the principle of calculating overall sediment volume rather than continuous measurement requires regular extraction of the material deposited in the settling tanks.

Since the set-up became operational on 21 October 2021, we have carried out eight maintenance visits, i.e. one visit every 1.5 months. This is an average, bearing in mind that after exceptional rainfall, the set-up is visited quite promptly.

During maintenance visits, not only is the equipment needed to download data from and repair the instruments (laptop, INSITU Bluetooth module, brush and shovel), but also more specific equipment is needed to repair the caissons or the rain gauge and DC holders (Figure 41).

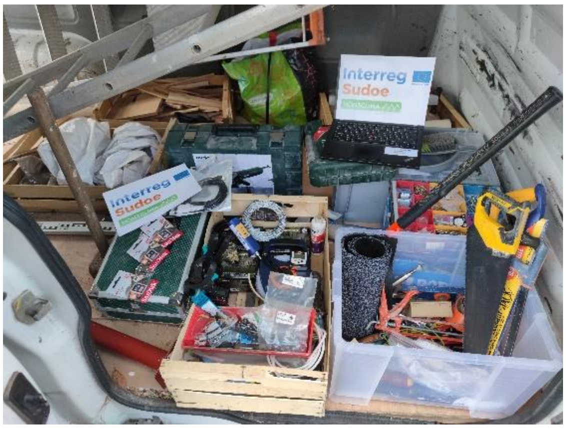

Figure 41: Maintenance equipment for monitoring and possible repairs

During a maintenance visit, the entire set-up is examined to visually detect any potential disruption. Then, as the visit progresses, the instruments are checked and their data downloaded. *Figure 42* gives a sample of the interventions carried out during these maintenance visits.

Figure 42: Equipment visited during periodic maintenance, and points requiring attention.

(a): General visual inspection, downloading from the rain gauge, checking time synchronisation and battery status

(b): General visual inspection, cleaning of the probe, data download and time synchronisation

(c): The wells dry quickly due to evaporation (very frequent wind). Water must be re-supplied, with verification of the level

(d): General visual inspection and sampling of sediments in the settling tanks

(e): Checking the condition of the borders

As the download times for the probes are quite long due to the large amount of data, a complete maintenance of an erosion plot usually takes about an hour.

Regarding the DCs, the acquisition time is highly variable, depending on the number of movements that have occurred in front of the detector. In spring, the sensitivity of the detector was too high, and the wind-blown vegetation triggered too many shots. The memory was quickly saturated and the batteries discharged (operating time of only about 1 month). The sensitivity was then reduced and the size of the images reduced.

3 RESULTS OF THE MEASUREMENTS

The experiment was launched in the autumn of 2021 and is still in operation today. The results presented below are for the period from 21/10/2021 to 17/09/2022, i.e. for almost a year. Only one hydrological season (autumn 2021 - spring 2022) was studied. The results are therefore not very robust, but they do allow trends to be identified.

3.1 RAINFALL CONTEXT

Before proceeding with the analysis of runoff, it is interesting to characterise the precipitation regime in this 2021/2022 hydrological season in relation to the average of the other years.

Table 4 lists the rainfall events recorded by the experiment's rain gauge. Not all these episodes generated runoff on the erosion plots. The duration of these episodes varied greatly, from less than 2 hours to more than 56 hours.

The maximum hourly intensities are also quite disparate, with values ranging from 2 to 56 mm/h. Only one rainfall episode exceeded a cumulative total of 100 mm (over 38 hours).

Table 4: Significant rainfall events that occurred between 21 Oct. 2021 and 17 Sep. 2022 (date of the last reading)

Rainfall episode	Start	End	**Duration (h)**	**Total (mm)**	Max total over 6 min (mm)	**Max intensity (mm/h)**	Average intensity (mm/h)	Rain index* (mm/h)
10 to 12 Nov. 2021	10/11/2021 10:30	12/11/2021 19:12	**56.7**	**62.8**	2	**20**	1.11	4.7
23 and 24 Nov. 2021	23/11/2021 12:48	24/11/2021 18:18	**29.5**	**80**	5.6	**56**	2.71	12.3
10 Dec. 2021	09/12/2021 22:36	10/12/2021 18:18	**19.7**	**22.8**	0.8	**8**	1.16	3.0
9 and 10 Jan. 2022	09/01/2022 19:36	10/01/2022 11:54	**16.3**	**29.8**	0.6	**6**	1.83	3.3
16 Feb. 2022	16/02/2022 07:30	16/02/2022 09:12	**1.7**	**2**	0.2	**2**	1.18	1.5
11 to 13 March 2022	11/03/2022 18:36	13/03/2022 08:42	**38.1**	**100.6**	3.4	**34**	2.64	9.5
20 and 21 March 2022	20/03/2022 06:06	21/03/2022 07:36	**25.5**	**22.8**	1.2	**12**	0.89	3.3
29 and 30 March 2022	30/03/2022 02:36	30/03/2022 11:42	**9.1**	**14.2**	0.6	**6**	1.56	3.1
20 to 21 April 2022	20/04/2022 14:06	21/04/2022 15:06	**25**	**36.2**	3.2	**32**	1.45	6.8
24 May 2022	-	-	**24**	**19.6**	-	**-**	-	-
3 Sep. 2022	03/09/2022 06:30	03/09/2022 08:42	**2.2**	**8**	3.6	**36**	3.64	11.4

* The rainfall index is an arbitrary construction for this study in order to establish a parameter that can characterise the onset of runoff. This index is the square root of the product of the average intensity and the maximum intensity. Its unit is expressed in mm/h.

Figure 43 gives the number of observed occurrences of episodes over the last 50 years that brought more than 100 mm in one climatological day on at least one measurement point per *département*. In the PYRÉNÉES-ORIENTALES *département*, rainfall with a daily total of 100 mm occurs on average 3 to 5 times a year.

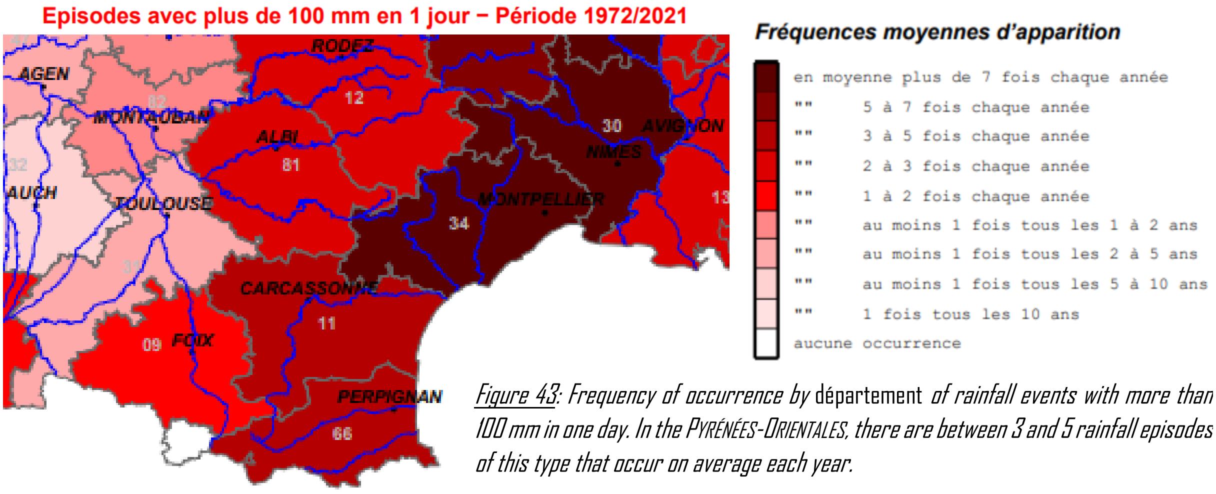

Figure 43: Frequency of occurrence by département *of rainfall events with more than 100 mm in one day. In the PYRÉNÉES-ORIENTALES, there are between 3 and 5 rainfall episodes of this type that occur on average each year.*

Taken from http://pluiesextremes.meteo.fr/france-metropole/Nombre-de-jours-par-departement.html

Strictly speaking, the results of *Figure 43* cannot be compared with the rainfall recorded on the CERBÈRE rain gauge, as the first is a departmental synthesis of all the rain gauge stations, and the second is a very localised measurement. Nevertheless, on a departmental scale, the number of observations of rainfall events causing damage was significantly lower in the 2021/2022 season than in previous years.

Autumn 2021 and **spring 2022 were fairly calm in terms of rainfall episodes** on the Vermeille coast; the Mediterranean episodes occurred more over the Cévennes (Gard and Hérault) due to an upwelling of air masses in a southerly flow rather than a south-easterly flow, which had previously been observed more frequently. This change in the orientation of the flows means that exceptional rainfall episodes tend to occur out at sea along the Catalan coasts before impacting the first foothills of the Cévennes. This change in wind patterns is quite recent (within the last few years) and could be a marker of climate change.

The results of an experimental erosion monitoring set-up in real conditions after a fire are strongly dependent on the intensity of the rainfall that may occur. In the case of the MONTCLIMA project, we were unfortunately unable to benefit from the occurrence of many exceptional rainfall events. However, some episodes were sufficiently intense to generate measurable runoff and allow an assessment of hydro-sedimentary processes in relation to soil degradation.

3.2 INCREASED HYDROLOGICAL REGIME

The change in hydrology on the burnt land was assessed by comparing the results of flows obtained on Fire Plots 1 and 2 with the reference or Control Plot.

The runoff values are not produced directly as data by the measuring probes. The following paragraphs detail the methodology for determining these values from the water level recorded by a probe:

- from the raw water-level data measured in the external well, a preliminary analysis must be carried out to distinguish between normal operation and measurement artefacts linked to maintenance operations;
- once the raw data have been analysed, the raw level values must be subtracted from the "zero" checked at each maintenance visit. This gives the actual value of the water level in the HS-Flume;
- from the water level in the HS-Flume, it is possible to calculate the runoff rate from the rating curve, and then compare the values obtained on the burnt plots with those from the Control Plot.

3.2.1 RAW WATER-LEVEL DATA

Figure 44 shows the water-level measurements of the probes in their respective external wells.

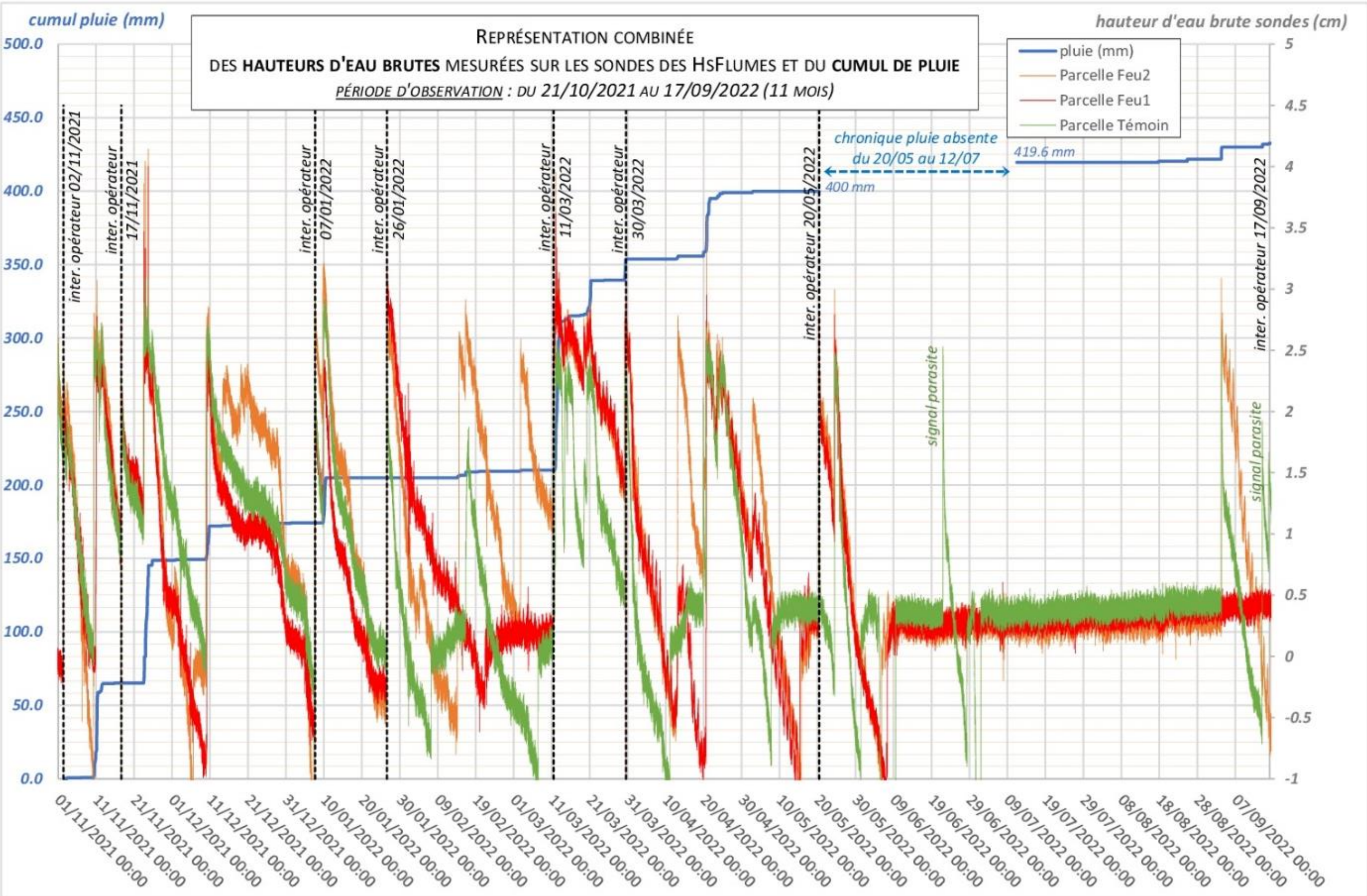

Figure 44: Raw water levels of the measurement probes on the three plots, as well as the cumulative rainfall given by the rain gauge of the set-up. The measurement wells are replenished during maintenance visits. These visits are indicated in the graph in order to differentiate between natural (rain induced flow) and artificial (operator levelling for calibration) replenishment.

The time period covers one hydrological season, between 21/10/2021 and 17/09/2022. The most suitable periods for measuring runoff are autumn and spring, when Mediterranean-type rainfall events usually occur.

This graph shows:

- The progressive accumulation of rainfall over the season. At the end of the season, a total accumulation of around 430 mm was measured. Usually, in this sector, an annual total of about 680 mm of rain is recorded *(Météo France data; Aurélhy procedure - average over the period [1981-2010])*. This highlights the fact that rainfall was rather low during the period covered by the MONTCLIMA project.

  During the summer of 2022, due to the rather mild weather, we did not make any maintenance visits. Due to the limited memory capacity of the rain gauge, the measurements between 20 May 2022 and 12 July 2022 were not recorded (only the rain gauge, the probes remaining fully functional). This lack of data is not detrimental to the interpretation of the results since no runoff was recorded on the erosion plots.

- The water-level values measured in the external wells, with:
  - in green, the values from the Control Plot probe,
  - in red, the values from the Fire Plot 1 probe,
  - in orange, the values from the Fire Plot 2 probe.

  With a measurement acquisition step of every 5 minutes, the curves are very "noisy". Rapid and systematic decreases are observed after each manual re-supplying of the measurement wells; this phenomenon reflects a high evaporation potential linked to the fact that the study area is very windy.

- The vertical black lines indicate maintenance visits. During these visits, the wells and probes are cleaned and then the well is re-supplied with water to determine the "zero" level, i.e. the height of water recorded by the probe, which corresponds to the level of the floor (sill plate) of the HS-Flume.

  Re-supplying with water at each maintenance visit is indicated by a sudden rise in the water level of the probe.

From these raw data, the following observations can be made:

- rainfall events do constitute a forcing that modifies the water level, being followed by a sudden rise;
- maintenance visits are clearly visible because of a sudden rise in water level;
- the windier the weather after a rainy spell, the faster the water-level curves decrease;
- the signal noise produced by the probes is consistent with the manufacturer's specifications (accuracy to within + or - 1.75 mm);
- there are few measurement artefacts.

3.2.2 WATER LEVEL IN THE HS-FLUME

The water levels measured in the HS-Flume are deduced from the raw measurements by subtracting the "zero" level of each probe, and for each period.

At each maintenance visit, the probe is taken out of the well, cleaned, and then put back into the well, not necessarily in exactly the same place. Consequently, the previous calibration can be modified and it is imperative to define for each period, the new "zero" level of the probes, so as to know precisely the real water levels in the HS-Flume.

Table 5 summarises the evolution over time of the "zero" levels to be taken into account for each of the probes. These levels vary by up to 0.6 cm. This variation is non-negligible in the level-to-flow transformation, hence the need to periodically check the "zero" levels.

Table 5: Values of the "zero" levels

		Value to be subtracted from the "raw" water levels to determine the **actual water levels** in the HS-Flume		
Time period		Control Plot (in cm)	Fire Plot 1 (in cm)	Fire Plot 2 (in cm)
from 21/10/2021	to 17/11/2021	2.20	2.20	2.25
from 17/11/2021	to 07/01/2022	2.30	2.25	2.30
from 07/01/2022	to 26/01/2022	2.50	2.40	2.80
from 26/01/2022	to 11/03/2022	2.45	3.00	2.80
from 11/03/2022	to 30/03/2022	2.30	2.80	2.70
from 30/03/2022	to 20/05/2022	2.25	2.90	2.75
from 20/05/2022	to 16/09/2022	2.30	2.30	2.40

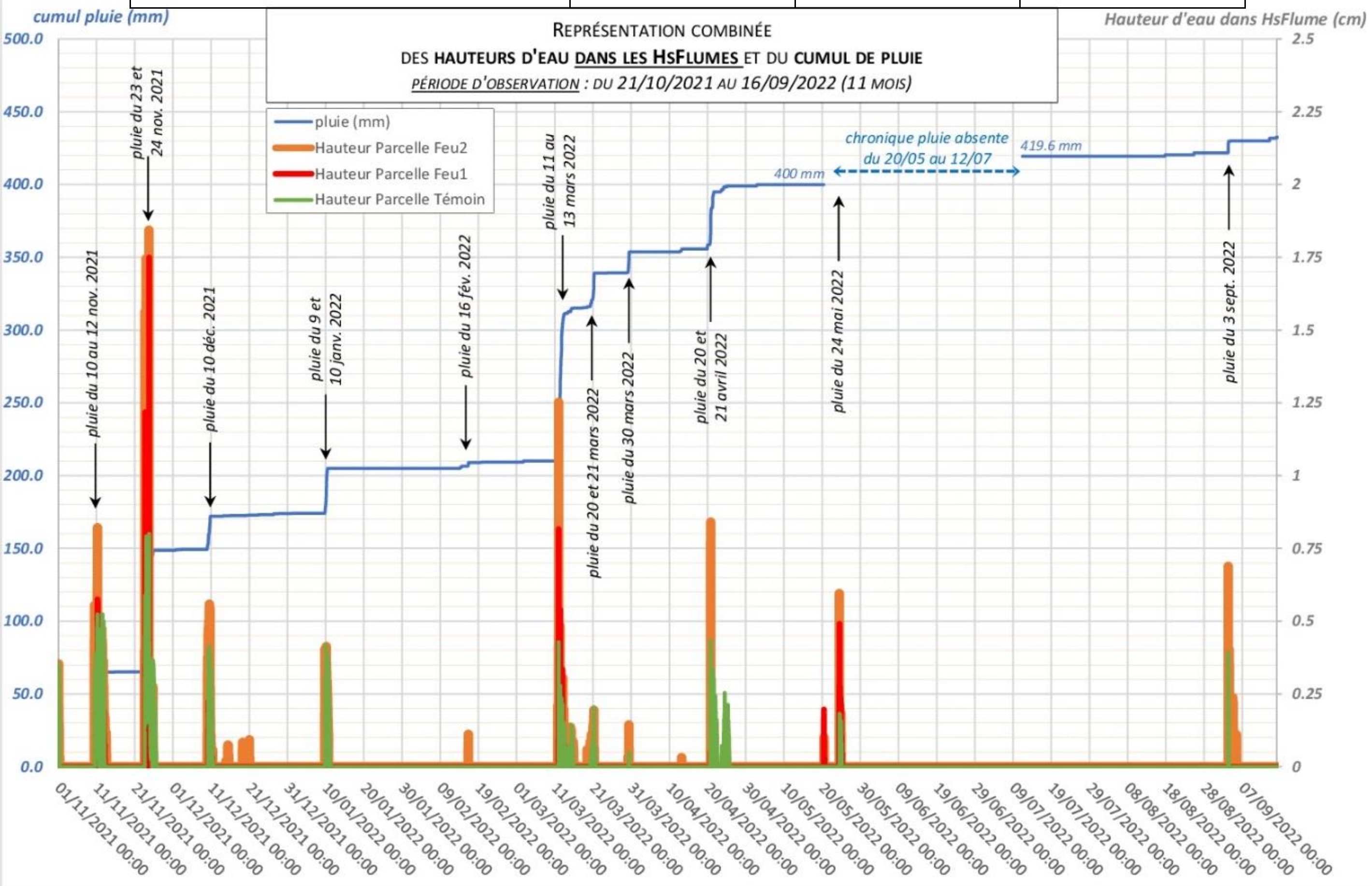

Figure 45: Processed water levels that correspond to the actual levels in the HS-Flume. It should be remembered that below a level of 6 mm the rating curve does not guarantee the calculated value of the corresponding flow.

The actual water levels in the HS-Flume are shown in *Figure 45*. The rainfall events that generated the most exceptional hydrological responses are indicated on the cumulative rainfall curve.

From this graph, the following observations can be made:

- the heavier the rainfall episodes, the stronger the hydrological responses of the plots;
- the burnt plots react more often than the Control Plot;
- Fire Plot 2 produced a stronger hydrological response than Fire Plot 1;
- Fire Plot 2 is steeper than Fire Plot 1. There is a consistency in the level of intensity of the hydrological responses of the different plots: Fire Plot 2 reacts more strongly than Fire Plot 1, which in turn reacts more strongly than the Control Plot.

3.2.3 MEASURED FLOWS

By design, the 0.8-foot Hs-Flume gives a rating curve over the range [0.61 cm - 24.08 cm] of water level. Below the value of 0.61 cm, the rating curve cannot be used to establish a level/flow relationship.

Using the data from *Figure 45*, the actual water-level values are filtered, keeping only those with a value greater than 0.61 cm. With this new dataset, we can establish a runoff dataset (*Figure 46*).

From this graph, the following observations can be made:

- there were five rainfall episodes during which runoff was observed on at least one plot:
  - rainfall from 10 to 12 November 2021 (max. intensity = 20 mm/h)
  - rainfall on 23 and 24 November 2021 (max. intensity = 56 mm/h)
  - rainfall from 11 to 13 March 2022 (max. intensity = 34 mm/h)
  - rainfall on 20 and 21 April 2022 (max. intensity = 32 mm/h)
  - rainfall on 3 September 2022 (max. intensity = 36 mm/h)
- Fire Plot 2 (the steeper burnt plot) reacted very quickly and most strongly.
- Fire Plot 1 (the less steeply sloping burnt plot) reacted less quickly and more moderately than Fire Plot 2.
- the Control Plot reacted little.

The hydrological responses of these small experimental plots **were more closely related to rainfall intensity** than to total rainfall accumulation.

The first hydrological responses (Fire Plot 2) occurred when rainfall intensity reached 20 mm/h.

Fire Plot 1 and the Control Plot only seemed to react to higher rainfall intensities (> 34 mm/h).

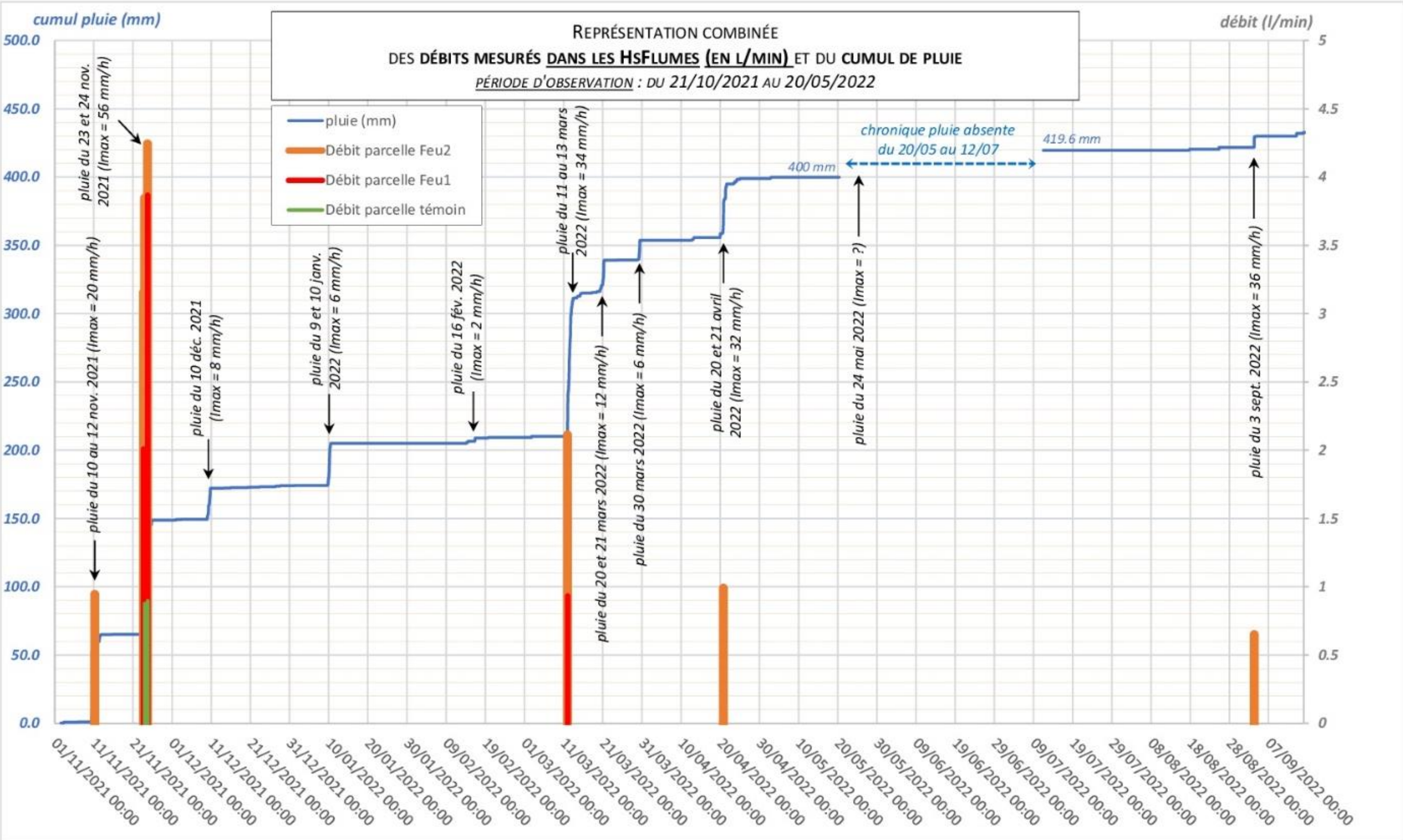

Figure 46: Flow rates measured on the three erosion plots in comparison with the cumulative and hourly intensities of rainfall events. In green, the results from the Control Plot; in red: the results from Fire Plot I; in orange: the results from Fire Plot 2.

3.2.4 CLOSE-UP ON THE NOVEMBER 2021 RAIN EVENT

A detailed analysis of the rainfall episode of 23 and 24 November 2021 provides a better understanding of the rainfall thresholds that triggered the hydrological responses of the plots (*Figure 47*).

With a maximum intensity of 56 mm/h, the rainfall of 23 and 24 November 2021 was the most intense rainfall episode recorded during the experiment. Looking at the details of this rainfall episode, we can see that it is composed of three rain peaks, which generated three peaks of runoff.

❖ The first rain peak occurred on 23/11/21 at 16:50, with an intensity of **30 mm/h**:
   - only burnt plots generated measurable runoff;
   - Fire Plot 2 reacted more strongly (3.2 l/min) than Fire Plot 1 (2 l/min).

❖ The second rain peak occurred on 24/11/21 at 00:02, with an intensity of **40 mm/h**:
   - all plots produced a hydrological response;
   - Fire Plot 2 reacted most strongly (3.8 l/min), followed by Fire Plot 1 (1.6 l/min) and then the Control Plot (0.9 l/min).

❖ The third rain peak occurred on 24/11/21 at 18:10, with an intensity of **56 mm/h**:
   - all plots produced a hydrological response;

- Fire Plot 2 reacted most strongly (4.3 l/min), followed by Fire Plot 1 (3.9 l/min) and then the Control Plot (0.9 l/min).

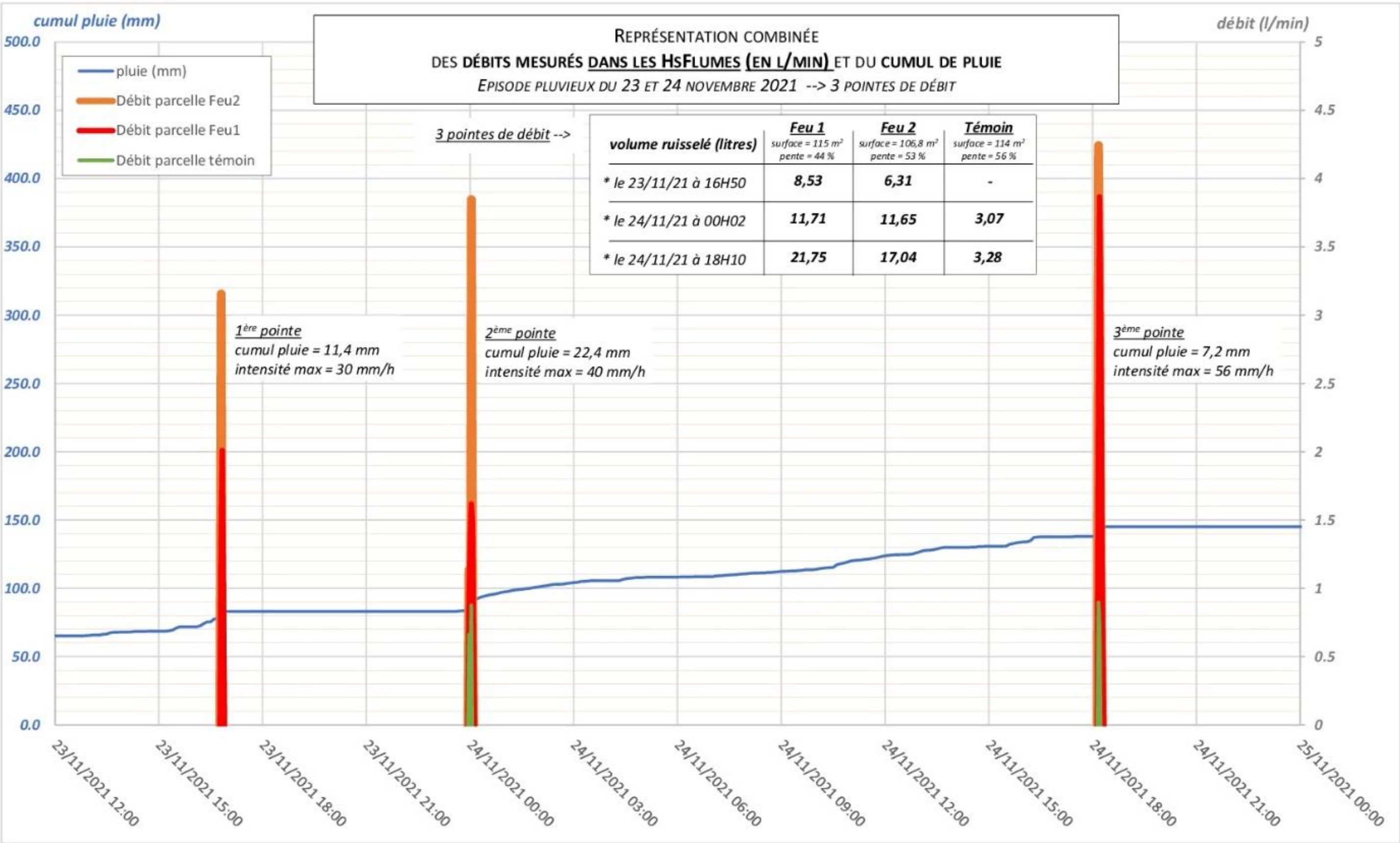

Figure 47: Flow rates measured during the rainfall of 23 and 24 November 2021. Several peak flow s were measured. For each of them it is possible to characterise the reaction of the plots.

It can be seen that **the hourly intensity (in mm/h) was the main forcing factor** for hydrological responses. The accumulated rainfall had little effect on the amount of runoff; for example, with an accumulation of 22.4 mm and an intensity of 40 mm/h, the hydrological response of the 2nd rainfall peak was weaker than that of the 3rd rainfall peak, which had a low accumulation (7.2 mm) but a higher hourly intensity (56 mm/h).

With regard to the volumes of runoff on each of the plots, the rainfall episode at the end of November 2021 highlighted the consequences of the fire *(Table 6)*: The volumes produced by the Control Plot were 3 to 6 times lower than those produced on the burnt plots.

Table 6: Runoff volumes during the rainfall episode of 23 and 24 November 2021

volume ruisselé (litres)	Feu 1 surface = 115 m² pente = 44 %	Feu 2 surface = 106,8 m² pente = 53 %	Témoin surface = 114 m² pente = 56 %
* le 23/11/21 à 16H50	8,53	6,31	-
* le 24/11/21 à 00H02	11,71	11,65	3,07
* le 24/11/21 à 18H10	21,75	17,04	3,28

Fire Plot 1 produced a larger volume than Fire Plot 2, despite a lower flow rate. This can be explained by the slope of Fire Plot 1 being shallower than that of Fire Plot 2, and therefore the flow is more spread out over time.

Table 7 summarises the observations made during the two rainfall peaks of 24 November 2021. Taking the Control Plot as a reference, it can be deduced that:

- for **Fire Plot 1**
  - the flow rate is 1.6 to 2.5 times higher
  - the volume is 3.8 to 6.6 times greater
- for **Fire Plot 2**
  - the flow rate is 4.7 to 5.8 times higher
  - the volume is 3.8 to 5.2 times greater

These results are based on only two rainfall peaks and cannot be generalised. However, they show trends that demonstrate that fires have a significant effect on changing hydrology for at least 4 months after a fire.

Table 7: Evaluation of the increase in flows and volumes on the burnt plots compared to the Control Plot

Rain on 24/11 at 00:02	**Max. measured flow rate** (l/min)	*Multiplier coeff.*	**Runoff volume** (litres)	*Multiplier coeff.*
Control Plot *(with vegetation) slope = 56%*	0.66	*Reference*	3.07	*Reference*
Fire Plot 1 *slope = 44%*	1.62	*x 2.5*	11.71	*x 3.8*
Fire Plot 2 *slope = 53%*	3.85	*x 5.8*	11.65	*x 3.8*
Rain on 24/11 at 18:10	**Max. measured flow rate** (l/min)	*Multiplier coeff.*	**Runoff volume** (litres)	*Multiplier coeff.*
Control Plot *(with vegetation) slope = 56%*	0.90	*Reference*	3.28	*Reference*
Fire Plot 1 *slope = 44%*	1.42	*x 1.6*	21.75	*x 6.6*
Fire Plot 2 *slope = 53%*	4.24	*x 4.7*	17.04	*x 5.2*

3.2.5 RESULTS FROM ANOTHER FIRE NEARBY

During the project, the RTM department studied another wildfire that occurred in the communes of OPOUL-PÉRILLOS and SALSES-LE-CHÂTEAU (in the north-east of the PYRÉNÉES-ORIENTALES *département*). This 1,000 ha fire burned a wooded area (pines, eucalyptus) and areas of shrubby scrubland. The geology was dominated by marl and limestone, with areas of skeletal soils.

In order to quantify the increase in runoff generated by the passage of fire, we measured water percolation in the soil at different locations, and according to several configurations of vegetation cover degradation. The objective of this type of measurement is to compare the infiltration capacity on the surface according to soil cover, and thus to deduce the runoff potential.

The methodology used was not standardised. It was inspired by Nasberg-type drilling tests for geotechnical permeability. The main difference was that in our case we were trying to quantify the permeability at the soil surface, without drilling. The limitation of the experiment lay mainly in the difficulties of avoiding water leakage at the interface between the measuring installation and the soil. Due to the gravelly soils encountered, it was somewhat difficult to embed the measuring cone in the soil in an ideal manner. But given that this difficulty appeared similarly for all the trials, even if the absolute percolation values **are wrong**, we can consider that the **relative comparisons are relevant**.

These percolation measurements were taken at the following locations:

- **Site 1**: pine stand near the DFCI tank located at the entrance to the state forest from the Vilaplana ridge track
- **Site 2**: pine stand in the state forest at a place called Les Fontanilles
- **Site 3**: pine and eucalyptus stands on the Serrat Negre, near the Bois de Pins campsite.

At each of these sites, percolation measurements *(Figure 48)* were taken to determine the rate of water infiltration into the soil in the following configurations:

- soils in **unburnt forest**: presence of a forest canopy and plant litter;
- soils in **burnt forest** with a **Low Severity Index**: the fire had spread through the lower vegetation, the litter had disappeared but the pines remained green on the upper third. The ground was scattered with pine needles.
- soils in **burnt forest** with a **High Severity Index**: the fire had burnt all the litter and the crowns of the trees.

Figure 48: Percolation measurements in different configurations:
(a): soils in **unburnt forest**
(b): soils in **burnt forest** with a **Low Severity Index**
(c): soils in **burnt forest** with a **High Severity Index**

Figure 49: Taking the percolation measurements. The metal cone is driven into the ground and then filled with water. An automatic probe measures the lowering of the water level in the cone.

Each percolation measurement performed is quite simple and requires little equipment *(Figure 49)*:

- a metal container of sufficient capacity, to be sunk into the ground (cylinder or cone);
- a water supply of about 10 litres;
- a builder's level to check horizontality;
- an automatic probe to measure water level;
- a smartphone to download the data recorded by the probe.

The results of the percolation measurements are shown in *Figure 50*:

- the tests on ground where the Fire Severity Index is High appear as black curves;
- the test on ground where the Fire Severity Index is Low appears as an orange curve;
- the tests on ground where the vegetation was not burnt appear as green curves.

It can be seen that percolation in unburned or lightly burned soils (Low Severity Index) was higher. This means that conversely, **the higher the Fire Severity Index, the higher the runoff rate**.

The results of the percolation measurements indicate a ratio of 1 to 5 between unburnt and heavily burnt soil.

This means that the runoff rate would be 5 times higher on heavily burnt soils than on unburnt soils.

It should be borne in mind that these measurements include approximations of implementation which call for caution with these values (difficulty of fully confining the infiltration surface, lateral losses observed). These results are also strongly dependent on the scale of analysis: at the point-by-point scale of percolation measurements, the values can be very high compared to the scale of an entire watershed over which the high values are reduced and averaged by large-scale integration.

The experiments carried out following the OPOUL fire (surface percolation measurements), despite the uncertainties of implementation, give ratios of the order of 1 to 5 in terms of increased runoff (for equivalent heavy rainfall) between vegetated soil and burnt soil with a High Fire Severity Index.

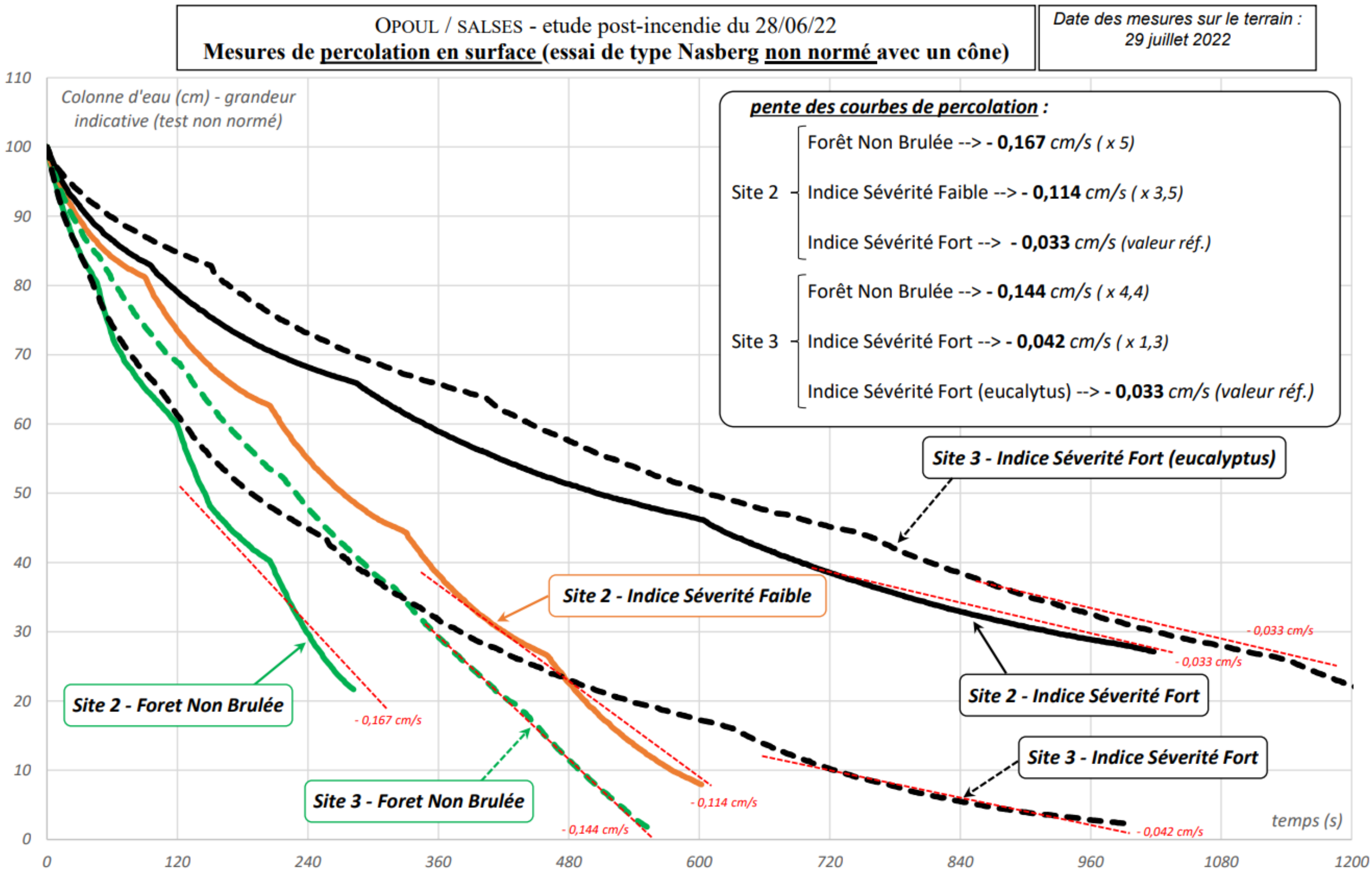

Figure 50: Results of percolation measurements following the OPOUL fire.

3.2.6 CONCLUSIONS CONCERNING HYDROLOGY

With regard to the hydrological results, it can be seen that the burnt plots produced more runoff volume with a higher flow rate than the plot with vegetation used as a reference.

The flow values were 1.6 to 5.8 times higher than the flow measured on the reference plot.

As far as runoff volume is concerned, the values were 3.8 to 6.6 times higher than the volume produced by the reference plot.

Furthermore, this experiment showed that runoff was much more sensitive to the intensity of rainfall than to its total volume.

Runoff from the **plot with vegetation** started when rainfall intensities exceeded **40 mm/h**.

In contrast, runoff from the **burnt plots** started as soon as rainfall intensity exceeded the threshold of 20 mm/h.

These results show that runoff on burnt soil occurs twice as easily as on vegetated soil. Therefore, in a context of Mediterranean vegetation of the shrubby scrubland type on schistose soils, and for light and moderate rainfall, only half the rainfall intensity is required to generate runoff on burnt soil as on non-burnt soil.

The experimental MONTCLIMA project on CERBÈRE, reinforced by the investigations carried out following the fire in OPOUL-PÉRILLOS and SALSES-LE-CHÂTEAU, give results established from localised measurements limited in space and time. It is therefore risky to extrapolate these unconsolidated results to an entire catchment area. Indeed, a more comprehensive approach at the level of a catchment area has the effect of mitigating the extremes of individual measurements. We believe that the 5-fold increase in the runoff coefficient does not apply at larger scales. Moreover, our review of the literature indicates that the values are closer to a ratio of **1:2 for runoff coefficients** between unburned soil and burnt soil for rainfall episodes, while also capping the runoff coefficient, which cannot be higher than 0.8.

3.3 INCREASED EROSION

3.3.1 RESULTS OF THE EXPERIMENTAL MEASUREMENTS

The erosion products are taken from the sedimentation tanks of each plot during periodic maintenance visits. These sediments are then dried naturally, sorted to remove plant debris (needles, leaves, pieces of bark) and weighed.

Sediments were collected three times in the course of the experiment: on 17 November 2021, 7 January 2022 and 16 September 2022. During the other maintenance visits, the quantity deposited was not sufficient to be measured. The material collected consists of sand, soot, pebbles and plant debris, as shown in *Figure 51*.

On the Control Plot, the majority of the material was plant debris and very fine sand. On Fire Plot 1, the deposits were composed of sand and pebbles, while on Fire Plot 2 the deposits were mainly pebbles.

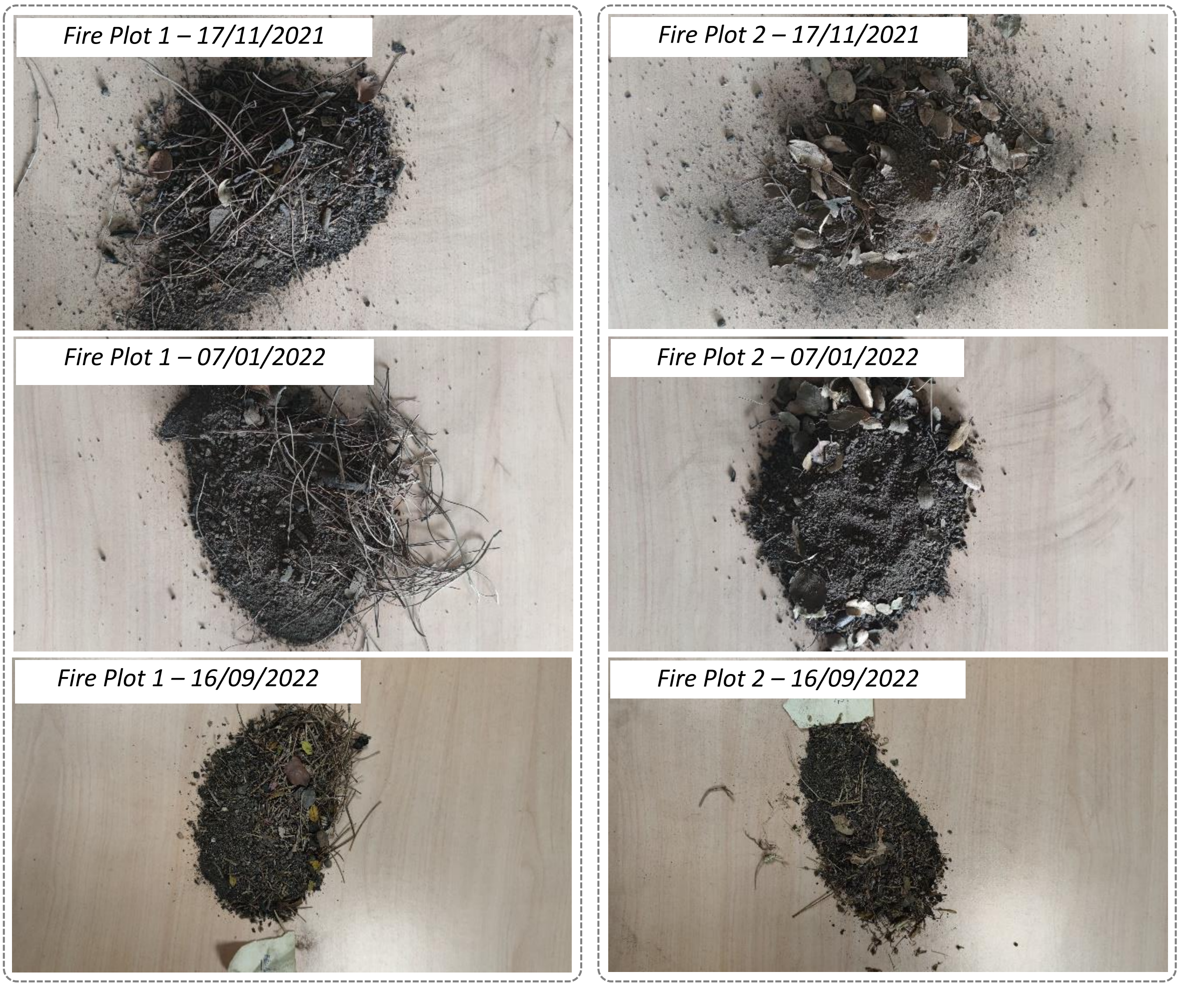

Figure 51: Sediments collected from erosion plots on different dates: on the burnt plots Fire 1 and Fire 2 there was enough material to take three samples (17 Nov. 2021, 7 Jan. 2022 and 16 Sep. 2022). For the Control Plot, there was little material; only one sample was possible (17 Nov. 2021).

Table 8 presents the results of samples taken from the sedimentation tanks. Some of the sediment had been transported by wind erosion, but most was transported by hydraulic erosion after significant rainfall events.

Given the regularity of maintenance visits between rain events, it is possible to determine the rainfall contexts that produced the deposited sediment masses:

- sampling dated 17/11/2021 → rain event: 10 to 12 Nov. 2021 (max. intensity 20 mm/h)
- sampling dated 07/01/2022 → rain event: 23 to 24 Nov. 2021 (max. intensity 56 mm/h)
- sampling dated 16/09/2022 → rain event: 3 Sep. 2022 (max. intensity 36 mm/h)

Rather paradoxically, following the rainfall event that generated a significant hydrological response (rainfall of 11-13 March 2022), the sedimentation tanks were quite clean and free of material. This suggests that the sampled masses are underestimated in relation to the reality of erosive processes.

Table 8: Measurement of erosion during the experiment: masses of sediment taken from the sedimentation tanks of each plot

	date de relevés des sédiments				
	17/11/2021 masse en grammes	**07/01/2022** masse en grammes	**16/09/2022** masse en grammes	*bilan du 21/10/2021 au 16/09/2022*	
	cumul pluviométrique antérieur = 65 mm *nombre d'épisodes pluvieux = 1* *intensité maximal de la pluie = 20 mm/h*	*cumul pluviométrique antérieur = 109 mm* *nombre d'épisodes pluvieux = 2* *intensité maximal de la pluie = 56 mm/h*	*cumul pluviométrique antérieur = 33 mm* *nombre d'épisodes pluvieux = 2* *intensité maximal de la pluie = 36 mm/h*	Cumul (Kg) sur la parcelle	***érosion équivalente t/ha/an***
parcelle Feu 1	**170**	**440**	**108**	0.718	***0.069***
type de dépôts	*nombreux sables et cailloux* *beaucoup de suie et débris de végétaux*	*nombreux sables et cailloux* *beaucoup de suie et débris de végétaux*	*nombreux sables et cailloux* *débris de végétaux*		
parcelle Feu 2	**315**	**540**	**85**	0.94	***0.097***
type de dépôts	*nombreux sables et cailloux* *beaucoup de suie et débris devégétaux*	*nombreux sables, forte proportion de cailloux* *beaucoup de suie et débris de végétaux*	*nombreux sables et cailloux* *débris de végétaux*		
parcelle Témoin	pas de sédiments	**75**	pas de sédiments	0.075	***0.007***
type de dépôts	-	*sables très fins et suie* *beaucoup de débris de végétaux*	-		

Given the low rainfall during the season studied and the limited number of rainfall episodes, the erosion processes were moderate. The sedimentation tank in the Control Plot was only sampled once. In contrast, we were able to sample the sedimentation tanks of Fire Plots 1 and 2 three times. This suggests that erosion is more frequent over time on burnt plots.

In addition, the sediment masses collected were much higher on the burnt plots than on the Control Plot. During the visit of 7 January 2021, when it was possible to take samples from all plots, there was approximately **6 and 7 times more** erosion on Fire Plots 1 and 2 respectively, compared to the Control Plot.

The equivalent erosion rates were very variable, between the Control Plot with vegetation (7 Kg/ha), Fire Plot 1 (69 Kg/ha) and Fire Plot 2 (97 Kg/ha).

Taking the erosion rate on the Control Plot as a reference, *Table 9* shows that the erosive potential was **10 times higher on Fire Plot 1** and **14 times higher on Fire Plot 2**. These values do not reflect absolute values; they should be considered as **comparative trends** between plots for this project.

Table 9: Sediment measurement for the period 21/10/2021 to 16/09/2022

	Mass of sediment measured (kg)	**Equivalent erosion** (t/ha/year)	*Multiplier coeff.*
Plot **with vegetation** *Slope = 56%*	0.075	0.007	*Reference*
Fire Plot 1 *Slope = 44%*	0.718	0.069	***x 10***
Fire Plot 2 *Slope = 53%*	0.940	0.097	***x 14***

3.3.2 QUALIFICATION OF EROSION: NATURAL DYNAMICS OF VEGETATION RECOLONISATION

The impact of a fire on the potential for increased soil erosion is immediate, as soon as the fire occurs. This potential remains high as long as the vegetation cover remains insufficient to regain its capacity to locally fix the soil and offer protection against the impacts of raindrops (splash effect).

The literature on the subject of the resilience of the environment from a temporal point of view indicates that it is commonly accepted that the critical period with regard to the soil's sensitivity to erosion before a return to a "normal" situation is on average **between 1 and 5 years**. After this time, the vegetation is restored to its pre-fire protective role. This temporal range is highly variable depending on the intensity of the fire, geology, rainfall (and the weather more generally), vegetation present, etc.

In the specific case of the CERBÈRE fire, the maintenance visits provided a very regular visual assessment of the set-up. By compiling the photographic evidence from the fire up until September 2022, it is possible to assess the natural dynamics of vegetation recolonisation and to get an idea of the timing of the critical period for soil erosion. This comparative analysis is illustrated in the series of photos shown in Figure 52 to Figure 56.

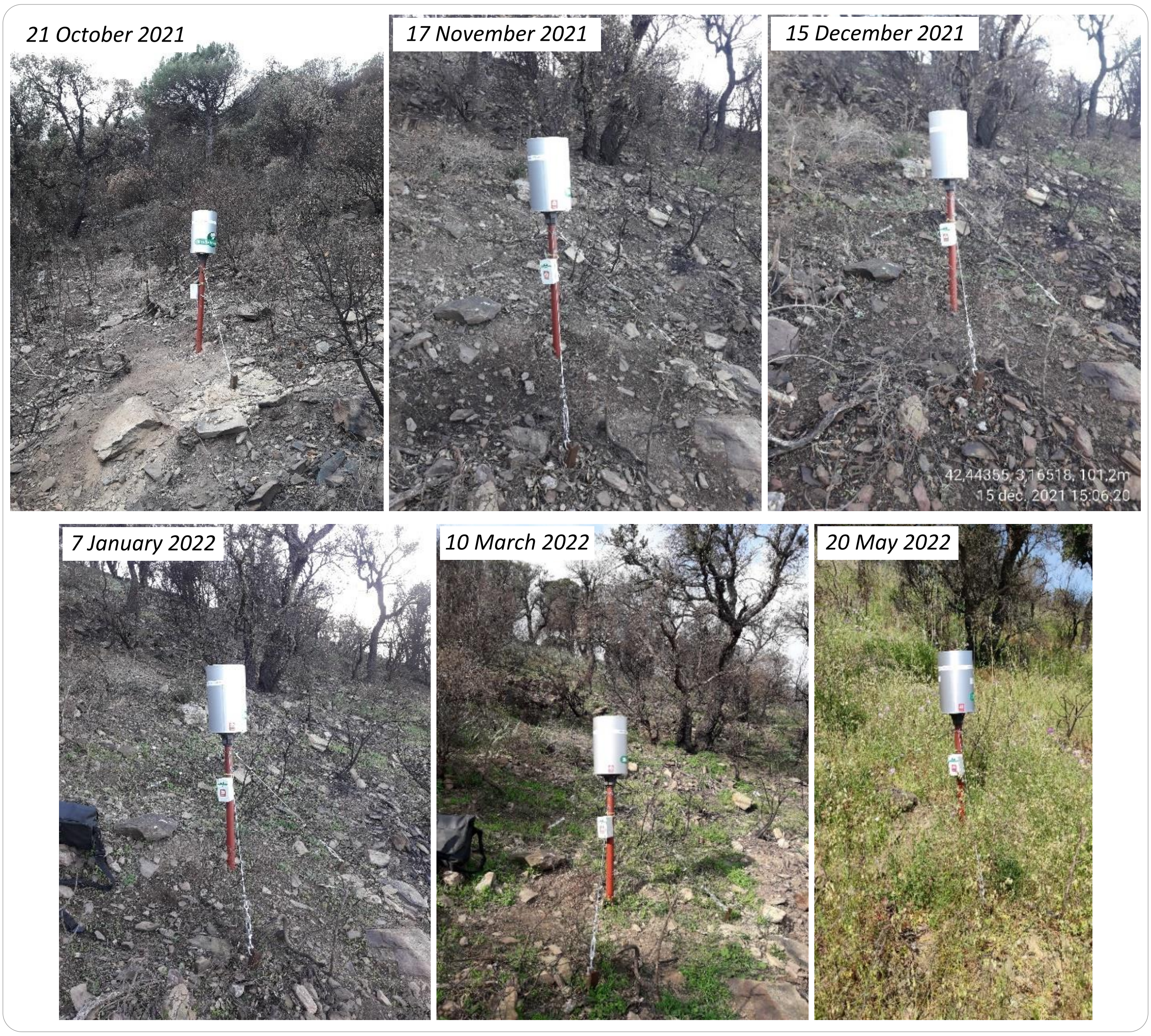

Figure 52: Natural revegetation dynamics around the rain gauge between October 2021 and May 2022

Figure 53: Natural revegetation dynamics of Fire Plot 1 between October 2021 and September 2022

Figure 54: Natural revegetation dynamics of Fire Plot 2 between November 2021 and September 2022

Fire Plot 2 – 17/11/2021

Fire Plot 2 – 26/01/2022

Fire Plot 2 – 11/03/2022

Fire Plot 2 – 30/03/2022

Fire Plot 2 – 20/05/2022

Fire Plot 2 – 16/09/2022

Figure 55: Natural revegetation dynamics of the Control Plot between October 2021 and September 2022

Figure 56: Natural revegetation dynamics of the international border ridge between August 2021 and May 2022

Pre-existing weather station - 27/08/2021

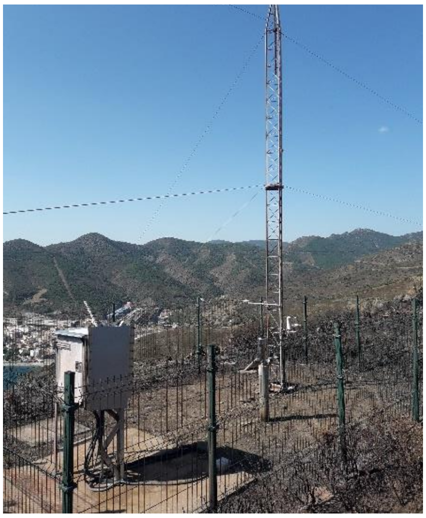

Pre-existing weather station - 20/05/2022

From these photos, the following observations can be made:

- near the rain gauge *(Figure 52)*: the site was affected by a Moderate Severity Index fire:
  - the ground remained devoid of vegetation until the end of November 2021 (fire + 4 months);
  - in December 2021, young shoots of herbaceous plants started to appear here and there;
  - in January 2022, this herbaceous revegetation expanded to cover about 30% of the surface;
  - in March 2022 (fire + 8 months) the herbaceous stratum spread further to cover 50% of the ground;
  - in May 2022 (fire + 10 months) the vegetation cover was very good and covered more than 90% of the soil with a significant thickness of vegetation.
- on Fire Plot 1 *(Figure 53)*: the site was affected by a High Severity Index fire.
  - the ground remained devoid of vegetation until the end of November 2021 (fire + 4 months);
  - in January 2021, the soil remained bare on the whole and very timid herbaceous growth could be observed;
  - at the beginning of March 2022, herbaceous vegetation was spreading but covered barely 20% of the soil surface;
  - at the end of March 2022, a carpet of vegetation was becoming established and covered 40% of the soil;
  - in May 2022 (fire + 10 months), the vegetation cover reached about 70%;
  - in September 2022, the vegetation cover was still about 70% of the soil surface but was significantly thicker.

- on Fire Plot 2 *(Figure 54)*: the site was affected by a High Severity Index fire.
    - the ground remained devoid of vegetation until the end of November 2021 (fire + 4 months);
    - in January 2021, the soil remained bare on the whole and very timid herbaceous growth could be observed;
    - at the beginning of March 2022, herbaceous vegetation was spreading but covered barely 20% of the soil surface;
    - at the end of March 2022, a carpet of vegetation became established and covered more than 50% of the soil;
    - in May 2022 (fire + 10 months), the vegetation cover reached a significant proportion of about 80%;
    - in September 2022, the vegetation cover was still about 80% of the soil surface but was significantly thicker.
- on the Control Plot *(Figure 55)*: the site was not affected by fire.
    - the vegetation was dry until March 2022. The vegetation cover was around 90%;
    - in March and May 2022, the vegetation completely covered the entire surface of the soil (100%) and was very thick;
    - in September 2022, the grass layer turned yellow but its coverage was still optimal (90%).
- on the international border ridge *(Figure 56)*: the site was affected by a Moderate Severity Index fire.
    - in August 2021 (fire + 1 month), all the low vegetation had been burnt;
    - in May 2022 (fire + 10 months), the low vegetation covered more than 90% of the ground surface with a significant thickness.

These observations are summarised in *Figure 57*, which shows the evolution of the vegetation cover on the ground for each site observed. The estimated percentage of coverage was assessed visually.

From these observations, we can deduce that the **natural dynamics of vegetation recolonisation are strong overall, because 10 months after the fire the ground cover was satisfactory** (between 70% and 90% depending on the site).

On the Control Plot, the vegetation cover was very good and constant over time, except in spring when it reached a maximum.

On the burnt Fire Plots 1 and 2, the natural dynamics of vegetation recolonisation followed the same changes over time.

In the vicinity of the rain gauge, which is a little more sheltered by the surrounding trees, and was less severely impacted by the fire (Moderate Severity Index), the vegetation recovered more quickly.

These results of the comparative analysis of the natural dynamics of vegetation recolonisation are consistent with the results of sediment sampling in the tanks: the greater the vegetation cover on the ground, the lower the volumes of sediment collected.

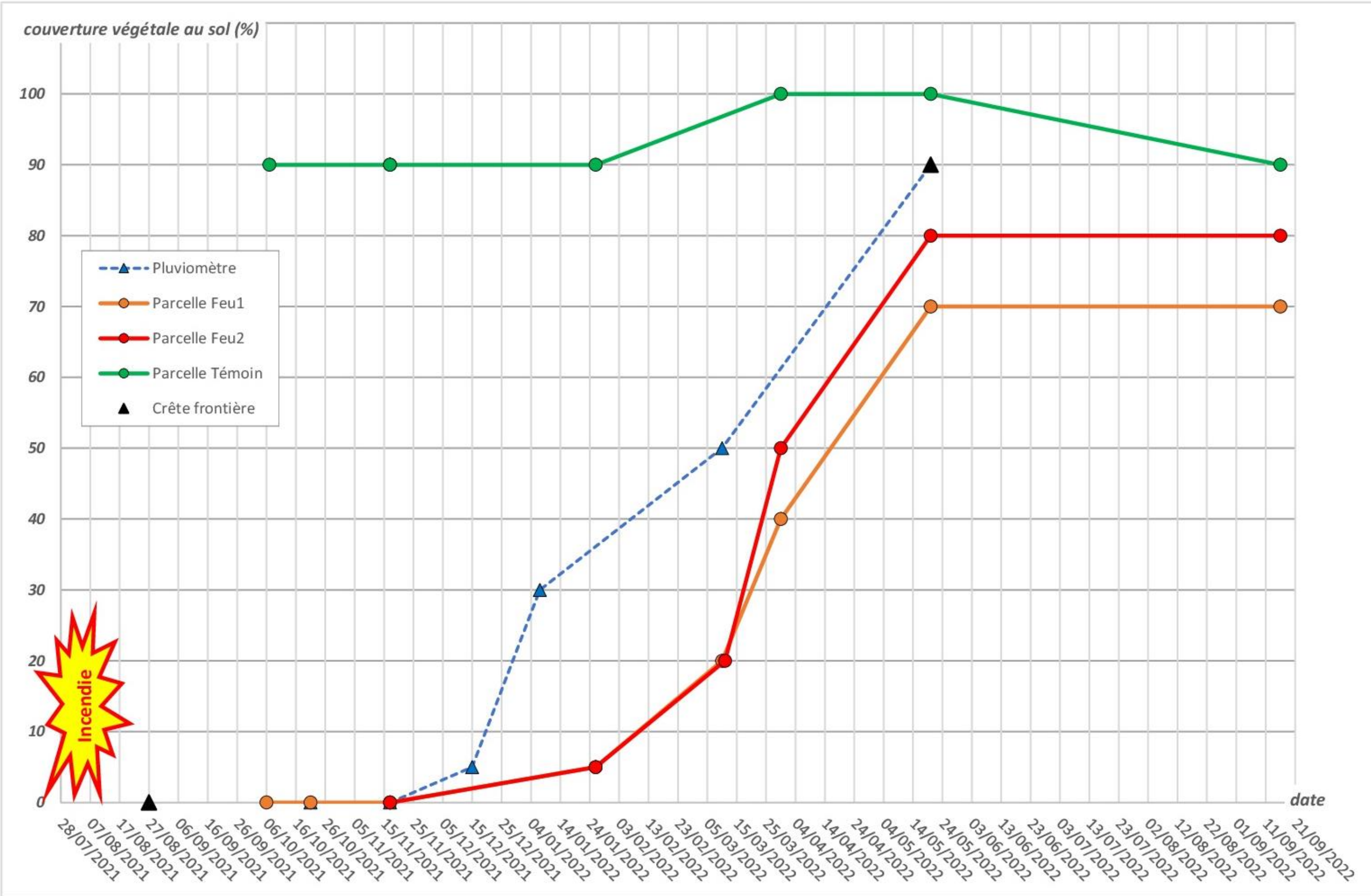

Figure 57: Natural dynamics of vegetation recolonisation after the fire on the erosion plots and near the rain gauge

3.4 RESERVATIONS ON THE INTERPRETATION OF THE RESULTS

The hydro-sedimentary results of the erosion plot experiment may appear accurate, but they must be contextualised and taken with certain reservations, particularly as:

- the very small size of the plots (about 100 m^2) means that the measurements are not averaged, unlike what would be obtained in a larger catchment area. The values obtained at this small spatial scale are consequently rather in the upper range of the real values;
- the short duration of the observation period does not allow for averaging the values over time. It would only require an unusually high or low volume of rainfall over the observation period to distort the realistic values that could be obtained over a longer observation. In this case, the rainfall was abnormally low;
- there are uncertainties about the proportion of natural erosion that can be measured as opposed to anthropogenic erosion generated during the installation of equipment;
- there are uncertainties about the effectiveness of plot containment using border markers;
- there are approximations regarding the setting to zero of the water-level probes.

4 LESSONS LEARNT AND FOLLOW-UP OF THE PROJECT

The MONTCLIMA project offered a real opportunity to improve local knowledge in part of the PYRÉNÉES-ORIENTALES *département* on the subject of the effects of fires on hydrological modifications and soil erosion.

The project was designed to be easily and quickly installed after a fire. All the work of analysis, sizing, installation, implementation and data processing can be used for possible similar experiments on other sites.

The MONTCLIMA project has shown that the quality of the experiment depends very much on the following factors:

- the objectives of the experiment must be clearly defined before the set-up is set up;
- the human resources for the supervision of the set-up and the analysis of the data should not be minimised;
- the choice of location and number of plots must be in line with the human resources available;
- the quality and robustness of the equipment must be consistent with the external threats (weather, risk of vandalism, etc.) and the duration of the experiment;
- the choice of equipment, and in particular its accuracy and reliability, must be consistent with the desired degree of accuracy of the quantities to be measured;
- power and storage capacities should be determined in relation to the ability to travel frequently to the site to monitor the set-up;
- overall design should include the possibility of working on longer timeframes than initially planned (extension of the experiment depending on funding);
- design should consider the ease and low cost of dismantling at the end of the experiment;
- the richness of the dataset and the quality of the measurements ultimately depend on a parameter that cannot be controlled: the occurrence immediately after a fire of rather exceptional rainfall, with numerous and intense episodes.

Despite deficient rainfall and the low number of exceptional rainfall episodes, this experiment shows that on schistose soils, with scrub-type vegetation and on slopes of around 40%-50%, fire has a real and highly significant impact on increasing hydro-sedimentary processes:

- soils become more reactive to precipitation; hydrological responses of burnt plots are more rapid and intense:
- runoff volumes on burnt plots are in a range of 3.8 to 6.6 times higher than the volume produced by the reference plot;
- flow values on burnt plots are 1.6 to 5.8 times higher than the flow measured on the reference plot;
- erosion by runoff is heavily increased, by ratios of 1 to 14, with intense erosive processes during the first year after the fire;

- the natural dynamics of vegetation recolonisation are remarkable, and suggest that by 10 months after the fire, the low vegetation starts to reduce the erosive potential exacerbated by the fire.

The results obtained show trends that would need to be consolidated over a longer period. As the MONTCLIMA project ends in late 2022, it seems necessary to build a partnership with a research institute or university in order to continue this work and to confirm the results over longer time periods.

---------- End of the Report ----------

AGENCE RTM PYRENEES

RTM Department of the Pyrénées-Orientales and Aude

8, Rue des Variétés

CS 50003

66026 PERPIGNAN Cedex

Office National des Forêts

www.onf.fr

rtm
restauration des terrains en montagne